# The Role of PARP1 in cGMP Mediated Photoreceptor Degeneration

**Dissertation**

der Mathematisch-Naturwissenschaftlichen Fakultät

der Eberhard Karls Universität Tübingen

zur Erlangung des Grades eines

Doktors der Naturwissenschaften

(Dr. rer. nat.)

vorgelegt von

**Ayse Sahaboglu Tekgöz**

aus Kozan Türkei

Tübingen

2012

| | |
|---|---|
| Tag der mündlichen Prüfung: | **16.05.2012** |
| Dekan: | **Prof. Dr. Wolfgang Rosenstiel** |
| 1. Berichterstatter | **Prof. Dr. Eberhard Zrenner** |
| 2. Berichterstatter | **Prof. Dr. Konrad Kohler** |

*"I am among those who think that science has great beauty. A scientist in his laboratory is not only a technician: he is also a child placed before natural phenomena which impress him like a fairy tale."*

*"You cannot hope to build a better world without improving the individuals. To that end each of us must work for his own improvement, and at the same time share a general responsibility for all humanity, our particular duty being to aid those to whom we think we can be most useful."*

*Marie Curie*

*To my family*

# Contents

# Publications that are part of this thesis

**Paper I** Huber G, Beck SC, Grimm C, **Sahaboglu-Tekgoz, A**, Paquet-Durand F, Wenzel A, Seeliger MW, Fischer MD. (2009) Spectral domain optical coherence tomography in mouse models of retinal degeneration. Investigative Ophthalmology & Visual Science 50(12):5888-5995.

**Paper II** Sancho-Pelluz J, Alavi M, **Sahaboglu A**, Kustermann S, Farinelli P, Azadi S, Van Veen T, Romero FJ, Paquet-Durand F, Ekström P. (2010) Excessive HDAC activation critical for neurodegeneration in the *rd1* mouse. Cell Death & Disease, e24; doi:10.1038/cddis.2010.4.

**Paper III** **Sahaboglu A**, Tanimoto N, Kaur J, Sancho-Pelluz J, Huber G, Fahl E, Arango-Gonzalez B, Zrenner E, Ekström P, Löwenheim H, Seeliger MW, Paquet-Durand F. (2010) PARP1 gene knock-out increases resistance to retinal degeneration without affecting retinal function. PLoS ONE 5(11): e15495.

# Abbreviations

| | |
|---|---|
| ADP | Adenin diphosphate |
| ADPRT | ADP-ribosyltransferases |
| AIF | apoptosis inducing factor |
| ARVO | Association for Research in Vision and Ophthalmology |
| ATP | Adenosin triphosphate |
| β | Beta |
| BER | Base excision repair |
| BRCT | BRCA1 C-terminus-like |
| $Ca^{2+}$ | Calcium |
| cAMP | cyclic adenosine monophosphate |
| cGMP | cyclic guanosine monophosphate |
| CNG | cation nucleotide-gated |
| CNS | central nervous system |
| CREB | cAMP response element-binding protein |
| cSLO | Confocal scanning laser ophthalmoscopy |
| CTx | chlolera toxin |
| DAPI | 4',6-diamidino-2-phenylindole |
| DBD | DNA-binding domain |
| DMSO | Dimethylsulfoxide |
| DNA | deoxyribonucleic acid |
| ERG | electroretinography |
| GC | guanylate cyclase |
| GCL | ganglion cell layer |
| GDP | guanosine diphosphate |
| GMP | guanosine monophosphate |
| GP | glycogen phosphorylase |
| GTP | guanosine triphosphate |
| HAT | histone acetyltransferase |
| HDAC | histone deacetylase |
| ICER | inducible cAMP early repressor |
| ILM | inner limiting membrane |
| INL | inner nuclear layer |
| IPL | inner plexiform layer |
| IS | inner segment |

| | |
|---|---|
| KO | knock-out |
| $NAD^+$ | nicotinamide adenine dinucleotide |
| NAM | nicotinamide |
| NMDA | N-Methyl-D-aspartic acid |
| OCT | optical coherence tomography |
| OLM | outer limiting membrane |
| ONL | outer nuclear layer |
| OPL | outer plexiform layer |
| OS | outer segment |
| PAR | Poly (ADP-ribose) |
| PARG | poly(ADP-ribose) glycohydrolase |
| PARP | poly(ADP-ribose) polymerase |
| PARS | poly(ADP-ribose) synthetase |
| PBS | phosphate buffered saline |
| PDE5 | phosphodiesterase 5 |
| PDE6 | phosphodiesterase 6 |
| PKG | protein kinase G |
| PN | post-natal day |
| PTx | pertussis toxin |
| *rd1* | retinal degeneration 1 |
| RETNET | retinal information network |
| ROS | Reactive oxygen species |
| RP | retinitis pigmentosa |
| RPE | retinal pigment epithelium |
| RT | room temperature |
| SD OCT | spectral domain optical coherence tomography |
| SEM | standard error of the mean |
| TBS | TRIS buffered saline |
| TSA | trichostatin A |
| TUNEL | terminal deoxynucleotidyl transferase dUTP nick end labelling |
| WB | Western blot |
| *wt* | wild-type |

# Summary

Retinitis Pigmentosa (RP) is an inherited eye disease which causes progressive photoreceptor degeneration and consequently blindness in humans. So far, there has been no found cure or reliable treatment for RP. The retinal degeneration 1 (*rd1*) mouse model is a well-studied model of human autosomal recessive RP. In 2007, it was found that over-activation of poly(ADP-ribose) polymerases (PARP) contributed to photoreceptor degeneration in the *rd1* mouse. However, it was still unclear which PARP family member exactly was involved in photoreceptor degeneration. Therefore, the aim of this thesis was to investigate the role of PARP1, the most prominently expressed and extensively studied member of the PARP family, in photoreceptor degeneration in the *rd1* retina.

Electroretinography, optic coherence tomography (OCT), scanning laser ophthalmoscopy (SLO), and histology identified no significant differences between PARP1 knock-out (KO) and wild-type (*wt*) animals in terms of retinal function, thickness, and structure. In addition to PARP, histone deacetylase (HDAC) activity was shown to be involved in *rd1* photoreceptor degeneration. Double-label immunohistochemistry showed poly(ADP-ribose) (PAR) accumulation - *i.e*. the product of PARP activity - in photoreceptor nuclei that were devoid of acetylated proteins, indicating a causal link between PARP and HDAC activity. We emulated the *rd1* situation in organotypic retinal cultures derived from PARP1 KO and *wt* animals using zaprinast, a selective inhibitor of PDE6. Accumulation of cyclic guanosine monophosphate (cGMP) in zaprinast treated PARP1 KO retina was significantly reduced compared to zaprinast treated *wt*. At the same time, PAR accumulation and cell death were also significantly reduced in zaprinast treated PARP1 KO when compared with *wt*.

In conclusion, PARP1 appears to have an important role in the progression of photoreceptor cell death. In *rd1* photoreceptors, PARylation was linked to cell death as well as to deacetylation and HDAC activity, while PARP1 KO retina showed increased resistance to pharmacologically induced photoreceptor degeneration. Because of the involvement of PARP in photoreceptor degeneration and since retinal function and morphology in PARP1 KO retina appeared normal, PARP1 promises to be an interesting target for future therapy development.

# Zusammenfassung

Retinitis Pigmentosa (RP) ist eine erbliche Augenkrankheit, die progressive Degeneration von Photorezeptorzellen und damit Blindheit beim Menschen verursacht. Bisher gibt es keine Heilung oder zuverlässige Behandlung für RP. Das Retinadegeneration-1 (*rd1*) Mausmodell ist ein gut untersuchtes Modell der menschlichen autosomal-rezessiven RP. Im Jahr 2007 wurde festgestellt, dass die Überaktivierung von Poly(ADP-Ribose) Polymerase (PARP) zur Photorezeptordegeneration in der *rd1* Maus beiträgt Allerdings war unklar, welche Isoform der PARP-Enzymfamilie an der Photorezeptordegeneration beteiligt ist. Daher war es das Hauptziel dieser Arbeit, die genaue Rolle von PARP1 in der Photorezeptordegeneration der *rd1* Retina zu untersuchen.

Elektroretinographie (ERG), optische Kohärenztomographie (OCT), Scanning Laser Ophthalmoskopie (SLO) und Histologie zeigten keine signifikanten Unterschiede zwischen PARP1 Knock-out (KO) und Wildtyp (*wt*) Tieren, im Hinblick auf die retinale Funktion, die Schichtdicke oder die retinale Struktur. Zusätzlich zu PARP konnte gezeigt werden, dass HDAC-Aktivität in der *rd1* Photorezeptordegeneration involviert war. Immunohistochemische Doppel-Markierung zeigte eine Akkumulation von PAR – d.h. dem Produkt von PARP Aktivität – in Photorezeptorkernen die negativ für acetylierte Proteine waren. Dies weis auf einen ursächlichen Zusammenhang zwischen PARP- und HDAC-Aktivität hin. Anhand von organotypischen Retina-Kulturen die aus PARP1 KO und *wt* Tieren gewonnen wurden, haben wir die *rd1* Situation durch Verwendung des selektiven PDE6-Inhibitors Zaprinast emuliert. Die Akkumulation von cGMP in der Zaprinast-behandelten PARP1 KO Retina war deutlich reduziert im Vergleich zur Zaprinast-behandelten *wt* Retina. Außerdem waren die PAR Akkumulation und der Zelltod ebenfalls signifikant reduziert in der PARP1 KO Situation, verglichen mit *wt*.

Zusammenfassend scheint es, dass PARP1 eine wichtige Rolle beim Voranschreiten des Photorezeptor-Zelltods hat. In *rd1* Photorezeptoren war PAR Akkumulation ursächlich sowohl mit Proteindeacetylierung und HDAC Aktivität, als auch mit dem Zelltod verbunden. Dahingegen zeigte PARP1 KO Retina eine erhöhte Resistenz zur pharmakologisch induzierten Photorezeptordegeneration. Wegen der offensichtlichen Beteiligung von PARP an der Photorezeptordegeneration und weil die retinale Funktion und Morphologie in PARP1 KO Retina normal erscheinen, könnte PARP1 ein interessantes Target für die Entwicklung von zukünftigen Therapien sein.

# 1. Introduction

Blindness is a devastating condition that severely affects the quality of human life. Retinitis Pigmentosa (RP) is a group of inherited neurodegenerative diseases that result in selective cell death of photoreceptors and is regarded as the main cause of blindness among the working age population in the developed world (Herse 2005). Although causative mutations in more than 44 genes have been identified in recent years (Wright *et al.* 2010), the precise mechanisms eventually leading to cell death remain unknown and to date no adequate treatment for RP is available (Sancho-Pelluz *et al.* 2008). The inherited forms of retinal degeneration are largely due to mutations in photoreceptors or the retinal pigment epithelium. Often the phototransduction cascade and visual pigment activation or de-activation are altered by gene mutations leading to the RP phenotype (Kalloniatis and Fletcher 2005). RP may be classified into autosomal dominant, autosomal recessive, or X-chromosome-linked inheritance patterns with additional and very rare mitochondrial and digenic forms.

## 1.1. Photoreceptor degeneration and clinical symptoms in RP

Photoreceptor cells, rods and cones, convert the energy absorbed from photons into neuronal signals. Rod photoreceptors are responsible for scotopic visions (*i.e.* night vision). Cone photoreceptors are responsible for colour vision and high contrast vision (*i.e.* daylight conditions) in photopic conditions (Figure 1). In humans, there are three different types of cone photoreceptors which are activated at different wavelengths of light. Long wavelength cones are referred to as L-cones or red cones and respond to light at wavelengths near 564–580 nm. Medium wavelength cones, abbreviated M-cones or green cones, responds to light at around 534–545 nm. Short wave length cones, S-cones, are also referred to blue cones respond at near 420-440 nm (Wald 1951;Roorda and Williams 1999).

The photoreceptor degeneration process in RP starts in the mid-periphery and progresses towards the macula and fovea (Daiger *et al.* 2007). In the progressive RP photoreceptor degeneration, the rod photoreceptors firstly die due to the genetic mutation, while secondarily, through an unknown pathway, death of cone photoreceptors follows. This two-stage degenerative process causes the commonly observed clinical symptoms in RP patients, such as night blindness followed by

decreasing visual fields, leading to tunnel vision, loss of central vision and eventually legal or total blindness (Daiger *et al.* 2007;Sancho-Pelluz *et al.* 2008).

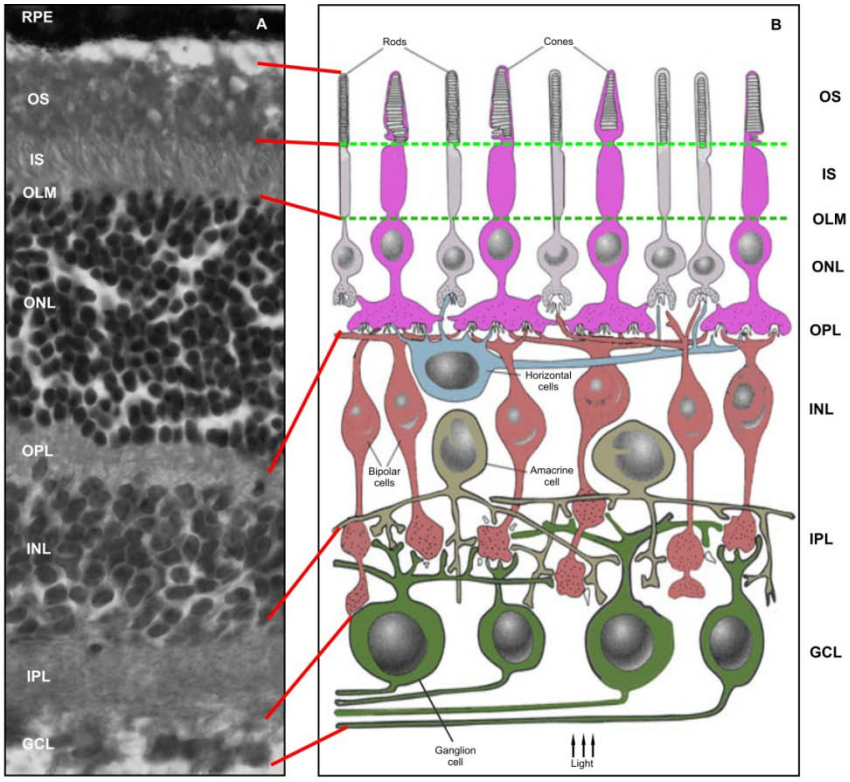


***Figure 1: Retinal structure**. Histology of wild-type mice retina **(A)** Functional organisation of vertebrate retina (Cartoon on right adapted from http://wdict.net/word/Retina+horizontal+cell) **(B)**. RPE: Retinal Pigment Epithelium, OS/IS: Outer segment/Inner Segment, OLM: Outer Limiting Membrane, ONL: Outer Nuclear Layer, OPL: Outer Plexiform Layer, INL: Inner Nuclear Layer, IPL: Outer plexiform layer, GCL: Ganglion Cell Layer.*

### 1.1.1. The *rd1* mouse model

Different animal models for RP have been investigated to try and improve the understanding of photoreceptor cell death mechanisms. The retinal degeneration 1 (*rd1* or *rd*) human homologous mouse model is the most studied RP model and characterized by a loss-of-function mutation in exon 7 of the gene encoding for the beta-subunit of rod photoreceptor cGMP phosphodiesterase 6 (PDE6) (Bowes *et al.* 1990). The *rd1* mouse is considered a relevant model for human RP, since about 4-5% of patients suffer from mutations in the PDE6 beta gene (McLaughlin *et al.* 1995). Accumulation of cGMP due to non-functional PDE6 causes $Ca^{2+}$ influx into the cytoplasm. Excessive $Ca^{2+}$ influx via constitutively opened CNG channels may trigger numerous signaling pathways potentially involved in photoreceptor degeneration (Farber and Lolley 1974;Paquet-Durand *et al.* 2009;Paquet-Durand *et al.* 2011).

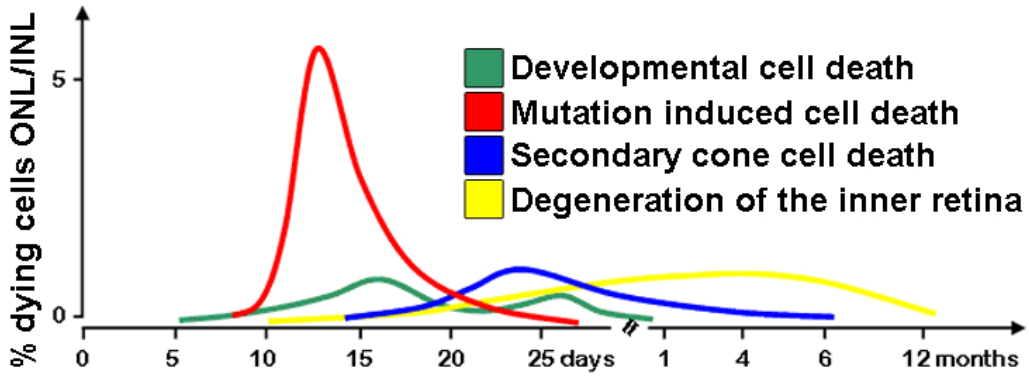


***Figure 2: Progression of photoreceptor cell death in rd1 mouse.*** *Retinal developmental cell death occurs between post-natal day PN5 and 30 in wt and rd1 retina. Mutation-induced rd1 rod photoreceptor cell death starts around PN10, peaks at PN13, and ends approximately at PN25. The secondary cone photoreceptor degeneration which follows primary rod photoreceptor degeneration starts around PN15. Only one or two rows of photoreceptors which are mainly cone photoreceptors remain at PN21 and eventually degenerate within the following six months (Pierce 2001). Both rod and cone photoreceptor degeneration affect the inner retina and may cause tertiary degeneration of various inner retinal cells. Due to the fast degeneration in the rd1 model, it is difficult to distinguish between these different degenerative processes. Figure adapted from Sancho-Pelluz et al. 2008.*

The *rd1* mutation-induced degeneration affects mostly rods and starts at around post-natal (PN) day 10 (Schoppner and Kindl 1984;Portera-Cailliau *et al.* 1994;Otani *et al.* 2004), peaking between PN12-14 (Punzo and Cepko 2007) (Paquet-Durand *et al.* 2007b) (Figure 2) and is almost complete at PN18 when mostly cone photoreceptor remain (Figure 3).

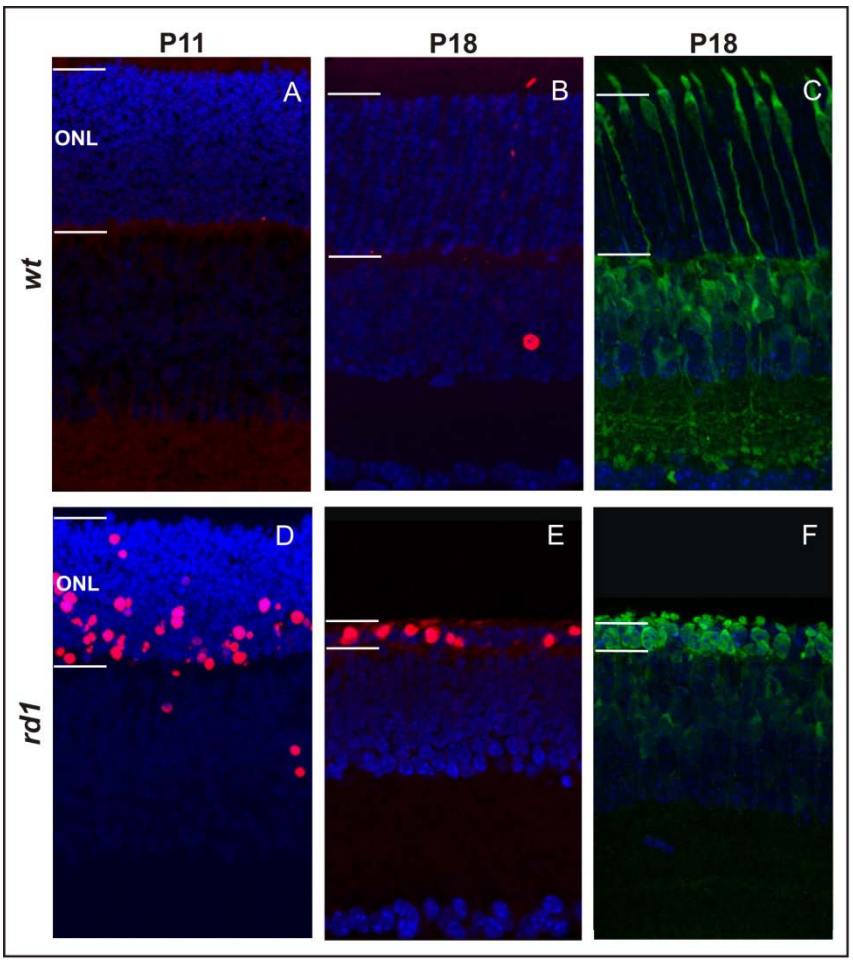


***Figure 3: Progression of photoreceptor degeneration and cone photoreceptor viability in rd1 mice****. The retinal thickness of wild-type (wt) revealed no significant difference between P11 and P18* ***(A,B)****, however there was significant difference between retinal degeneration 1 (rd1) P11 and P18* ***(D,E)*** *due to mutation in PDE6 gene. TUNEL staining (red color) showed significant difference between wt and rd1 at P11* ***(A,D)****. Glycogen Phosphorylase (GP) staining (green color) showed a clearly reduced number of cones in wt retina at P18. In rd1 retina, ONL was reduced to single layer of cone cell bodies and cone inner segment was flattened* ***(C,F)****. ONL: Outer nuclear layer.*

## 1.2. Poly ADP ribose polymerase (PARP) family

Approximately 40 years ago, a study with rat liver nuclear extracts showed that the addition of nicotinamid adenine dinucleotide ($NAD^+$) stimulated the formation of polyadenylic acid, which was later called poly(ADP-ribose) or PAR. With that observation, increasing research on PAR led to the discovery of the first PAR polymerase (PARP) (Jagtap and Szabo 2005).

Many cellular processes are regulated by protein post-translational modifications, such as (ADP-ribosyl)ation or poly(ADP-ribosyl)ation of proteins (Hottiger *et al.* 2010). This family of enzymes is called PARPs or poly(ADP-ribose) synthetases (PARS). Hottiger *et al.* proposed a new unified nomenclature for mammalian poly(ADP-ribose) transferases as ADP-ribosyltransferases (ADPRT/ARTs) to facilitate communication of researchers in the PAR field (Hottiger *et al.* 2010).

PARP family members catalyze mono- and poly-ADP-ribosylation of proteins which are implicated in a wide range of cellular processes (Hassa *et al.* 2006). Although in many instances the precise molecular consequences are not known, these catalytic cellular processes are involved in important processes such as maintenance of genomic stability, transcriptional regulation, energy metabolism and cell death (Hassa *et al.* 2006). It has been suggested that mono-ADP-ribosylation is an important cellular process for regulation of intracellular signaling cascades, gene expressions, cell differentiation and proliferation (Corda and Di 2003;Hassa *et al.* 2006).

PARP family members share highly conserved catalytic domains, which are also referred to as the “PARP signature” (Kim *et al.* 2005). On the other hand, the PARP motif contains sufficient variations such as zinc fingers, breast cancer associated protein C terminus (BRCT), ankyrin repeats, macro domains, W,W, and E (WWE) residues to allow phylogenetic discrimination (Ame *et al.* 2004) (Figure 4).

PARPs are involved in many aspects of regulation of cellular functions including DNA repair, transcriptional control, genomic stability, transformation and cell death (Herceg and Wang 2001;Hong *et al.* 2004). On the other hand, PARP also plays a role in cell cycle progression, cell proliferation, and neoplastic transformation (Tanuma *et al.* 1978;Masutani *et al.* 1995;Horton *et al.* 2005). It was proposed that poly(ADP-ribosyl)ation is associated with the stimulation of cell proliferation (Cesarone *et al.* 1990;Kun *et al.* 2006;Pagano *et al.* 2007).

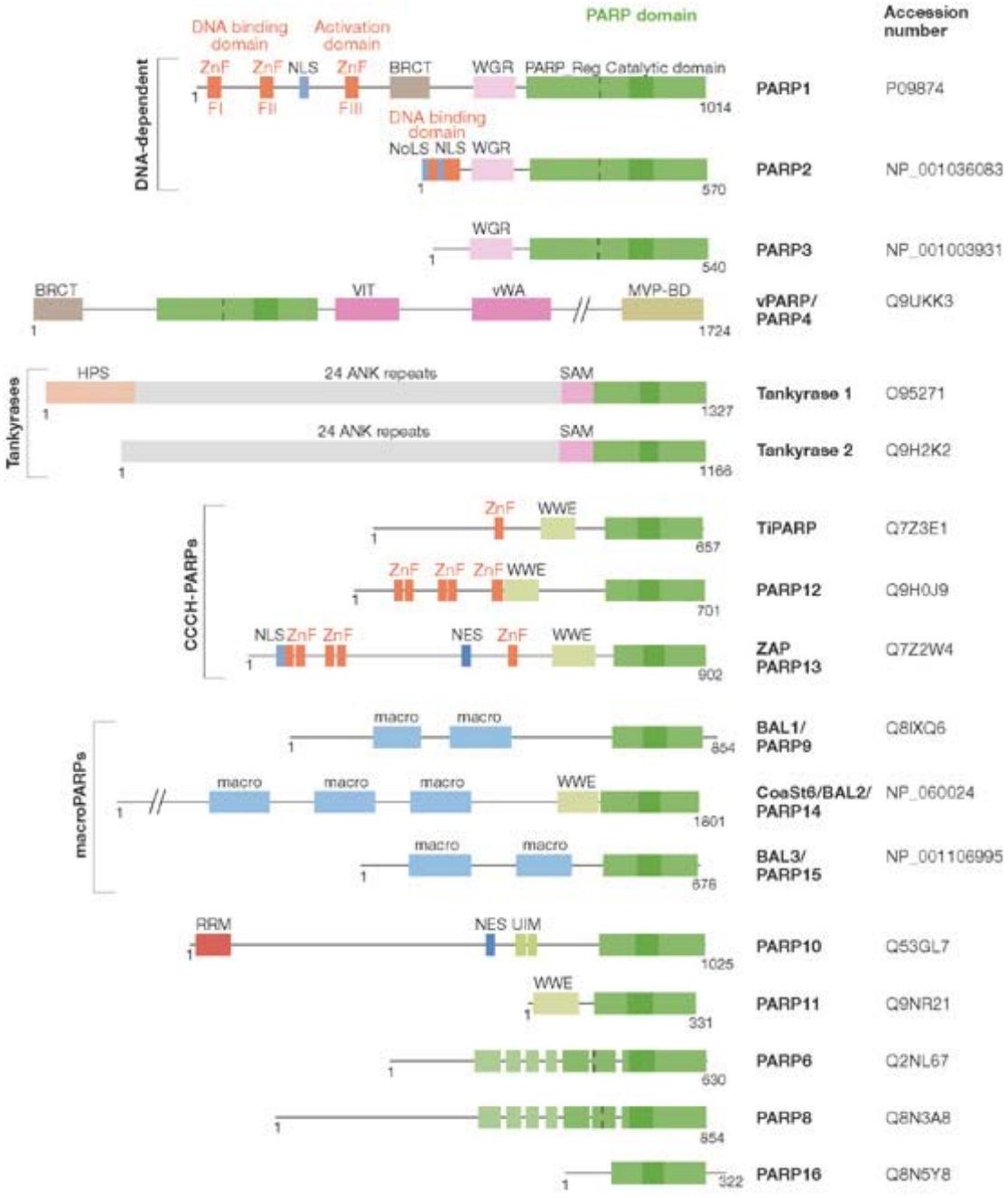


***Figure 4: Domain structure of human PARP family members**. Darker green colour represents the PARP signature. Breast Cancer suppressor Protein-1 (BRCA1), BRCA1-carboxy-terminus (BRCT), TiPARP is also known as PARP7 and induced by 2,3,7,8-tetrachlorodibenzo-p-dioxin, sterile α-motif TiPARP (SAM), ubiquitin-interacting motif (UIM), Major-vault particle (MVP)-binding (MVP-BD), von Willebrand factor type A (VWA) and ankyrin (ANK) are protein interaction modules. Homopolymeric runs of His, Pro and Ser (HPS); domain involved in ADP-ribose and poly(ADP-ribose) binding (macro); nuclear export signal (NES), nuclear localization signal (NLS), poly(ADP-ribose) polymerase (PARP); putative regulatory domain (PARP_reg), RNA binding motif (RRM); vault inter-α-trypsin (VIT); vault poly(ADP-ribose) polymerase (vPARP); conserved W,G and R residues (WGR); conserved W,W, and E residues (WWE); DNA or RNA binding zinc fingers (except PARP1 ZnFIII, which contains coordinates DNA-dependent enzyme activation) (ZnF). Figure adapted from (Hakme et al. 2008).*

PARP family members abundant nuclear enzymes and found in many eukaryotes except yeast (Uchida 2001;Herceg and Wang 2001). PARP2 is another DNA dependent enzyme of 62 kDa in the PARP family, shares considerable homology with the catalytic domain of PARP1 thus suggesting a biological role in the cellular response to DNA damage and base excision repair (BER) (Ame 1999;Schreiber *et al.* 2002;Isabelle *et al.* 2010). Within the PARP family, only PARP1 and PARP2 are activated by DNA strand breaks (Hottiger *et al.* 2010). PARP3 is involved in the maintenance of genomic integrity and activates the PARP1 in absence of DNA (Loseva *et al.* 2010). PARP4/vPARP is dispensable for normal development and can interact with telomerase-associated protein 1 (TEP1) (Hassa and Hottiger 2008). PARP5/Tankyrase-1 is involved in the maintenance of telomere length (Kraus and Lis 2003;Hassa and Hottiger 2008). To date, the activities and functions of the other members of PARP family have not been studied to the same extent as PARP1 and still further studies are needed to understand their exact roles.

### 1.2.1. PARP1

There are at least 17 different PARP isoforms and in this family PARP1, 116 kDa protein, has become the major focus of research due to its multi-faceted roles in many cellular activities. PARP1 contains three highly conserved structural and functional domains: an amino (N)-terminal double zinc finger DNA-binding domain (DBD) of 46 kDa, an automodification domain (AMD) of 22 kDa and a carboxy (C)-terminal catalytic domain of 54 kDa (Jagtap and Szabo 2005;Kim *et al.* 2005).

Single and double stranded DNA breaks are recognized by zinc fingers of PARP1. The DBD contains two zinc fingers and a nuclear localization signal (NLS) in the caspase cleavage site (DEVD) and acts as a DNA nick sensor. The AMD contains auto-poly(ADP-ribosyl)ation sites, which regulate PARP-DNA interactions and a BRCT motif for protein-protein interactions (Oliver 1999;D'Amours 1999;Kim *et al.* 2005). The C-terminal catalytic domain performs poly(ADP-ribose) synthesis and its binding to target protein (Oliver 1999) (Figure 4).

### 1.2.2. PARP1 and cell death

Cell death and cell division are fundamental biological processes and are required for regulation of tissue homeostasis and normal development (Zhivotovsky and Orrenius 2010). This orchestrated balance between cell death and survival is regulated by genetic and epigenetic factors (Zhivotovsky and Orrenius 2010). Dysregulation of cell

death and survival processes is involved in many human diseases such as cancer, stroke, infection, and neurodegenerative disorders (Zhivotovsky and Orrenius 2010;Fuchs and Steller 2011). Pharmacological inhibition of PARP1 activity or genetic knock-down of PARP1 protects from several pathophysiological conditions which lead to cell death such as streptozotocin-induced diabetes, traumatic spinal cord injury, cerebral ischemia (*reviewed in* (Jagtap and Szabo 2005;Hassa and Hottiger 2008)).

DNA damage by mild genomic stress activates PARP1 whereas massive DNA disruption in several diseases causes excessive PARP1 activation which leads to cell death (Hassa and Hottiger 2008;Andrabi *et al.* 2008). Excessive activation of PARP1 may lead to excessive utilization of nicotine amide adenine dinucleotide ($NAD^+$). Restoration of decreased $NAD^+$ requires two or four molecules of adenosine-5'-triphosphate (ATP). Consequently cellular ATP levels become depleted, leading to an energetic collapse, cellular dysfunction and death (Hong *et al.* 2004;Hassa *et al.* 2006). PARP is a key factor in a novel form of cell death which involves accumulation of poly(ADP-ribose) (PAR) and nuclear translocation of apoptosis inducing factor (Hong *et al.* 2004) from mitochondria. This PARP-dependent cell death mechanism is tentatively termed *PARthanatos*. In response to DNA damage, PARP1 covalently attaches oligo or poly (ADP ribose) chains on to various acceptor proteins such as histones, DNA polymerases, topoisomerases, and transcription factors or PARP1 itself by transfer of ADP-ribose units from $NAD^+$ (Tong W.M. 2001;Jagtap and Szabo 2005;Andrabi *et al.* 2008) (Figure 5).

PARthanatos is distinct from apoptosis and necrosis and has special features such as PARP1 activation, PAR accumulation, mitochondrial depolarization, early nuclear AIF translocation, cellular $NAD^+$ and ATP depletion and late caspase activity (Wang *et al.* 2011). Caspases are known as mediators of neuronal apoptosis. However PARthanatos is not prevented by caspase inhibitors which suggest that caspases do not have an executioner role for PARthanatos (Yu *et al.* 2002;Andrabi *et al.* 2008). However, the exact mechanism of PARP1 activation during cell death is not fully understood.

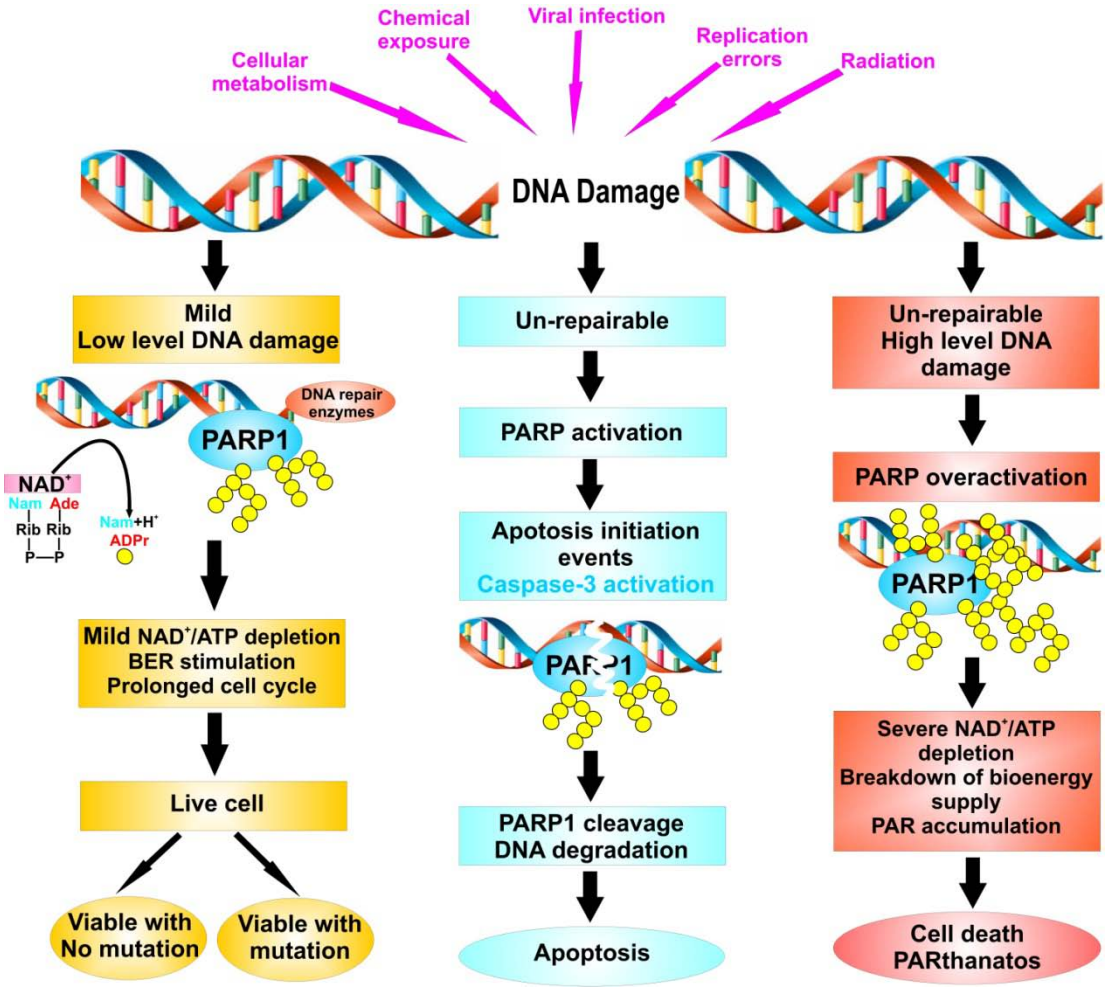


***Figure 5: Activation of PARP1 by several genotoxic stressors.*** *PARP1 activation facilitates base excision repair (BER) with moderate nicotine amide adenine dinucleotide ($NAD^+$)/ adenosine-5'-triphosphate. When cells have DNA damage, PARP1 regulates cell cycle check proteins for facilitation of DNA repair. PARP1 activation by irreparable DNA damage leads to apoptosis with PARP1 cleavage by caspase3 and DNA degradation. Severe genotoxic stress leads to large amounts of DNA damage and consequently PARP1 overactivation. This situation depletes $NAD^+$/ATP, and consequently changing energy metabolism and eventually causing cell death. Figure modified from Agarwal et al., 2009.*

### 1.2.3. Cell death by PARylation

Poly(ADP-ribosyl)ation is a post-translational modification of proteins and is regulated by the synthesizing enzyme PARP. PARP activity is found in multicellular organisms, but is absent in prokaryotes and yeast (Burkle 2005). $NAD^+$ is an essential cofactor in energy metabolism and also a substrate for synthesis of poly(ADP-ribose) (D'Amours 1999;Burkle 2005;Andrabi *et al.* 2008). PARP catalyzes the polymerisation of ADP-ribose units and adds them to acceptor proteins or itself using $NAD^+$ (Hassa and

Hottiger 2008). Poly(ADP-ribose) metabolism is involved in several biological processes such as DNA repair and maintenance of genomic stability, transcription, centromere and centrosomal function and mitotic spindle formation, structure and function of vault particles, telomere dynamics, trafficking of endosomal vesicles, and cell death (Ueda and Hayaishi 1985;Burkle 2005).

One of the explanations for the involvement of PARP in cell death is that poly(ADP-ribosyl)ation causes cellular energy depletion due to utilization of $NAD^+$. Consequently, overactivation of PARP1 may lead to cell death due to energetic collapse (Andrabi *et al.* 2008). On the other hand, it was shown that PARP1 activation may also lead to cell death independent of energy depletion (Moubarak *et al.* 2007;Andrabi *et al.* 2008). Excessive activation of PARP1 causes cell death due to a toxic level of PAR (Andrabi *et al.* 2006). Excessive production of PAR by PARP1 in response to extensive DNA damage may serve as a potential signal to nuclear AIF translocation (Kim *et al.* 2005). Yu *et al*. showed an increase of PAR polymers to induce release and translocation of mitochondrial AIF, consequently PAR polymers may act as AIF-releasing factor. Furthermore, they showed that a reduced level of AIF protects cells from PAR polymer cytotoxicity (Yu *et al.* 2006). PARP1-dependent AIF release is prevented by degradation of PAR polymers by PARG (Yu *et al.* 2006;Wang *et al.* 2009). On the other hand, which type of PAR polymers exactly cause AIF release is not known (Wang *et al.* 2009).

Poly(ADP-ribosyl)ation is regulated by the synthesizing enzyme PARP1 and the degrading enzyme poly(ADP-ribose) glycohydrolase (PARG) in a coordinated fashion for proper cellular response to DNA damage and maintenance of genomic stability (Davidovic *et al.* 2001). Degradation of PAR is catalyzed by endoglycosidic or exoglycosidic activity of PARG (Davidovic *et al.* 2001;Andrabi *et al.* 2008). PARG activity was first demonstrated by Miwa and Sigumura in 1971 (Miwa and Sugimura 1971). In mammalian systems there are four PARG isoforms: PARG110/111 is a nuclear isoform with low abundance, PARG 102 and PARG 99 are cytoplasmic isoforms and detected mostly in humans, and PARG 59/60 is exclusively cytoplasmic and mostly detected in mice (Meyer-Ficca *et al.* 2004;Hassa *et al.* 2006) (Figure 6).

Protein free PAR polymers are generated by endoglycosidic activity of PARG (D`Amours 1999). Even in low levels, endoglycosidic activity is effective in preventing hyper-modification of nuclear proteins with very long chains of PAR. This endoglycosidic activity of PARG also serves to maintain PARP1 activity by removing

PAR polymers from the PARP1 automodification domain (Zahradka 1982; D`Amours 1999) (Figure 7).

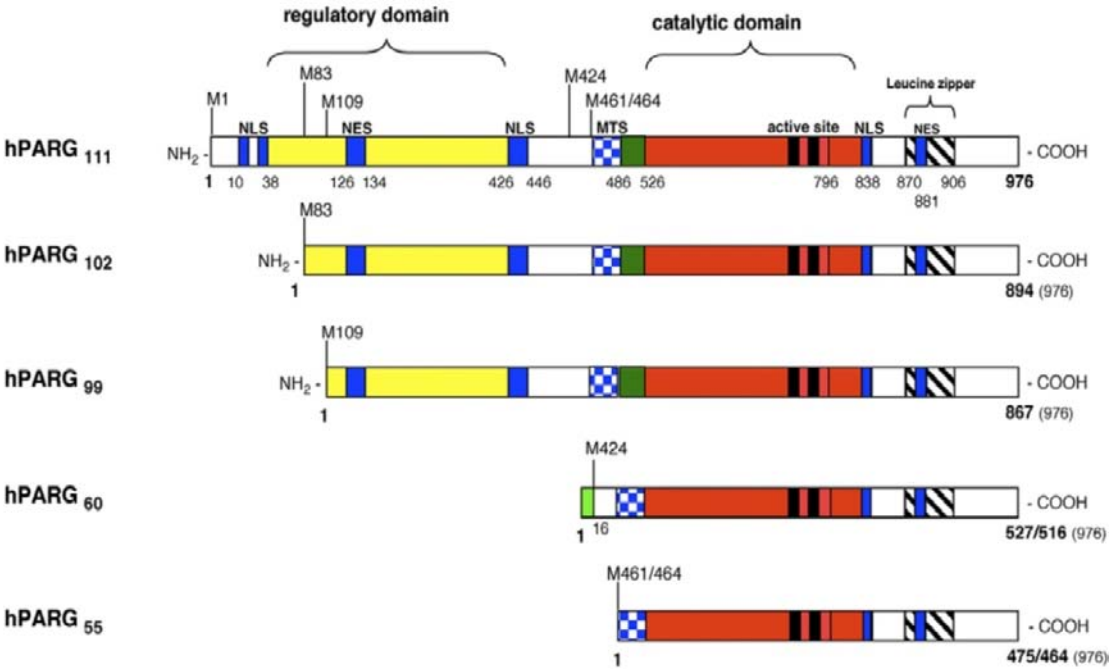


***Figure 6: Domain structure of the four human PARG isoforms.*** *Poly(ADP-ribose) glycohydrolase (PARG) is involved in the catabolism of poly(ADP-ribose) to produce free or branched ADP-ribose in the cell. NES: nuclear export signals; MTS: mitochondrial targeting sequence; Active sites: E728, E738, E756, E757 and T995. NLS: nuclear localization signals (aa 10-16, aa32-38, aa421-446, aa838-844). Figure adapted from (Hassa and Hottiger 2008).*

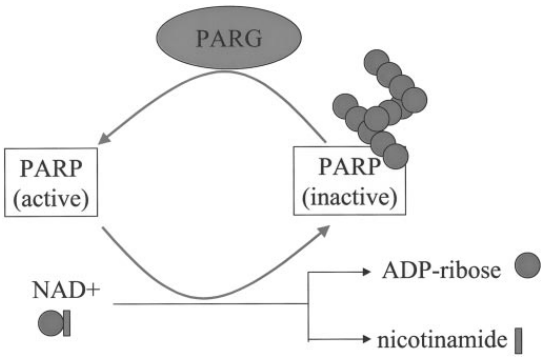


***Figure 7: Reactivaction of PARP by PARG****. Auto-ADP-ribosylation of PARP is the best characterized mechanism for PARP inhibition. PARG removes poly-ADP-ribose polymers from PARP, thereby contributing to PARP activation. It is also known that nicotinamide, a product of $NAD^+$ cleavage, exerts inhibitory effect on PARP. Poly(ADP-ribose) polymerase (PARP), poly(ADP-ribose) glycohydrolase (PARG), adenine dinucleotide ($NAD^+$). Figure adapted from (Virag and Szabo 2002).*

## 1.3. Knock-out mice for PARP

Until 1995, many studies to demonstrate the function of PARP in many biological processes were performed by inhibition of poly (ADP-ribosyl)ation with employing $NAD^+$ analogs (Wang 1995). But inhibition of PARP with these substances may affect the cellular metabolism (Willmore and Durkacz 1993) or may interact with unrelated PARP family members, possibly consequently influencing the results obtained from those studies (Wang 1995). On the other hand, some studies have been made to circumvent the side effects by expression of PARP in mutant cell lines, but this was tedious and time-consuming effort (Shall and de Murcia 2000).

In 1995, Wang *et al.* generated mice with a disrupted PARP1 gene using homologous recombination in embryonic stem (ES) cells (Wang 1995). These mice lacking PARP1 showed normal fetal and postnatal development and were fertile. But on the other hand, PARP1 knock-out (KO) mice exhibit hypersensitivity to DNA damage induced by gamma radiation and alkylating agents (Shall and de Murcia 2000). Furthermore, aged PARP1 KO mice are susceptible to epidermal hyperplasia and obesity in a mixed genetic background (Wang *et al.* 1997). PARP1 KO mice which were used for this PhD project were kindly provided by Prof. Zhao-Qi Wang, Leibniz Institute for Age Research indirectly via Prof. Hubert Löwenheim, Tübingen University.

***Figure 8:*** *Adult PARP1 KO mouse which was generated from embryonic stem cells with a disrupted PARP1 gene by Prof. Zhao-Qi Wang. Although PARP1 KO mice display normal fetal and postnatal development, they are susceptible to environmental stresses such as gamma radiation and alkylating agents.*

Mouse fibroblasts derived from PARP1 KO mice can synthesize PAR after DNA damage (Shieh *et al.* 1998) suggesting the presence of other PARP family members in mammals which are capable of synthesizing (ADP-ribose) polymerase. Indeed, we

obtained similar results when PARP1 KO retina was treated with zaprinast to induce cGMP and PARP dependent cell death. While PARP activity and PARylation was strongly reduced in PARP1 KO retina, it was not completely abolished **(Paper 3, *Results*, page 3, figure 3E)**.

# 2. Aims of study

Up until now no cure or reliable treatments have been discovered for Retinitis Pigmentosa. Studies on the *rd1* mouse model for RP showed an important causative role of PARP activity in inherited retinal degeneration. However, there is no information about which PARP family member is (predominantly) involved in *rd1* retinal degeneration. Therefore, the principal purpose of this thesis was to investigate the role of PARP1, among the PARP family, in inherited retinal degeneration.
Hence the aims of thesis work are:

## 2.1. Study retinal degeneration in PARP1 KO retina

Previously, PARP overactivation was found to be involved in retinal degeneration in the *rd1* mouse while PJ34 - an inhibitor of PARP - was shown to decrease retinal degeneration (Paquet-Durand *et al.* 2007b). PJ34 is a potent PARP inhibitor, but it does not specifically inhibit a particular PARP isoform. Therefore, the first aim of this study was to mimic the *rd1* situation in PARP1 KO retina and genetically matched wild-type (*wt*) to understand the role of PARP1, in pharmacologically induced retinal degeneration caused by PDE6 inhibition.

To this end, we analyzed PARP1 KO retina *in vivo* using OCT, SLO and ERG **(Paper I, *Results*, page 5893, figure 5)** and *ex vivo* histological techniques **(Paper III, *Results*, page 3,5 figure 1,2)** to see whether PARP1 KO retina shows signs of degeneration and whether or not PARP1 KO retinal function and retinal thickness are normal **(Paper III, *Results*, page 5, figure 2)**. Zaprinast, an inhibitor of PDE6 was used to inhibit PDE6 in PARP1 KO and *wt* retina culture **(Paper III, *Results*, page 6, figure 3)**.

## 2.2. Establish cell death markers in PARP1 KO

The cell death mechanisms which lead to photoreceptor degeneration in RP retina have been mainly unknown to date (Sancho-Pelluz *et al.* 2008). Studies with *rd1* mice showed that there are several markers causatively related to cell death such as increased cGMP accumulation, excessive activation of calpain (Paquet-Durand *et al.* 2007a), HDAC activity **(Paper 2, *Results*, page 3, figure 3)**, PARP activity, and PAR accumulation (Paquet-Durand *et al.* 2007b). The second aim was to analyze cell death markers by mimicking the *rd1* situation in PARP1 KO and *wt* retina. cGMP level, calpain activity, HDAC activity, PARP activity, PAR accumulation, and caspase 3 were

analyzed with *in vivo* and *in vitro* on zaprinast treated retina **(Paper III, *Results*, page 2, figure 2-3)**.

## 2.3. Define the sequence of degenerative processes

Although some cell death markers and their putative role were established in *rd1* retina (Paquet-Durand *et al.* 2007b;Sancho-Pelluz *et al.* 2008), the links between these and others as of yet unidentified markers, is not clear. The third aim, therefore, was to define differences in the degenerative processes in photoreceptors lacking PARP1 gene activity in an *rd1*-like situation.

## 2.4. Identify opportunities for treatment of RP

The definition of cell death pathways in the *rd1* retina is important for the identification of the novel therapeutic targets for inherited retinal degenerations. Therefore, we investigated the role of PARP1 in photoreceptor degeneration in *rd1* retina to see whether PARP1 or PARP1-related proteins were possible targets for the treatment of RP. Our findings suggested that PARP1 inhibitors providing a new potential therapeutic may delay or a stop the progression of photoreceptor degeneration for RP patients in the future.

# 3. Results

## 3.1. Investigation of retinal degeneration in *rd1* retina by optical coherence tomography (OCT) *(Summary of Paper I)*

### 3.1.1 Background

Optical coherence tomography (OCT) techniques provide three-dimensional slice images of morphological structures with a resolution close to the cellular level. OCT is also a cheap, safe and useful tool to generate cross-sectional images of tissue microstructure and characterization of disease *in vivo* (Fercher 2003;Gambichler *et al.* 2007). Therefore, OCT techniques have become an important diagnostic tool in clinical ophthalmology and other medical applications (Fercher 2003). While the quality of first and second generation time domain OCT was relatively poor, the latest commercially available spectral domain (SD) OCT devices provide better depth resolution and scanning speed sufficient for analyzing the eyes of even small animals (Kim *et al.* 2008). SD-OCT analysis is an extensively studied non-invasive method to observe changes of retinal function and structure (Chang *et al.* 2002). OCT analysis allows longitudinal studies and observations of retinal diseases with or without treatment, leading to a reduction in the number of animals needed. The technique also reduces some of the disadvantages of histological analysis such as undetected or masked structures by handling procedure (Fischer *et al.* 2009). Our study provided *in vivo* cross-sectional visualization of retinal structure in *wild-type* and mouse models for retinal degenerations including the *rd1* model which was used for this PhD project.

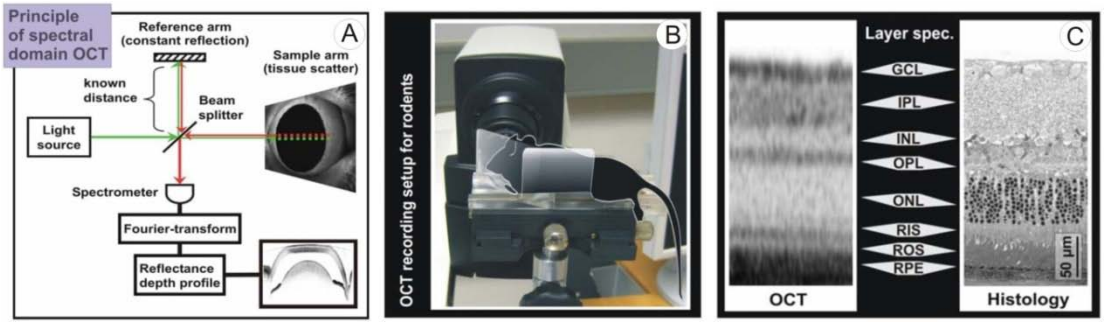


***Figure 9: Principle of optical coherence tomography (OCT). A)*** *Schematic diagram of spectral-domain (SD) OCT.* ***B)*** *OCT recording set up for imaging mice retina.* ***C)*** *Comparison of OCT and histological structure of retina. Figure adapted from (Fischer et al. 2009). GCL: Ganglion Cell Layer**,** IPL: Outer plexiform layer, INL: Inner Nuclear Layer, OPL: Outer Plexiform Layer, ONL: Outer Nuclear Layer, RIS: Rod Outer Segment, ROS: Rod Inner Segment, RPE: Retinal Pigment Epithelium.*

### 3.1.2. Summary of the results of Paper I

**Photoreceptor degeneration in *rd1* retina can be detected *in vivo* by SD-OCT, comparison with PARP1 KO and *wt* retina (Paper I, *Results*, page 5892, figure 5).** SD-OCT and SLO analysis of *rd1* mice was performed to monitor the progressive anatomical changes in the retinas of *rd1* mice and detect the thinning of retinal layer caused by the degeneration. Thickness of inner and outer retina was evaluated by SD-OCT, cSLO and compared with the histological results. Because mice open their eyes only between PN12-13, detection of photoreceptor degeneration with *en face* imaging SD-OCT and cSLO was not possible for *rd1* at PN11. Histological results of *rd1* at PN11 confirmed the results of SD-OCT and cSLO.

At PN28, SD-OCT and cSLO analysis showed that in *rd1* mice the size of the outer nuclear layer was significantly reduced. Histological analysis of *rd1* mice at PN28 confirmed the results of SD-OCT and cSLO. Analysis of *rd1* mice at PN28 revealed intact retinal structure of inner nuclear layer, however the INL was very close to the RPE due to photoreceptor degeneration. Outer plexiform layer, outer nuclear layer and photoreceptor segments were not distinguished in the *rd1* retinal structure at PN28. The thickness of the central retina in *rd1* mice at PN11 was 246 ± 2 μm, whereas at PN28 it was markedly reduced to 145 ± 5 μm. SD-OCT, cSLO and histological analysis of wild-type retina at PN28 showed all retinal layers without any signs of retinal degeneration.

### 3.1.3. Contributions to paper I: *"Spectral domain optical coherence tomography in mouse models of retinal degeneration"*

For this paper, I performed and evaluated a comparative histological analysis of *wt* and *rd1* retina. To this end, the eyes were embedded in cryomatrix, frozen, and sectioned in a Microtome. I performed the majority of this sectioning with some help from a technical assistant. For visualization of retinal structure, hematoxylin/eosin staining was used. Pictures were taken by Imager Z1 Apotome-Zeiss and images were captured using corresponding software. I assisted Dr. Gesine Huber when performing the *in vivo* OCT and SLO analysis. I read and revised the manuscript.

## 3.2. Investigation of interplay between HDAC and PARP1 (*Summary of Paper II*)

### 3.2.1. Background

Epigenetic mechanisms such as protein acetylation by histone acetyltransferases (HATs) and deacetylation by histone deacetylases are involved in transcription and DNA repair mechanisms (Kruszewski and Szumiel 2005). The HDAC family includes three main classes; HDAC I, II and III. Class I and class II comprise HDAC1-3, HDAC8 and HDAC 4-7, HDAC9, HDAC10, respectively, and are inhibited by trichostatin (TSA). The third class of HDAC is called Sirtuins (Sirt 1-7). The chromatin structure is condensed when transcription is inactivated and decondensed, opened when there is active gene transcription, replication, or repair. Post translational modifications of histones are essential factors for changes in the chromatin structure (Kruszewski and Szumiel 2005).

Although few publications have addressed the role of PARP activity in retinal degeneration, it was previously shown that overactivation of PARP is an important factor to the contribution of *rd1* photoreceptor degeneration (Paquet-Durand *et al.* 2007b). After this observation, we showed that HDAC activity was also involved in photoreceptor degeneration in the *rd1* mouse. The following publication addressed the role of HDACs in retinal degeneration and the relationship between PARP and HDAC activity in photoreceptor degeneration in *rd1* mouse.

### 3.2.2. Summary of the results of Paper II

**HDAC activity and acetylation are involved in photoreceptor retinal degeneration in the *rd1* retina (Paper II, *Results*, page 2-3, figure 2-3).** We investigated and compared the acetylation patterns of *rd1* and *wt* photoreceptors and showed that there was a decreased acetylation level in the *rd1* situation. Consequently, we investigated the relationship between decreased *rd1* acetylation and increased HDAC activity. The results suggested that excessive HDAC activation, most likely stemming from HDACI/II was the cause of hypoacetylation in *rd1* photoreceptors.

**HDAC I/II inhibitor protects *rd1* photoreceptors (Paper II, *Results*, page 5, figure 5).** To test whether HDAC I/II inhibitors could prevent photoreceptor degeneration in

*rd1* retina, organotypic retinal explants cultures were treated with the HDAC I/II inhibitor TSA. TSA treatment showed decreased numbers of TUNEL positive cells in a short-term treatment paradigm, which translated into a strong pro-survival effect in long-term treatment on *rd1* retinal cultures.

**HDAC activity regulates PARP activity during photoreceptor cell death (Paper II, *Results*, page 6, figure 6).** The next question concerned the potential interaction between activity of HDAC and PARP. Here, we performed double label immunohistochemistry for acetylated lysines and PAR, the product of PARP activity. Co-localization images revealed that only non-acetylated photoreceptor nuclei were positive for PAR. In addition TSA treatment decreased PAR accumulation in ONL. These results suggested that there was an interaction between deacetylation and poly(ADP-ribosyl)ation, in other words, HDAC activity and PARP activity. Somehow deacetylation affected PARP activity and consequently PAR accumulation. Therefore it was concluded that PARP activation occurred downstream of HDAC I/II. Since most PARP activity stems from activation of the PARP1 isoform specifically, our future investigations focused on this isoform.

### 3.2.3. Contributions to **paper II: "*Excessive HDAC activation critical for neurodegeneration in the rd1 mouse*"**

I performed analysis of western blot (together with Javier Sancho Pelluz) and quantified the *in vivo* HDAC activity in *wt and rd1* retinae. I read and revised the manuscript.

## 3.3. PARP1 KO increases resistance to retinal degeneration (*Summary of Paper III*)

### 3.3.1. Background

Previously, excessive activation of enzymes belonging to the poly-ADP-ribose polymerase (PARP) group was shown to be involved in photoreceptor cell death in the human homologous *rd1* mouse model for RP (Paquet-Durand *et al.* 2007b). Since there are at least 17 different PARP isoforms, we investigated the exact relevance of the predominant isoform - PARP1 - for photoreceptor cell death and survival, using PARP1 KO mice.

### 3.3.2. Summary of the results of Paper III

*In vivo* and *ex vivo* retinal morphology was analysed using optic OCT and conventional histology. There were no major alterations of retinal phenotype between PARP1 KO and *wt*. ERG results showed that retinal function of PARP1 KO was normal. Retinal explant cultures derived from *wt* and PARP1 KO animals were treated with zaprinast, a selective inhibitor of PDE6 to emulate an *rd1*-like situation on non-*rd1* genotypes. PDE6 inhibition caused massive photoreceptor degeneration in *wt* retina, in contrast, PARP1 KO retina showed relatively little degeneration after inhibition of PDE6. These results demonstrated that under pathological conditions PARP1 activity is important for photoreceptor degeneration.

**PARP1 KO retina has normal retinal function and normal morphology and layering (Paper III, *Results*, page 2, figure 1).** SD-OCT was performed in *wt* and PARP1 KO mice retina and compared with *rd1* mice retina, to see whether PARP1 KO showed signs of retinal degeneration *in vivo*. Comparison of SD-OCT and histological data showed normal retinal morphology and layering together with a slightly thinner ONL in PARP1 KO. Retinal function analysis using ERG suggested normal photoreceptor signaling in PARP1 KO rods and cones, since neither scotopic nor photopic measurements revealed any signs of impaired retinal function.

**No PARP1 protein expression in PARP1 KO mice (Paper III, *Results*, page 2, figure 1).** The deficiency in protein expression in PARP1 KO was confirmed by western blot analysis, which showed that the characteristic 116 kDa PARP1 band was missing in KO tissue.

**Cell death markers in *wt*, *rd1* and PARP1 KO retinae (Paper III, *Results*, page 2, figure 2).** Cell death markers which were found to relate to photoreceptor cell death in *rd1* retina were analyzed on *in vivo wt* and PARP1 KO retina. Many positive cells were observed in *rd1* retina due to PDE6 dysfunction while *wt* retina showed very few and rarely PARP1 KO positive cells. There were no significant differences between *in vivo* PARP1 KO and *wt* but a significant difference between PARP1 KO and *rd1.*

The analysis of *in situ* PARP activity showed few positive cells in the *wt* retina, large numbers of positive cells in *rd1* ONL and no PARP activity positive cells for PARP1 KO retina. PAR accumulation, an indirect evidence for PARP activity, was studied using immunohistochemistry and identified few positive cells in *wt* retina and in PARP1 KO retina. Western blot confirmed the immunohistochemical results showing

a strong accumulation of high molecular weight PARylated proteins only in *rd1* retinal tissue samples.

To detect degenerating cells in PARP1 KO retina, TUNEL assay was performed for *wt*, *rd1* and PARP1 KO. Retina from *wt* mice showed very few dying cells, much higher numbers were detected for *rd1* situation and PARP1 KO also showed very few positive cells like *wt*. The histological data indicated that there was no major degeneration phenotype in the ONL of the PARP1 KO, which therefore, in all aspects studied here, appeared to behave like *wt*.

**PARP1 KO reduces photoreceptor cell death induced by PDE6 inhibition (Paper III, *Results*, page 2, figure 3).** Zaprinast is a selective PDE5/6 inhibitor (Morin *et al.* 2001;Zhang *et al.* 2005) which consequently increases intracellular cGMP level and causes photoreceptor degeneration. 100 µM zaprinast was used to mimic the *rd1* situation in *wt* and PARP1 KO retina. Organotypic retinal explants with *wt* and PARP1 KO retina were cultured during postnatal days 5-11. PDE6 inhibition was confirmed by an increased cGMP immunofluorescence. While untreated *wt* ONL is essentially devoid of cGMP immunoreactivity, zaprinast treated *wt* ONL showed large numbers of cGMP positive cells comparable to *rd1* situation. Untreated PARP1 KO showed very low numbers of cGMP positive cells while strong increases were found in zaprinast treated PARP1 KO retina. The zaprinast induced increase in cGMP positivity was significantly lower in PARP1 KO when compared to *wt*. However, in relative terms the zaprinast induced elevation in cGMP was more pronounced in PARP1 KO than in *wt*.

Accumulation of PAR is another, independent marker for PARP activity, PAR immunohistochemistry showed few positive cells for untreated *wt* and larger number of cells for zaprinast treated *wt* retina and in the *rd1* situation. Very few PAR positive cells were observed in either untreated PARP1 KO or zaprinast treated PARP1 KO retina.

TUNEL staining for dying cells identified very few positive cells for untreated *wt* while zaprinast treated *wt* showed large number of positive cells comparable to untreated *rd1* retina. Untreated PARP1 KO displayed very low numbers of TUNEL positive cells similar to untreated *wt*. Importantly, very low numbers of positive cells were observed for zaprinas treated PARP1 KO retina. In relative terms, zaprinast treatment resulted in a 200% elevation of cell death in *wt* retina, compared to only a 17% increase in PARP1 KO.

These results suggested that the photoreceptor cell death that follows upon PDE6 inhibition and subsequent accumulation of cGMP is, to a major extent, dependent on PARP1 activity, since PARP1 KO displayed strong resistance to this paradigm of induced photoreceptor degeneration.

### 3.3.3. Contributions to paper III: "*PARP1 gene knock-out increases resistance to retinal degeneration without affecting retinal function*"

I performed the culturing of *wt*, PARP1 KO and *rd1* retinae and treatment with zaprinast to inhibit PDE6. I also performed embedding of cultures and eyes, freezing, most of the sectioning, and staining, western blotting (all steps). I took pictures using Zeiss Imager Z1 Apotome Microscope. Images were captured using corresponding Zeiss Axiovision software. I evaluated the immunohistochemical and WB data for *in vivo* and *in vitro* experiments. I prepared the figures and wrote a first draft of the manuscript and revised the final manuscript. I also prepared the second revision of the manuscript after initial peer review at the journal PLoS One.

## 3.4. Additional observations

### 3.4.1. Calpain and HDAC activity in PARP1 KO retina

In addition, several other cell death markers, which were not included in paper III, were also studied on *in vivo wt, rd1* and PARP1 KO retinae. This involved an analysis of calpain and HDAC activity.

Immunohistochemical results confirmed the previous result for calpain and HDAC activity at PN11 (Paquet-Durand *et al.* 2006;Sancho-Pelluz *et al.* 2010). Calpain activity for *wt* was 0.2 % (± 0.0 SEM, n=3), considerably lower than the high levels observed in the *rd1* situation 3.4 % (± 0.3 SEM, n=3). PARP1 KO 0.02 % (± 0.0 SEM, n=3) showed calpain activity levels comparable to *wt*. There were statistically significant differences between *in vivo* PARP1 KO and *rd1* ($p<0.01$), but no differences between *in vivo* PARP1 KO and *wt*.

In *wt* retina, HDAC activity assay showed few positive cells while high numbers of cells were detected in the *rd1* situation (1.3% ± 0.05 SEM, n=3) and PARP1 KO showed very few positive cells (0.01 % ± 0.0 SEM, n=3). There were significant differences between *in vivo* PARP1 KO and *rd1* ($p<0.01$) and no differences between

PARP1 KO and *wt*. These results suggested that calpain and HDAC activity in the PARP1 KO ONL at PN11 were within the normal, *wt* range.

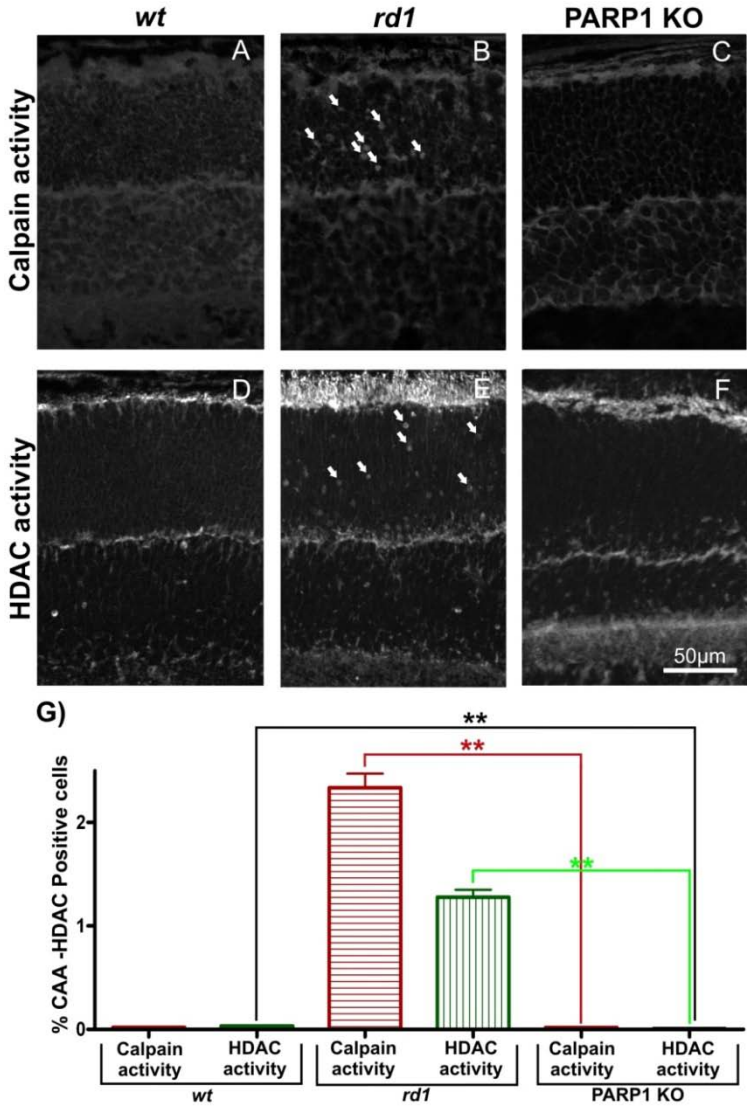


***Figure 10: Calpain and HDAC activity in wt, rd1 and PARP1 KO retina.*** *The in situ calpain activity assay (**A-C**) and HDAC activity assay (**D-F**). The bar graphs display the quantification of the percentages of ONL cells positive for calpain and HDAC activity (**G**). Retinae from n=3-6 animals were used for each analysis and genotype. Error bars represent SEM. Statistical analysis for calpain and HDAC activity showed that there were significant differences between PARP1 KO and rd1. In addition, there was a significant difference between PARP1 KO and wt for HDAC activity.*

# 4. Discussion

Animal studies on PARP using either pharmacologically inhibition or genetic deletion of PARP1 indicate that PARP has a considerable role in neurodegenerative diseases such as stroke and neurotrauma (Komjati et al. 2005). In terms of neurodegenerative eye diseases excessive PARP activation was causally connected to photoreceptor cell death (Paquet-Durand et al. 2007b). However, at the beginning of this study it was not clear which PARP family member was most important for the photoreceptor degeneration. In this thesis, we showed that morphology and function of PARP1 KO retina was normal. There was an interplay between PARP activity and HDAC activity in photoreceptor degeneration. PARP activity during cGMP-induced photoreceptor neurodegeneration is caused to a major extent by the PARP1 isoform specifically. While wt photoreceptors were highly susceptible to a stress paradigm mimicking the rd1 type of inherited retinal degeneration, PARP1 KO photoreceptors were resistant to such stress.

## 4.1. Morphology and function of PARP1 KO and *rd1* retina

Although PARP1 KO mice are healthy and fertile, they show hypersensitivity to DNA damage induced by gamma radiation and alkylating agents (Wang *et al.* 1997). Before our study, there has been no specific information about retinal morphology and function in PARP1 KO animals. Therefore, we analyzed *in vivo* PARP1 KO, *wt* and *rd1* retinal morphology and function, before mimicking *rd1* photoreceptor degeneration. Our findings showed that PARP1 KO retina has normal retinal morphology and function and consequently that lack of PARP1 expression did not affect retinal development and function.

## 4.2. Modulation of PARP activity by HDAC activity

Histone deacetylases (HDACs) modify chromatin conformation. They remove acetyl groups which were added by histone acetyltransferases (HATs). Thus, chromatin is formed into a compact structure to prevent transcription (Kruszewski and Szumiel 2005). Among HDACs, type III histone deacetylases (HDACIII, sirtuins) catalyze the cleavage of $NAD^+$ and protein deacetylation and their activity is inhibited by nicotinamide (Kruszewski and Szumiel 2005).

Kruszewski and Szumiel proposed that PARP is activated at the sites of DNA breaks. Utilization of $NAD^+$ by PARP leads to increase of nicotinamide concentration at the

damaged site of DNA. Thus, at these sites, sirtuins are inhibited by nicotinamide. All HDAC classes may contribute to DNA repair processes as a reason of a connection between acetylation of histones and repair of DNA breaks (Kruszewski and Szumiel 2005). Zimmerman *et al.* showed that two Histone deacetylase inhibitors (HDACi) valproic acid and AR-42, reduced proliferation of adult T-cell leukemia/lymphoma (ATL) cell lines and elicited a dose dependent increase of cytochrome C and cleaved PARP (Zimmerman *et al.* 2011). Studies with HEK 293 cells showed PARP1 activation in DNA damage was modulated by Sirtuin1 (Kolthur-Seetharam *et al.* 2006). Previously, a study with *rd1* retina indicated that PARP activity was involved in photoreceptor degeneration (Paquet-Durand *et al.* 2007b). After this observation, our result showed that HDAC activity also had a causative role in photoreceptor degeneration in *rd1* **(Paper II, *Results*, page 3, figure 3)**. Although PARP and HDAC activity were shown to be involved in photoreceptor degeneration, there has been no publication about their relationship in *rd1* retina to date. In paper II, there was no acetylation in the PAR positive photoreceptors. And treatment of *rd1* retinae by TSA, a HDACI/II inhibitor, reduced PAR positive cells in *rd1* retina suggests that HDAC activity preceded PARP activity. **(Paper II, *Results*, page 5, figure 5)**. Nevertheless, further studies are needed to understand the exact interaction between PARP and HDAC activity completely.

## 4.3. PARP activity in cellular physiology

PARP enzymes play ambiguous roles in cellular physiology. Within the PARP family, PARP1 is mostly involved in DNA repair and strongly protects cells against genotoxic stressors (Schreiber *et al.* 2006). This is notably poly(ADP-ribosyl)ation of DNA associated histones causes relaxation of the chromatin structure allowing DNA repair enzymes to access the site of the strand break, thereby facilitating the DNA repair process (Herceg and Wang 2001;Rouleau *et al.* 2010). On the other hand, an excessive PARP activation may overstrain the cellular metabolism, leading to an energetic collapse and eventually cell death (Sims *et al.* 1983;Du *et al.* 2003). In this respect, excessive consumption of the PARP substrate $NAD^+$ seems to be of particular importance, since this will indirectly result in depletion of cellular ATP (Du *et al.* 2003;Rouleau *et al.* 2010).

PARP synthesizes poly-ADP-ribose which is a homopolymer of ADP-ribose units linked by glycosidic bonds. On the other hand, poly-ADP-ribose glycohydrolase (PARG) hydrolyzes the glycosidic bonds between the ADP-ribose units (Hassa *et al.*

2006). PAR accumulation caused by excessive PARP activity leads to cleavage of apoptosis inducing factor (AIF) (Yu *et al.* 2002;Hong *et al.* 2004) by calpain proteases (Moubarak *et al.* 2007) and translocation of AIF from the nucleus to the mitochondria. Translocation of cleaved AIF to the nucleus triggers widespread DNA fragmentation and cell death (Susin *et al.* 1999;Yu *et al.* 2002). On the other hand, PAR degradation by PARG activation reduces PARP1-dependent AIF release (Yu *et al.* 2002). Alternatively, free ADP-ribose may activate transient-receptor-potential (TRP) ion channels, inducing excessive $Ca^{2+}$ influx (Kraft *et al.* 2004;Buelow *et al.* 2008) something that could potentially cause photoreceptor cell death (Paquet-Durand *et al.* 2006).

Although PARP1 KO mice develop normally and show no particular phenotype, these animals are susceptible to developing epidermal hyperplasia and obesity at older ages (Wang 1995) and cells lacking PARP1 are susceptible to genotoxic stress (Trucco 1998). Interestingly, PARP1 KO animals display increased resistance to streptozotocin induced cell death of pancreatic beta cells (Masutani *et al.* 1999;Virag and Szabo 2002), ischemic brain injury (Endres *et al.* 1997), and ocular deprivation induced cell death in the lateral geniculate nucleus (Nucci *et al.* 2000). Pharmacological inhibition of PARP1 activity or knock-out of the PARP1 gene showed that PARP1 has a central role in a novel form of caspase-independent cell death. This new cell death mechanism has as a central element PARP overactivation and is consequently termed PARthanatos. This unique form of cell death caused by PARP1 over-activation is mostly mediated via accumulation of PAR, translocation of AIF protein from mitochondria to the nucleus, chromatin condensation and DNA fragmentation (Andrabi *et al.* 2008).

## 4.4. PARP and cGMP

Cyclic guanosine monophosphate cGMP is a common second messenger derived from guanosine triphosphate (GTP) and regulates many cell functions. Immunohistochemical comparisions with *wt* and *rd1* retina showed an elevated cGMP levels in *rd1* photoreceptors which lack a functional beta subunit of cGMP phosphodiesterase (PDE) activity (Lem *et al.* 1992). After this observation, increased PARP activity was also shown in *rd1* photoreceptors (Paquet-Durand *et al.* 2007b). So far, there has been no information about the relationship between cGMP and PARP activity in *rd1* photoreceptor degeneration. ADP-ribosylation is involved in post-translational modification of proteins. GTP-binding proteins in cell membrane are one

of the acceptors of ADP-ribose (Cohen-Armon *et al.* 1996). Cohen-Armon *et al.* showed a depolarization-induced ADP-ribosylation of cysteine residues of GTP-binding proteins in the nuclei of cells in rat brain stem and cortex (Cohen-Armon *et al.* 1996).

The heterodimeric GTP-binding proteins are involved in transmitting chemical signals outside the cell, consequently leading to changes inside the cell. They regulate metabolic enzymes, ion channels, transporters, and other parts of the cell machinery (Neves *et al.* 2002). It was shown that PARP catalyzes ADP-ribosylation of arginine residues in GTP-binding proteins (Abood *et al.* 1982) and there was an endogenous ADP-ribosylation of cysteine residues of GTP-binding proteins (Abood *et al.* 1982;Neves *et al.* 2002) in cell membranes (Cohen-Armon *et al.* 1996). On the other hand, Bornancin showed that ADP-ribosylation of Cholera toxin (CTx) and Pertussis toxin (PTx) lead to functional modifications of transducin (Bornancin *et al.* 1992). Transducin is a G protein and expressed in rod and cone photoreceptors and involved in phototransduction in vertebrate retina (Lerea *et al.* 1986). In response to photoexcitation of rhodopsin, transducin mediates activation of cGMP phosphodiesterase (Medynski 1985). ADP ribosylated transducin by Pertussis toxin blocks the light stimulated hydrolysis of GTP and cGMP (Van *et al.* 1984). These studies suggest that ADP-ribosylation may have important roles in the phototransduction cascade and a potential connection between ADP-ribosylation of GTP-binding proteins and cGMP levels in photoreceptors. PARP1 may have a role for ADP-ribosylation of GTP-binding proteins and consequently contributing to the depolarization of photoreceptor cells and thus to accumulation of cGMP. These studies may be one explanation of our findings about the relationship between PARP1 and cGMP **(Paper 3, *Results*, page 2, figure 3)**. In photoreceptors, lack of PARP1 may result in less cGMP accumulation due to lack of ADP-ribosylation in G protein or, the other way around, excessive PARP1 activation contributing to cell death by cGMP accumulation due to excessive ADP-ribosylation of G protein, together with changing energy metabolism and PAR toxicity. On the other hand, cGMP accumulation in PDE6 inhibited PARP1 KO retina may be due to ADP-ribosylation of G protein by PARP2 together with PAR accumulation **(Paper 3, *Results*, page 2, figure 3)**. Together with all these results, further experiments are needed to understand the exact relationship between PARP1 and cGMP.

## 4.5. PARP and photoreceptor cell death mechanisms

Photoreceptor cell death in the *rd1* mouse was found to be associated with nuclear translocation of AIF and oxidative DNA damage, factors which both colocalized with PARP activity in photoreceptor nuclei (Paquet-Durand *et al.* 2007b). Recently, excessive PARP activity was also shown to be correlated to oxidative DNA damage and causally involved in photoreceptor cell death in P23H and S334ter rats (Kaur *et al.* 2011).

Our finding that PARP1 KO photoreceptors are highly resistant to PDE6 inhibition induced degeneration (**paper 3**), is in line with previous results (Paquet-Durand *et al.* 2007b) and points to the PARP1 isoform as a major contributor to PARP dependent photoreceptor cell death. However, while PARP1 KO dramatically reduced the accumulation of PAR in all situations tested, PAR accumulation was not abolished altogether. One explanation might be that other PARP isoforms such as PARP2 (Ame 1999;Shieh *et al.* 1998;Schreiber *et al.* 2002) may, to a more limited extent, compensate for the lack of PARP1 expression.

As a consequence of excessive PARP1 activity, PARylation of nuclear or other related proteins and energy depletion may cause photoreceptor cell death in *rd1* retinal degeneration. On the other hand, it is also important to know potential regulators of PARP1 during photoreceptor cell death. Kauppinen *et al.* showed a drastic reduction of PARP1 enzymatic activity by dephosphorylation of the human recombinant PARP1 with calf intestinal alkaline phosphatase (CIAP) (Kauppinen *et al.* 2006). This suggests that PARP1 catalytic activity depends on phophorylation by kinases. The molecular structure of PARP1 allows for a higher phosphorylation potential in the N-terminal zinc finger domains including the region which is centered around the BRCT domain (Isabelle *et al.* 2010). It was shown that PARP1 may be regulated by phosphorylation and this was related to the activities of several kinases such as protein kinase C (PKC) (Hegedus *et al.* 2008), IGF-I (Beckert *et al.* 2006), c-Jun-N-terminal kinase 1(JNK1) (Zhang *et al.* 2007;Bogoyevitch and Arthur 2008), extracellular signal-regulated kinase (ERK1/2) (Kauppinen *et al.* 2006;Cohen-Armon 2007;Gagne *et al.* 2008) calcium/calmodulin-activated protein kinase II (CaMK-II), casein kinase 2 (CKII), aprataxin- and PNK-like factor (APFL), cyclin-dependent kinase 5 (CDK5), integrin-linked kinase (ILK), and AMP-activated protein kinase (AMP-K) (Gagne *et al.* 2008). Midorikawa *et al.* showed that CaMK-II mediated membrane depolarization and calcium signaling induces dissociation of kinesin

superfamily protein 4 (KIF4) from PARP1 in juvenile neurons (Midorikawa *et al.* 2006). Under physiological conditions, PARP1 repairs DNA damage, serving as a transcriptional regulator and consequently maintaining cell homeostasis. Tight regulation of PARP activity thus is beneficial for neuronal survival. Midorikawa *et al*. suggested that KIF4 binds directly to PARP1 and regulates it to consequently control PARP activity dependent survival of postmitotic neurons in brain. While the activity of most of the mentioned kinases has not been studied in the context of retinal degeneration, increased activation of CaMK-II was found in *rd1* retinal degeneration and could thus relate to downstream of PARP activation (Hauck *et al.* 2006). In addition, the up-regulation and increased phosphorylation of PKC (Azadi *et al.* 2006) and increased activation of cGMP-dependent-protein kinase or protein kinase G (PKG) (Paquet-Durand *et al.* 2009) in the degenerating *rd1* mouse retina might also be connected to PARP activity.

Photoreceptor cell death in *rd1* mouse retina is preceeded by an elevation of intracellular cGMP and possibly $Ca^{2+}$ levels (Fox *et al.* 1999;Farber and Lolley 1974), and involves activation of PKG (protein kinase G) (Paquet-Durand *et al.* 2009), calpains (Paquet-Durand *et al.* 2006) and HDACs (histone deacetylases) (Sancho-Pelluz 2009). There are links between PARP1 and mitochondrial calpain activation (Vosler *et al.* 2009), PARP1 and HDACs (Sancho-Pelluz 2010). Calpain activation and N-terminus cleavages of AIF is necessary for AIF truncation in PARP1 dependent cell death (Vosler *et al.* 2009) and could be very similar to what is observed in photoreceptor cell death in *rd1* retina. There are limited publications about these cell death markers and links between them in the *rd1* photoreceptor degeneration. Therefore, further studies need to be done to understand the exact interplays between PARP1 and cGMP, PARP1 and PKG, PARP1 and HDAC activity, PARP1 and calpain activity.

In the past, photoreceptor cell death in *rd1* mouse has often been addressed as an apoptotic process however it is independent of critical features of apoptosis such as *de novo* protein biosynthesis, caspase activation, or cytochrome *c* release. The finding that photoreceptor degeneration induced by PDE6 inhibition was strongly reduced in PARP1 deficient animals also supports the idea that PARthanatos or a closely related mechanism is responsible for cell death in this situation.

## 4.6. Neuroprotection of photoreceptors by PARP inhibition

Inhibitors of PARP have demonstrated neuroprotective capabilities in a variety of neurodegenerative disease models (Virag and Szabo 2002). In the NMDA treated rat retina, the PARP inhibitor PJ34 decreased retinal ganglion cell damage and attenuated formation of PAR and the decline of ATP (Goebel and Winkler 2006). In experimental retinal ischemia, PARP inhibition with HO3089 preserved the normal morphological structure of the retina as well as the thickness of retinal layers compared to control (Szabadfi *et al.* 2010). In the N-methyl-N-nitrosourea (MNU) animal model photoreceptor cell death was prevented by subcutaneous injection of the PARP inhibitor nicotinamide (Uehara *et al.* 2006). PARP1 regulates the transcription factor, NF-κB (Kauppinen *et al.* 2011) which has been shown to be involved in retinal degeneration in *rd1* retina (Zeng *et al.* 2008). Similarly, in *rd1* organotypic retinal cultures, inhibition of PARP with PJ34 decreased accumulation of PAR in photoreceptors and reduced their degeneration (Paquet-Durand *et al.* 2007b). In line with the latter findings, cGMP-induced photoreceptor death was strongly reduced in PARP1 retina when compared to congenic wild-type, implying that PARP1 specifically, played a major role in photoreceptor death (**paper 3**). Thus, long term PARP1 inhibition should preserve and restore the cellular energetic pools at the expense of decreased DNA repair and hence, a possible increase in mutagenesis (Komjati *et al.* 2005).

Although there are a variety of possible approaches to treat inherited photoreceptor degeneration, such as gene therapy and cell replacement, PARP inhibition appears as a promising neuroprotective strategy that could significantly delay or even stop photoreceptor degeneration in the future. Alternatively, PARP1 gene knock-down using viral construct delivery might be another therapeutic approach.

# 5. Conclusion and future prospects

In this thesis, a retinal photoreceptor degeneration paradigm that mimics inherited neurodegeneration, as it occurs in the human homologous *rd1* mouse model, was used to show a causal involvement of PARP1 in the photoreceptor cell death. Progressive cell death in *rd1* retina was a unique caspase-independent suggesting the execution of non-apoptotic mechanisms. The precise sequence of events and the components of the photoreceptor cell death pathways are still unclear, although we could demonstrate an interaction between PARP1 and HDAC activity in this progressive cell death pathway in *rd1* retina. Our findings suggested that inhibited or a reduced PARP1 activity does not alter retinal function. In addition, PARP1 KO retina was resistance to chemically induced retinal degeneration *in vitro*. This promising finding suggests PARP1 as a novel therapeutic target in retinal degeneration both for pharmacological and genetic treatment approaches. These findings also propose an alternative cell death mechanism which has been recently described tentatively termed PARthanatos.

Although, it was clearly shown here that PARP1 is involved in photoreceptor degeneration in *rd1* mice, further experiments are needed to understand the exact mechanism of PARP1 activity in photoreceptor degeneration in the *rd1* retina.

For instance, cross breeding of *rd1* and PARP1 KO and *in vivo* treatment with PARP1 specific inhibitors in *rd1* retina could yield a number of important insights on PARP interaction partners, if this was combined with genomic and/or proteomic analysis. Furthermore, investigations into the roles of other PARP family members, such as PARP2 could be done in further experiments to understand more clearly the interplay of different PARP isoforms during *rd1* photoreceptor degeneration.

# Education and Research Experience

## Education

| | |
|---|---|
| **2001-2003** | Master student, Gazi University, Department of Biological Sciences, Ankara, Turkey |
| **2003-2006** | MSc in Biology, Harran University, Department of Biological Sciences, S. Urfa, Turkey.<br>Thesis: *The investigations of apoptosis in ischemia reperfusion induced rat retina.* |
| **since June 2008** | PhD student and Research Training Fellowship awarded by the Kerstan foundation and DFG, Institute For Ophthalmic Research, Tubingen, Germany. Focus on *"The role of PARP and PARG in photoreceptor degeneration in rd1 mouse".* |

## Research Experience

| | |
|---|---|
| **2007-2008** | Expert, Harran University, S.Urfa, Turkey |
| **2005-2006** | Research assistant at Biology Department at Harran University, S.Urfa, Turkey |

## Publications


1. Trifunović D, **Sahaboglu A**, Kaur J, Mencl S, Zrenner E, Ueffing M, Arango-Gonzalez B, Paquet-Durand F. (2012) Neuroprotective Strategies for the Treatment of Inherited Photoreceptor Degeneration. Current Molecular Medicine. 12, 598-612.

2. Kaur J, Mencl S, **Sahaboglu A**, van Veen T, Zrenner E, Ekstrom P, Paquet Durand F, Arango-Gonzalez B. (2011) Calpain and PARP Activation during Photoreceptor Cell Death in P23H and S334ter Rhodopsin Mutant Rats. PLoS ONE. PLoS One. 6 (7):e22181.

3. **Sahaboglu A**, Tanimoto N, Kaur J, Sancho-Pelluz J, Huber G, Fahl E, Arango-Gonzalez B, Zrenner E, Ekström P, Löwenheim H, Seeliger MW, Paquet-Durand F. (2010) PARP1 gene knock-out increases resistance to retinal degeneration without affecting retinal function. PLoS ONE 5(11): e15495.

4. Sancho-Pelluz J, Alavi M, **Sahaboglu A**, Kustermann S, Farinelli P, Azadi S, van Veen T, Romero FJ, Paquet-Durand F, Ekström P. (2010) Excessive HDAC activation critical for neurodegeneration in the *rd1* mouse. Cell Death & Disease, doi:10.1038/cddis.2010.4.

5. Huber G, Beck SC, Grimm C, **Sahaboglu-Tekgoz, A**, Paquet-Durand F, Wenzel A, Seeliger MW, Fischer MD. (2009) Spectral domain optical coherence tomography in mouse models of retinal degeneration. Investigative Ophthalmology & Visual Science 50(12):5888-5995.

6. Dilsiz N, **Sahaboglu A**, Yıldız MZ, and Reichenbach A. (2006) Protective effects of various antioxidants during ischemia-reperfusion in the rat retina. Graefe's Archive for Clinical and Experimental Ophthalmology 244 (5): 627-633

**Oral Presentations**

1. **Sahaboglu A,** van Veen T, Zrenner E, Paquet-Durand F. (2010) The Role of PARP in Photoreceptor Cell Death. **Talk,** Young Researcher Vision Camp 2010, Wildenstein, Germany, July 25-27.

2. **Sahaboglu A,** Paquet-Durand F. (2008) The role of PARP and PARG in retinal degeneration. **Talk,** Neurotrain 3rd Annual Meeting, Tübingen, Germany, November 06-07.

**Poster Presentations**

1. **Sahaboglu A**, Löwenheim H, Zrenner E, Paquet-Durand F. (2011) The roles of PARP and PARG in inherited photoreceptor degeneration. European Retina Meeting (ERM). Amsterdam, Holland, September 21-24.

2. **Sahaboglu A,** Tanimoto N, Kaur J, Sancho-Pelluz J, Huber G, Fahl E, Arango-Gonzalez B, Zrenner E, Ekström P, Löwenheim H, Seeliger M, Paquet-Durand F. (2011) Increased resistance to retinal degeneration in PARP1 gene knock-out animals. Göttingen Meeting of the German Neuroscience Society. Göttingen, Germany, March 23-27.

3. Arango-Gonzalez B, Mencl S, **Sahaboglu A**, Paquet-Durand F, Kaur J (2011) Activity and expression of calpain and PARP in P23H-1 and S334ter-3 mutant rhodopsin transgenic rats. Göttingen Meeting of the German Neuroscience Society. Göttingen, Germany, March 23-27.

4. **Sahaboglu A**, Tanimoto N, Kaur J, Sancho-Pelluz J, Huber G, Fahl E, Arango-Gonzalez B, Zrenner E, Ekström P, Löwenheim H, Seeliger M, Paquet-Durand F. (2010) PARP1 in photoreceptor degeneration. PARP 2010: 18th International Conference on ADP-ribose metabolism. Zürich, Switzerland, August 18-21.

5. Sancho-Pelluz J, Alavi M, **Sahaboglu A**, Kustermann S, Farinelli P, Azadi S, van Veen T, Romero FJ, Paquet-Durand F, Ekstrom P. (2010) Histone deacetylase (HDAC) inhibition prevents photoreceptor cell death in the *rd1* mouse. XIV International symposium on retinal degeneration. Mont-Tremblant, Quebec, Canada, July 13-17.

6. Paquet-Durand F, Sancho-Pelluz J, Alavi M, **Sahaboglu A**, Kustermann S, van Veen T, Romero FJ, Ekström P. (2010) Interplay between HDAC and PARP activity during *rd1* mouse retinal degeneration. ARVO, Fort Lauderdale (Florida, USA), May 2-6.

7. **Sahaboglu A,** Sancho-Pelluz J, van Veen, T, Paquet-Durand F. (2010) Characterization of the retinal phenotype in PARP1 KO animals. Pro Retina 2010, Potsdam, Germany, 9-10 April.

8. **Sahaboglu A,** van Veen, T, Paquet-Durand F. (2009) Investigation of cGMP mediated PARP activity in retinal degeneration. European Retina Meeting, Oldenburg, Germany, October 8-10.

9. **Sahaboglu A,** van Veen, T, Paquet-Durand F. (2009) The roles of PARP in inherited retinal degeneration**.** ARVO/ISOCB Meeting, Ericeira, Portugal, September 9-12.

10. **Sahaboglu A,** van Veen T, Paquet-Durand F. (2009) Role of PARP and PARG in inherited retinal degeneration. ARVO, Fort Lauderdale (Florida, USA), May 3-7.

**11.** Sancho-Pelluz J, Alavi M, **Sahaboglu A**, Kustermann S, van Veen T, Romero FJ, Paquet-Durand F, Ekström P. (2009) Role of HDACs in retinal degeneration. ARVO, Fort Lauderdale (Florida, USA), May 3-7.

**12. Sahaboglu A,** van Veen T, Paquet-Durand F. (2009) Role of PARG in inherited retinal degeneration. Pro Retina, Potsdam, Germany, 17-18 April.

# Acknowledgements

This thesis would not possible without the moral and material support, advice and help from many other people. Therefore, here I would like to thank to all of these people.

First and foremost, I would like to sincerely thank **Dr. François Paquet-Durand** for the many hours he has taken from his busy schedule to guide me and for sharing his enthusiasm for cell death mechanism with me as well as his friendship.

I am grateful to **Prof. Dr. Eberhart Zrenner** for his encouragement and constant support to my work and to **Prof Dr. Konrad Kohler** for his kind willingness to supervise my PhD thesis and to **Prof. Dr. Theo van Veen** and **Prof. Dr. Marius Ueffing** for their support and helpful advices.

I would like to thank the members of my thesis *committee*, **Prof. Dr. Hanspeter A. Mallot** and **Prof. Dr. Peter Ruth** for their helpful feedback.

I would like to thank **Prof. Dr. Mathias W. Seeliger** for giving me an opportunity to perform *in vivo* analysis at his lab. And thanks to his lab members **Dr. Naoyuki Tanimoto, Dr. Gesine Huber, Dr. Edda Fahl** for their collaboration and great help.

I would like to also thank **Prof. Dr. Per Ekström** for his helpful advices and collaboration and **Prof. Dr. Hubert Löwenheim** for providing me with the opportunity to work with PARP1 KO mouse and **Dr. Karina Gueltig** for her help.

Many thanks to my lab mates; **Dr. Dragana Trifunović**, **Dr. Blanca Arango-Gonzales**, **Dr. Tao Wei**, **Stine Mencl**, **Jasvir Kaur**, **Dr. Javier Sancho-Pelluz**, **Dr. Anna Lekawa-Ilczuk, Wadood Haq** for their continuous friendship, professional advices, helps and great moments outside of work.

Furthermore, I would especially like to express my gratitude to **Sandra Bernhard-Kurz**, **Sylvia Bolz**, **Katja Dengler** (former lab worker), **Kubrom Bekure-Nemariam** (former lab worker), **Gordon Eske** for their great technical help for my work.

I would like to gratefully acknowledge the financial support from the European Union (**Neurotrain: MEST-CT-2005-020235**), **Charlotte and Tistou Kerstan Foundation** and the **Deutsche Forschungsgemeinschaft (DFG, PA1751/4-1)**.

Last but not least, I would like to express my special thanks to my family members especially to my husband **Mehmet Tekgöz** who encouraged, enabled and supported my studies.

# Reference List

Abood M. E., Hurley J. B., Pappone M. C., Bourne H. R. and Stryer L. (1982) Functional homology between signal-coupling proteins. Cholera toxin inactivates the GTPase activity of transducin. *J. Biol. Chem.* **257,** 10540-10543.

Agarwal A., Mahfouz R. Z., Sharma R. K., Sarkar O., Mangrola D., Mathur P. P. (2009) Potential biological role of poly(ADP-ribose) polymerase (PARP) in male gametes. *Reproductive Biology and Endocrinology **7,** 143.*

Ame J. C. (1999) PARP-2, A Novel Mammalian DNA Damage-dependent Poly(ADP-ribose) Polymerase. *The Journal of Biological Chemistry* **274,** 17860-17868.

Ame J. C., Spenlehauer C. and de M. G. (2004) The PARP superfamily. *Bioessays* **26,** 882-893.

Andrabi S. A., Dawson T. M. and Dawson V. L. (2008) Mitochondrial and nuclear cross talk in cell death: parthanatos. *Ann. N. Y. Acad. Sci.* **1147,** 233-241.

Andrabi S. A., Kim N. S., Yu S. W., Wang H., Koh D. W., Sasaki M., Klaus J. A., Otsuka T., Zhang Z., Koehler R. C., Hurn P. D., Poirier G. G., Dawson V. L. and Dawson T. M. (2006) Poly(ADP-ribose) (PAR) polymer is a death signal. *Proc. Natl. Acad. Sci. U. S. A.* **103,** 18308-18313.

Azadi S., Paquet-Durand F., Medstrand P., van Veen T. and Ekstrom P. A. (2006) Up-regulation and increased phosphorylation of protein kinase C (PKC) delta, mu and theta in the degenerating rd1 mouse retina. *Mol. Cell Neurosci.* **31,** 759-773.

Beckert S., Farrahi F., Perveen G. Q., Aslam R., Scheuenstuhl H., Coerper S., Konigsrainer A., Hunt T. K. and Hussain M. Z. (2006) IGF-I-induced VEGF expression in HUVEC involves phosphorylation and inhibition of poly(ADP-ribose)polymerase. *Biochem. Biophys. Res. Commun.* **341,** 67-72.

Bogoyevitch M. A. and Arthur P. G. (2008) Inhibitors of c-Jun N-terminal kinases: JuNK no more? *Biochim. Biophys. Acta* **1784,** 76-93.

Bornancin F., Franco M., Bigay J. and Chabre M. (1992) Functional modifications of transducin induced by cholera or pertussis-toxin-catalyzed ADP-ribosylation. *Eur. J. Biochem.* **210,** 33-44.

Bowes C., Li T., Danciger M., Baxter L. C., Applebury M. L. and Farber D. B. (1990) Retinal degeneration in the rd mouse is caused by a defect in the beta subunit of rod cGMP-phosphodiesterase. *Nature* **347,** 677-680.

Buelow B., Song Y. and Scharenberg A. M. (2008) The Poly(ADP-ribose) polymerase PARP-1 is required for oxidative stress-induced TRPM2 activation in lymphocytes. *J. Biol. Chem.* **283,** 24571-24583.

Burkle A. (2005) Poly(ADP-ribose). The most elaborate metabolite of $NAD^+$. *FEBS J.* **272,** 4576-4589.

Cesarone C. F., Scarabelli L., Scovassi A. I., Izzo R., Menegazzi M., Carcereri De P. A., Orunesu M. and Bertazzoni U. (1990) Changes in activity and mRNA levels of poly(ADP-ribose) polymerase during rat liver regeneration. *Biochim. Biophys. Acta* **1087,** 241-246.

Chang B., Hawes N. L., Hurd R. E., Davisson M. T., Nusinowitz S. and Heckenlively J. R. (2002) Retinal degeneration mutants in the mouse. *Vision Research* **42,** 517-525.

Cohen-Armon M. (2007) PARP-1 activation in the ERK signaling pathway. *Trends Pharmacol. Sci.* **28,** 556-560.

Cohen-Armon M., Hammel I., Anis Y., Homburg S. and Dekel N. (1996) Evidence for endogenous ADP-ribosylation of GTP-binding proteins in neuronal cell nucleus. Possible induction by membrane depolarization. *J. Biol. Chem.* **271,** 26200-26208.

Corda D. and Di G. M. (2003) Functional aspects of protein mono-ADP-ribosylation. *EMBO J.* **22,** 1953-1958.

D'Amours D. (1999) Poly(ADP-ribosyl)ation reactions in the regulation of nuclear functions. *Biochemical Society* **342,** 249-268.

Daiger S. P., Bowne S. J. and Sullivan L. S. (2007) Perspective on genes and mutations causing retinitis pigmentosa. *Arch. Ophthalmol.* **125,** 151-158.

Davidovic L., Vodenicharov M., Affar E. B. and Poirier G. G. (2001) Importance of poly(ADP-ribose) glycohydrolase in the control of poly(ADP-ribose) metabolism. *Exp. Cell Res.* **268,** 7-13.

Du L., Zhang X., Han Y. Y., Burke N. A., Kochanek P. M., Watkins S. C., Graham S. H., Carcillo J. A., Szabo C. and Clark R. S. (2003) Intra-mitochondrial poly(ADP-ribosylation) contributes to $NAD^+$ depletion and cell death induced by oxidative stress. *J. Biol. Chem.* **278,** 18426-18433.

Endres M., Wang Z. Q., Namura S., Waeber C. and Moskowitz M. A. (1997) Ischemic brain injury is mediated by the activation of poly(ADP-ribose)polymerase. *J. Cereb. Blood Flow Metab* **17,** 1143-1151.

Farber D. B. and Lolley R. N. (1974) Cyclic guanosine monophosphate: elevation in degenerating photoreceptor cells of the C3H mouse retina. *Science* **186,** 449-451.

Fercher A. F. (2003) Optical coherence tomography—principles and applications. *Reports on Progress in Physic* **03,** 18703-18712.

Fischer M. D., Huber G., Beck S. C., Tanimoto N., Muehlfriedel R., Fahl E., Grimm C., Wenzel A., Reme C. E., van de Pavert S. A., Wijnholds J., Pacal M., Bremner R. and Seeliger M. W. (2009) Noninvasive, in vivo assessment of mouse retinal structure using optical coherence tomography. *PLoS. ONE.* **4,** e7507.

Fox D. A., Poblenz A. T. and He L. (1999) Calcium overload triggers rod photoreceptor apoptotic cell death in chemical-induced and inherited retinal degenerations. *Ann. N. Y. Acad. Sci.* **893,** 282-285.

Fuchs Y. and Steller H. (2011) Programmed cell death in animal development and disease. *Cell* **147,** 742-758.

Gagne J. P., Isabelle M., Lo K. S., Bourassa S., Hendzel M. J., Dawson V. L., Dawson T. M. and Poirier G. G. (2008) Proteome-wide identification of poly(ADP-ribose) binding proteins and poly(ADP-ribose)-associated protein complexes. *Nucleic Acids Res.* **36,** 6959-6976.

Gambichler T., Moussa G., Regeniter P., Kasseck C., Hofmann M. R., Bechara F. G., Sand M., Altmeyer P. and Hoffmann K. (2007) Validation of optical coherence tomography in vivo using cryostat histology. *Phys. Med. Biol.* **52,** N75-N85.

Goebel D. J. and Winkler B. S. (2006) Blockade of PARP activity attenuates poly(ADP-ribosyl)ation but offers only partial neuroprotection against NMDA-induced cell death in the rat retina. *J. Neurochem.* **98,** 1732-1745.

Hakme A., Wong H. K., Dantzer F. and Schreiber V. (2008) The expanding field of poly(ADP-ribosyl)ation reactions. 'Protein Modifications: Beyond the Usual Suspects' Review Series. *EMBO Rep.* **9,** 1094-1100.

Hassa P. O., Haenni S. S., Elser M. and Hottiger M. O. (2006) Nuclear ADP-ribosylation reactions in mammalian cells: where are we today and where are we going? *Microbiol. Mol. Biol. Rev.* **70,** 789-829.

Hassa P. O. and Hottiger M. O. (2008) The diverse biological roles of mammalian PARPS, a small but powerful family of poly-ADP-ribose polymerases. *Front Biosci.* **13,** 3046-3082.

Hauck S. M., Ekstrom P. A., Ahuja-Jensen P., Suppmann S., Paquet-Durand F., van Veen T. and Ueffing M. (2006) Differential modification of phosducin protein in degenerating rd1 retina is associated with constitutively active Ca2+/calmodulin kinase II in rod outer segments. *Mol. Cell Proteomics.* **5,** 324-336.

Hegedus C., Lakatos P., Olah G., Toth B. I., Gergely S., Szabo E., Biro T., Szabo C. and Virag L. (2008) Protein kinase C protects from DNA damage-induced necrotic cell death by inhibiting poly(ADP-ribose) polymerase-1. *FEBS Lett.* **582,** 1672-1678.

Herceg Z. and Wang Z. Q. (2001) Functions of poly(ADP-ribose) polymerase (PARP) in DNA repair, genomic integrity and cell death. *Mutat. Res.* **477,** 97-110.

Herse P. (2005) Retinitis pigmentosa: visual function and multidisciplinary management. *Clin. Exp. Optom.* **88,** 335-350.

Hong S. J., Dawson T. M. and Dawson V. L. (2004) Nuclear and mitochondrial conversations in cell death: PARP-1 and AIF signaling. *Trends Pharmacol. Sci.* **25,** 259-264.

Horton J. K., Stefanick D. F., Naron J. M., Kedar P. S. and Wilson S. H. (2005) Poly(ADP-ribose) polymerase activity prevents signaling pathways for cell cycle arrest after DNA methylating agent exposure. *J. Biol. Chem.* **280,** 15773-15785.

Hottiger M. O., Hassa P. O., Luscher B., Schuler H. and Koch-Nolte F. (2010) Toward a unified nomenclature for mammalian ADP-ribosyltransferases. *Trends Biochem. Sci.* **35,** 208-219.

Isabelle M., Moreel X., Gagne J. P., Rouleau M., Ethier C., Gagne P., Hendzel M. J. and Poirier G. G. (2010) Investigation of PARP-1, PARP-2, and PARG interactomes by affinity-purification mass spectrometry. *Proteome. Sci.* **8,** 22.

Jagtap P. and Szabo C. (2005) Poly(ADP-ribose) polymerase and the therapeutic effects of its inhibitors. *Nat. Rev. Drug Discov.* **4,** 421-440.

Kalloniatis M. and Fletcher E. L. (2005) Retinal degeneration: challenge and opportunity. *Clin. Exp. Optom.* **88,** 265-266.

Kauppinen T. M., Chan W. Y., Suh S. W., Wiggins A. K., Huang E. J. and Swanson R. A. (2006) Direct phosphorylation and regulation of poly(ADP-ribose) polymerase-1 by extracellular signal-regulated kinases 1/2. *Proc. Natl. Acad. Sci. U. S. A* **103,** 7136-7141.

Kauppinen T. M., Suh S. W., Higashi Y., Berman A. E., Escartin C., Won S. J., Wang C., Cho S. H., Gan L. and Swanson R. A. (2011) Poly(ADP-ribose)polymerase-1 modulates microglial responses to amyloid beta. *J. Neuroinflammation.* **8,** 152.

Kaur J., Mencl S., Sahaboglu A., Farinelli P., van Veen T., Zrenner E., Ekstrom P., Paquet-Durand F. and Arango-Gonzalez B. (2011) Calpain and PARP Activation during Photoreceptor Cell Death in P23H and S334ter Rhodopsin Mutant Rats. *PLoS. ONE.* **6,** e22181.

Kim K. H., Puoris'haag M., Maguluri G. N., Umino Y., Cusato K., Barlow R. B. and de Boer J. F. (2008) Monitoring mouse retinal degeneration with high-resolution spectral-domain optical coherence tomography. *J. Vis.* **8,** 17-11.

Kim M. Y., Zhang T. and Kraus W. L. (2005) Poly(ADP-ribosyl)ation by PARP-1: 'PAR-laying' $NAD^+$ into a nuclear signal. *Genes Dev.* **19,** 1951-1967.

Kolthur-Seetharam U., Dantzer F., McBurney M. W., de M. G. and Sassone-Corsi P. (2006) Control of AIF-mediated cell death by the functional interplay of SIRT1 and PARP-1 in response to DNA damage. *Cell Cycle* **5,** 873-877.

Komjati K., Besson V. C. and Szabo C. (2005) Poly (adp-ribose) polymerase inhibitors as potential therapeutic agents in stroke and neurotrauma. *Curr. Drug Targets. CNS. Neurol. Disord.* **4,** 179-194.

Kraft R., Grimm C., Grosse K., Hoffmann A., Sauerbruch S., Kettenmann H., Schultz G. and Harteneck C. (2004) Hydrogen peroxide and ADP-ribose induce TRPM2-mediated calcium influx and cation currents in microglia. *Am. J. Physiol Cell Physiol* **286,** C129-C137.

Kraus W. L. and Lis J. T. (2003) PARP goes transcription. *Cell* **113,** 677-683.

Kruszewski M. and Szumiel I. (2005) Sirtuins (histone deacetylases III) in the cellular response to DNA damage--facts and hypotheses. *DNA Repair (Amst).* **4,** 1306-1313.

Kun E., Kirsten E., Bauer P. I. and Ordahl C. P. (2006) Quantitative correlation between cellular proliferation and nuclear poly (ADP-ribose) polymerase (PARP-1). *Int. J. Mol. Med.* **17,** 293-300.

Lem J., Flannery J. G., Li T., Applebury M. L., Farber D. B. and Simon M. I. (1992) Retinal degeneration is rescued in transgenic rd mice by expression of the cGMP phosphodiesterase beta subunit. *Proc. Natl. Acad. Sci. U. S. A* **89,** 4422-4426.

Lerea C. L., Somers D. E., Hurley J. B., Klock I. B. and Bunt-Milam A. H. (1986) Identification of specific transducin alpha subunits in retinal rod and cone photoreceptors. *Science* **234,** 77-80.

Loseva O., Jemth A. S., Bryant H. E., Schuler H., Lehtio L., Karlberg T. and Helleday T. (2010) PARP-3 is a mono-ADP-ribosylase that activates PARP-1 in the absence of DNA. *J. Biol. Chem.* **285,** 8054-8060.

Masutani M., Nozaki T., Wakabayashi K. and Sugimura T. (1995) Role of poly(ADP-ribose) polymerase in cell-cycle checkpoint mechanisms following gamma-irradiation. *Biochimie* **77,** 462-465.

Masutani M., Suzuki H., Kamada N., Watanabe M., Ueda O., Nozaki T., Jishage K., Watanabe T., Sugimoto T., Nakagama H., Ochiya T. and Sugimura T. (1999) Poly(ADP-ribose) polymerase gene disruption conferred mice resistant to streptozotocin-induced diabetes. *Proc. Natl. Acad. Sci. U. S. A* **96,** 2301-2304.

McLaughlin M. E., Ehrhart T. L., Berson E. L. and Dryja T. P. (1995) Mutation spectrum of the gene encoding the beta subunit of rod phosphodiesterase among patients with autosomal recessive retinitis pigmentosa. *Proc. Natl. Acad. Sci. U. S. A* **92,** 3249-3253.

Medynski D. C. (1985) Amino acid sequence of the a subunit of transducin deduced from the cDNA sequence. *Proc. Natl. Acad. Sci.* **82,** 4311-4315.

Meyer-Ficca M. L., Meyer R. G., Coyle D. L., Jacobson E. L. and Jacobson M. K. (2004) Human poly(ADP-ribose) glycohydrolase is expressed in alternative splice variants yielding isoforms that localize to different cell compartments. *Exp. Cell Res.* **297,** 521-532.

Midorikawa R., Takei Y. and Hirokawa N. (2006) KIF4 motor regulates activity-dependent neuronal survival by suppressing PARP-1 enzymatic activity. *Cell* **125,** 371-383.

Miwa M. and Sugimura T. (1971) Splitting of the ribose-ribose linkage of poly(adenosine diphosphate-robose) by a calf thymus extract. *J. Biol. Chem.* **246,** 6362-6364.

Morin F., Lugnier C., Kameni J. and Voisin P. (2001) Expression and role of phosphodiesterase 6 in the chicken pineal gland. *J. Neurochem.* **78,** 88-99.

Moubarak R. S., Yuste V. J., Artus C., Bouharrour A., Greer P. A., Menissier-de M. J. and Susin S. A. (2007) Sequential activation of poly(ADP-ribose) polymerase 1, calpains, and Bax is essential in apoptosis-inducing factor-mediated programmed necrosis. *Mol. Cell Biol.* **27,** 4844-4862.

Neves S. R., Ram P. T. and Iyengar R. (2002) G protein pathways. *Science* **296,** 1636-1639.

Nucci C., Piccirilli S., Rodino P., Nistico R., Grandinetti M., Cerulli L., Leist M., Nicotera P. and Bagetta G. (2000) Apoptosis in the dorsal lateral geniculate nucleus after monocular deprivation involves glutamate signaling, NO production, and PARP activation. *Biochem. Biophys. Res. Commun.* **278,** 360-367.

Oliver F. J. (1999) Poly(ADP-Ribose) Polymerase in the Cellular Response to DNA Damage, Apoptosis, and Disease. *The American Journal of Human Genetics* **64,** 1282-1288.

Otani A., Dorrell M. I., Kinder K., Moreno S. K., Nusinowitz S., Banin E., Heckenlively J. and Friedlander M. (2004) Rescue of retinal degeneration by intravitreally injected adult bone marrow-derived lineage-negative hematopoietic stem cells. *J. Clin. Invest.* **114,** 765-774.

Pagano A., Metrailler-Ruchonnet I., Aurrand-Lions M., Lucattelli M., Donati Y. and Argiroffo C. B. (2007) Poly(ADP-ribose) polymerase-1 (PARP-1) controls lung cell proliferation and repair after hyperoxia-induced lung damage. *Am. J. Physiol Lung Cell Mol. Physiol* **293,** L619-L629.

Paquet-Durand F., Azadi S., Hauck S. M., Ueffing M., van Veen T. and Ekstrom P. (2006) Calpain is activated in degenerating photoreceptors in the rd1 mouse. *J. Neurochem.* **96,** 802-814.

Paquet-Durand F., Beck S., Michalakis S., Goldmann T., Huber G., Muhlfriedel R., Trifunovic D., Fischer M. D., Fahl E., Duetsch G., Becirovic E., Wolfrum U., van Veen T., Biel M., Tanimoto N. and Seeliger M. W. (2011) A key role for cyclic nucleotide gated (CNG) channels in cGMP-related retinitis pigmentosa. *Hum. Mol. Genet.* **20,** 941-947.

Paquet-Durand F., Hauck S. M., van Veen T., Ueffing M. and Ekstrom P. (2009) PKG activity causes photoreceptor cell death in two retinitis pigmentosa models. *J. Neurochem.* **108,** 796-810.

Paquet-Durand F., Johnson L. and Ekstrom P. (2007a) Calpain activity in retinal degeneration. *J. Neurosci. Res.* **85,** 693-702.

Paquet-Durand F., Silva J., Talukdar T., Johnson L. E., Azadi S., van Veen T., Ueffing M., Hauck S. M. and Ekstrom P. A. (2007b) Excessive activation of poly(ADP-ribose) polymerase contributes to inherited photoreceptor degeneration in the retinal degeneration 1 mouse. *J. Neurosci.* **27,** 10311-10319.

Pierce E. A. (2001) Pathways to photoreceptor cell death in inherited retinal degenerations. *Bioessays.* **23,** 605-618.

Portera-Cailliau C., Sung C. H., Nathans J. and Adler R. (1994) Apoptotic photoreceptor cell death in mouse models of retinitis pigmentosa. *Proc. Natl. Acad. Sci. U. S. A* **91,** 974-978.

Punzo C. and Cepko C. (2007) Cellular responses to photoreceptor death in the rd1 mouse model of retinal degeneration. *Invest Ophthalmol. Vis. Sci.* **48,** 849-857.

Roorda A. and Williams D. R. (1999) The arrangement of the three cone classes in the living human eye. *Nature* **397,** 520-522.

Rouleau M., Patel A., Hendzel M. J., Kaufmann S. H. and Poirier G. G. (2010) PARP inhibition: PARP1 and beyond. *Nat. Rev. Cancer* **10,** 293-301.

Sancho-Pelluz J., Alavi M., Sahaboglu A., Kustermann S., Farinelli P., Azadi S., van Veen T., Romero F. J., Paquet-Durand F. and Ekstrom P. (2010) Excessive HDAC activation is critical for neurodegeneration in the rd1 mouse. *Cell Death & Disease* **1,** 1-9.

Sancho-Pelluz J., Arango-Gonzalez B., Kustermann S., Romero F. J., van Veen T., Zrenner E., Ekstrom P. and Paquet-Durand F. (2008) Photoreceptor cell death mechanisms in inherited retinal degeneration. *Mol. Neurobiol.* **38,** 253-269.

Schoppner A. and Kindl H. (1984) Purification and properties of a stilbene synthase from induced cell suspension cultures of peanut. *J. Biol. Chem.* **259,** 6806-6811.

Schreiber V., Ame J. C., Dolle P., Schultz I., Rinaldi B., Fraulob V., Menissier-de M. J. and de M. G. (2002) Poly(ADP-ribose) polymerase-2 (PARP-2) is required for efficient base excision DNA repair in association with PARP-1 and XRCC1. *J. Biol. Chem.* **277,** 23028-23036.

Schreiber V., Dantzer F., Ame J. C. and de M. G. (2006) Poly(ADP-ribose): novel functions for an old molecule. *Nat. Rev. Mol. Cell Biol.* **7,** 517-528.

Shall S. and de Murcia (2000) Poly(ADP-ribose) polymerase-1: what have we learned from the deficient mouse model? *Mutat. Res.* **460,** 1-15.

Shieh W. M., Ame J. C., Wilson M. V., Wang Z. Q., Koh D. W., Jacobson M. K. and Jacobson E. L. (1998) Poly(ADP-ribose) polymerase null mouse cells synthesize ADP-ribose polymers. *J. Biol. Chem.* **273,** 30069-30072.

Sims J. L., Berger S. J. and Berger N. A. (1983) Poly(ADP-ribose) Polymerase inhibitors preserve nicotinamide adenine dinucleotide and adenosine 5'-triphosphate pools in DNA-damaged cells: mechanism of stimulation of unscheduled DNA synthesis. *Biochemistry.* **22,** 5188-5194.

Susin S. A., Lorenzo H. K., Zamzami N., Marzo I., Snow B. E., Brothers G. M., Mangion J., Jacotot E., Costantini P., Loeffler M., Larochette N., Goodlett D. R., Aebersold R., Siderovski D. P., Penninger J. M. and Kroemer G. (1999) Molecular characterization of mitochondrial apoptosis-inducing factor. *Nature* **397,** 441-446.

Szabadfi K., Mester L., Reglodi D., Kiss P., Babai N., Racz B., Kovacs K., Szabo A., Tamas A., Gabriel R. and Atlasz T. (2010) Novel neuroprotective strategies in ischemic retinal lesions. *Int. J. Mol. Sci.* **11,** 544-561.

Tanuma S. I., Enomoto T. and Yamada M. A. (1978) Changes in the level of poly ADP-ribosylation during a cell cycle. *Exp. Cell Res.* **117,** 421-430.

Tong W.M. (2001) Poly(ADP-ribose) polymerase:a guardian angel protecting the genome and suppressing tumorigenesis. *Biochimica et Biophysica Acta* **1552,** 27-37.

Trucco C. (1998) DNA repair defect in poly(ADP-ribose) polymerase-deficient cell lines. *Nucleic Acids Research* **26,** 2644-2649.

Uchida M. (2001) Genetic and functional analysis of PARP, a DNA strand break-binding enzyme, (Hanai S., ed), pp. 89-96. Mutation Research.

Ueda K. and Hayaishi O. (1985) ADP-ribosylation. *Annu. Rev. Biochem.* **54,** 73-100.

Uehara N., Miki K., Tsukamoto R., Matsuoka Y. and Tsubura A. (2006) Nicotinamide blocks N-methyl-N-nitrosourea-induced photoreceptor cell apoptosis in rats through poly (ADP-ribose) polymerase activity and Jun N-terminal kinase/activator protein-1 pathway inhibition. *Exp. Eye Res.* **82,** 488-495.

Van D. C., Yamanaka G., Steinberg F., Sekura R. D., Manclark C. R., Stryer L. and Bourne H. R. (1984) ADP-ribosylation of transducin by pertussis toxin blocks the light-stimulated hydrolysis of GTP and cGMP in retinal photoreceptors. *J. Biol. Chem.* **259,** 23-26.

Virag L. and Szabo C. (2002) The therapeutic potential of poly(ADP-ribose) polymerase inhibitors. *Pharmacol. Rev.* **54,** 375-429.

Vosler P. S., Sun D., Wang S., Gao Y., Kintner D. B., Signore A. P., Cao G. and Chen J. (2009) Calcium dysregulation induces apoptosis-inducing factor release: cross-talk between PARP-1- and calpain-signaling pathways. *Exp. Neurol.* **218,** 213-220.

Wald G. (1951) The chemistry of rod vision. *Science.* **113,** 287-291.

Wang Y., Dawson V. L. and Dawson T. M. (2009) Poly(ADP-ribose) signals to mitochondrial AIF: a key event in parthanatos. *Exp. Neurol.* **218,** 193-202.

Wang Y., Kim N. S., Haince J. F., Kang H. C., David K. K., Andrabi S. A., Poirier G. G., Dawson V. L. and Dawson T. M. (2011) Poly(ADP-ribose) (PAR) binding to apoptosis-inducing factor is critical for PAR polymerase-1-dependent cell death (parthanatos). *Sci. Signal.* **4,** ra20.

Wang Z. Q. (1995) Mice lacking ADPRT and poly(ADPribosyl)ation develop normally but are susceptible to skin disease. *Genes & Development* **9,** 509-520.

Wang Z. Q., Stingl L., Morrison C., Jantsch M., Los M., Schulze-Osthoff K. and Wagner E. F. (1997) PARP is important for genomic stability but dispensable in apoptosis. *Genes Dev.* **11,** 2347-2358.

Willmore E. and Durkacz B. W. (1993) Cytotoxic mechanisms of 5-fluoropyrimidines. Relationships with poly(ADP-ribose) polymerase activity, DNA strand breakage and incorporation into nucleic acids. *Biochem. Pharmacol.* **46,** 205-211.

Wright A. F., Chakarova C. F., Abd El-Aziz M. M. and Bhattacharya S. S. (2010) Photoreceptor degeneration: genetic and mechanistic dissection of a complex trait. *Nat. Rev. Genet.* **11,** 273-284.

Yu S. W., Andrabi S. A., Wang H., Kim N. S., Poirier G. G., Dawson T. M. and Dawson V. L. (2006) Apoptosis-inducing factor mediates poly(ADP-ribose) (PAR) polymer-induced cell death. *Proc. Natl. Acad. Sci. U. S. A* **103,** 18314-18319.

Yu S. W., Wang H., Poitras M. F., Coombs C., Bowers W. J., Federoff H. J., Poirier G. G., Dawson T. M. and Dawson V. L. (2002) Mediation of poly(ADP-ribose) polymerase-1-dependent cell death by apoptosis-inducing factor. *Science.* **297,** 259-263.

Zeng H. Y., Tso M. O., Lai S. and Lai H. (2008) Activation of nuclear factor-kappaB during retinal degeneration in rd mice. *Mol. Vis.* **14,** 1075-1080.

Zhang S., Lin Y., Kim Y. S., Hande M. P., Liu Z. G. and Shen H. M. (2007) c-Jun N-terminal kinase mediates hydrogen peroxide-induced cell death via sustained poly(ADP-ribose) polymerase-1 activation. *Cell Death. Differ.* **14,** 1001-1010.

Zhang X., Feng Q. and Cote R. H. (2005) Efficacy and selectivity of phosphodiesterase-targeted drugs in inhibiting photoreceptor phosphodiesterase (PDE6) in retinal photoreceptors. *Invest Ophthalmol. Vis. Sci.* **46,** 3060-3066.

Zhivotovsky B. and Orrenius S. (2010) Cell cycle and cell death in disease: past, present and future. *J. Intern. Med.* **268,** 395-409.

Zimmerman B., Sargeant A., Landes K., Fernandez S. A., Chen C. S. and Lairmore M. D. (2011) Efficacy of novel histone deacetylase inhibitor, AR42, in a mouse model of, human T-lymphotropic virus type 1 adult T cell lymphoma. *Leuk. Res.* **35,** 1491-1497.

# Appendix

**Paper I** Huber G, Beck SC, Grimm C, **Sahaboglu-Tekgoz, A**, Paquet-Durand F, Wenzel A, Seeliger MW, Fischer MD. (2009) Spectral domain optical coherence tomography in mouse models of retinal degeneration. Investigative Ophthalmology & Visual Science 50(12):5888-5995.

**Paper II** Sancho-Pelluz J, Alavi M, **Sahaboglu A**, Kustermann S, Farinelli P, Azadi S, van Veen T, Romero FJ, Paquet-Durand F, Ekström P. (2010) Excessive HDAC activation critical for neurodegeneration in the *rd1* mouse. Cell Death & Disease, doi:10.1038/cddis.2010.4.

**Paper III** **Sahaboglu A**, Tanimoto N, Kaur J, Sancho-Pelluz J, Huber G, Fahl E, Arango-Gonzalez B, Zrenner E, Ekström P, Löwenheim H, Seeliger MW, Paquet-Durand F. (2010) PARP1 gene knock-out increases resistance to retinal degeneration without affecting retinal function. PLoS ONE 5(11): e15495.

# Spectral domain optical coherence tomography in mouse models of retinal degeneration.

*Huber G, Beck SC, Grimm C,* ***Sahaboglu-Tekgoz, A****, Paquet-Durand F, Wenzel A, Seeliger MW, Fischer MD.*

*Published in "Investigative Ophthalmology & Visual Science" 50(12):5888-5995. (2009)*

# Spectral Domain Optical Coherence Tomography in Mouse Models of Retinal Degeneration

*Gesine Huber,*[1,2] *Susanne C. Beck,*[1] *Christian Grimm,*[3] *Ayse Sahaboglu-Tekgoz,*[4] *Francois Paquet-Durand,*[4] *Andreas Wenzel,*[3,5] *Peter Humphries,*[6] *T. Michael Redmond,*[7] *Mathias W. Seeliger,*[1,8] *and M. Dominik Fischer*[1,8]

**Purpose.** Spectral domain optical coherence tomography (SD-OCT) allows cross-sectional visualization of retinal structures in vivo. Here, the authors report the efficacy of a commercially available SD-OCT device to study mouse models of retinal degeneration.

**Methods.** C57BL/6 and BALB/c wild-type mice and three different mouse models of hereditary retinal degeneration (*Rho*$^{-/-}$, *rd1*, *RPE65*$^{-/-}$) were investigated using confocal scanning laser ophthalmoscopy (cSLO) for en face visualization and SD-OCT for cross-sectional imaging of retinal structures. Histology was performed to correlate structural findings in SD-OCT with light microscopic data.

**Results.** In C57BL/6 and BALB/c mice, cSLO and SD-OCT imaging provided structural details of frequently used control animals (central retinal thickness, $CRT_{C57BL/6} = 237 \pm 2$ $\mu$m and $CRT_{BALB/c} = 211 \pm 10$ $\mu$m). *RPE65*$^{-/-}$ mice at 11 months of age showed a significant reduction of retinal thickness ($CRT_{RPE65} = 193 \pm 2$ $\mu$m) with thinning of the outer nuclear layer. *Rho*$^{-/-}$ mice at P28 demonstrated degenerative changes mainly in the outer retinal layers ($CRT_{Rho} = 193 \pm 2$ $\mu$m). Examining *rd1* animals before and after the onset of retinal degeneration allowed monitoring of disease progression ($CRT_{rd1\ P11} = 246 \pm 4$ $\mu$m, $CRT_{rd1\ P28} = 143 \pm 4$ $\mu$m). Correlation of CRT assessed by histology and SD-OCT was high ($r^2 = 0.897$).

**Conclusions.** The authors demonstrated cross-sectional visualization of retinal structures in wild-type mice and mouse models for retinal degeneration in vivo using a commercially available SD-OCT device. This method will help to reduce numbers of animals needed per study by allowing longitudinal study designs and will facilitate characterization of disease dynamics and evaluation of putative therapeutic effects after experimental interventions. (*Invest Ophthalmol Vis Sci.* 2009;50:5888–5895) DOI:10.1167/iovs.09-3724

Optical coherence tomography (OCT) has evolved over the past two decades to become an important diagnostic tool in clinical ophthalmology and other medical specialties.[1] Widespread application of this powerful tool in animal research, however, was restricted because of poor image quality in commercially available first- and second-generation time domain OCT devices.[2,3] Sufficiently high image quality could be achieved only with prototype devices with improved depth resolution that were specifically adapted for the respective animal visual system.[4–7] Only recently, latest generation SD-OCT devices have become commercially available that provide scanning speed and depth resolution sufficient for small animal experimentation.[8] Given that SD-OCT is ideally suited for studying changes of retinal integrity, wild-type mice and mouse models of retinal degeneration were chosen to explore the efficacy of this method.

Thus far, animal models of retinal degeneration have been studied extensively on both functional and structural levels. Morphologic changes were detected using either en face imaging methods such as funduscopy[9] and confocal scanning laser ophthalmoscopy (cSLO)[10] or, more commonly, ex vivo histologic approaches. Although light and electron microscopy provide (ultra-)high structural resolution, fixation procedures, dehydration preparatory to subsequent embedding, and staining, even the processes of cutting, flattening, and mounting histologic sections are potential sources for significant and variable alterations in dimensions.[11,12] Indeed, retinal thickness measures of rodent retina are reported to be 95 $\mu$m in one study[13] and 170 to 217 $\mu$m in other studies.[11,14] Taken together, ex vivo analysis of retinal tissue has certain limitations and should be interpreted accordingly. In vivo analysis of the retina has significant benefits as delicate, but functionally important changes such as retinal edema and focal neurosensory and pigment epithelial detachments can readily be detected by SD-OCT while potentially remaining undetected or masked by handling procedures in histologic analysis. Finally, monitoring of dynamic changes in individual animals requires a noninvasive study design. Here, SD-OCT has the potential to complement the existing in vivo methods in vision research by providing histology-analog structural details on retinal integrity. Because individual animals may be investigated at multiple time points, SD-OCT can also help to reduce the numbers of animals needed for such a study, which has both ethical and economic implications. To the best of our knowledge, this is the first study to demonstrate the efficacy of a commercially

From the [1]Division of Ocular Neurodegeneration and the [4]Division for Experimental Ophthalmology, Institute for Ophthalmic Research, Centre for Ophthalmology, Tuebingen, Germany; [2]Institute of Animal Welfare, Ethology and Animal Hygiene, Faculty of Veterinary Medicine, Ludwig-Maximilians-University, Munich, Germany; [3]Laboratory of Retinal Cell Biology, Department of Ophthalmology, University of Zurich, Zurich, Switzerland; [6]Ocular Genetics Unit, Trinity College, Dublin, Ireland; and [7]National Eye Institute, National Institutes of Health, Bethesda, Maryland.

[8]These authors contributed equally to the work presented here and should therefore be regarded as equivalent authors.

[5]Present affiliation: Novartis Pharma Schweiz AG, Bern, Switzerland.

Supported by Deutsche Forschungsgemeinschaft Grants Se837/5-2 & Se837/7-1 (KFO 134), Se837/6-1, and PA1751/1-1; German Ministry of Education and Research Grant 0314106; European Union Grants LSHG-CT-512036 and EU HEALTH-F2-2008-200234, Kerstan Foundation, EU (MEST-CT-2005-020235).

Submitted for publication March 17, 2009; revised May 29, 2009; accepted August 31, 2009.

Disclosure: **G. Huber**, None; **S.C. Beck**, None; **C. Grimm**, None; **A. Sahaboglu-Tekgoz**, None; **F. Paquet-Durand**, None; **A. Wenzel**, Novartis Pharma Schweiz (E); **P. Humphries**, None; **T.M. Redmond**, None; **M.W. Seeliger**, None; **M.D. Fischer**, None

The publication costs of this article were defrayed in part by page charge payment. This article must therefore be marked "*advertisement*" in accordance with 18 U.S.C. §1734 solely to indicate this fact.

Corresponding author: M. Dominik Fischer, Institute for Ophthalmic Research, Centre for Ophthalmology, University of Tuebingen, 72076 Tuebingen, Germany; dominik.fischer@med.uni-tuebingen.de.

available SD-OCT device to obtain cross-sectional images from wild-type mice and mouse models of retinal degeneration.

## Materials and Methods

### Animals

Animals were housed under standard white cyclic lighting (200 lux), had free access to food and water, and were used irrespective of gender. *Rho*$^{-/-}$[15] ($n$ = 46), *RPE65*$^{-/-}$[16] ($n$ = 10), BALB/c ($n$ = 15; Charles River Laboratories), C57/BL6/J ($n$ = 37; Charles River Laboratories), C3H *rd1/rd1* ($n$ = 6, *rd1*), and control C3H wild-type ($n$ = 6) mice[17] were used for imaging. All procedures were performed in accordance with the local ethics committee, German laws governing the use of experimental animals, and the ARVO Statement for the Use of Animals in Ophthalmic and Vision Research. Because of the critical changes after postnatal day (P) 11,[18,19] imaging in *rd1* and corresponding wild-type were carried out at P11 and P28. Because of the later onset and slower course of degeneration in the *Rho*$^{-/-}$ *and RPE65*$^{-/-}$ mouse models, imaging was performed at 1 and 11 months, respectively.

### Confocal Scanning Laser Ophthalmoscopy

For en face retinal imaging, we used the commercially available HRA 1 and HRA 2 (Heidelberg Engineering, Heidelberg, Germany) featuring up to two argon wavelengths (488/514 nm) in the short-wavelength range and two infrared diode lasers (HRA 1, 795/830 nm; HRA 2, 785/815 nm) in the long-wavelength range. A detailed protocol for anesthesia and imaging is described elsewhere.[10] Briefly, mice were anesthetized by subcutaneous injection of ketamine (66.7 mg/kg) and xylazine (11.7 mg/kg), and their pupils were dilated with tropicamide eye drops (Mydriaticum Stulln; Pharma Stulln GmbH, Stulln, Germany) before image acquisition. By applying hydroxypropyl methylcellulose (Methocel 2%; OmniVision, Puchheim, Germany) on the eye, the refractive power of the air corneal interface was effectively negated. A custom-made contact lens (focal length, 10 mm) was used to reduce the risk of corneal dehydration and edema and to act as a collimator.

### Spectral Domain Optical Coherence Tomography

SD-OCT imaging was performed in the same session as cSLO (i.e., animals remained anesthetized using identical preparatory steps). Mouse eyes were subjected to SD-OCT with a commercially available HRA+OCT device (Spectralis; Heidelberg Engineering, Heidelberg, Germany) featuring a broadband superluminescent diode at $\lambda$ = 880 nm as a low coherent light source. Each two-dimensional B-scan recorded at 30° field-of-view consists of 1536 A-scans acquired at a speed of 40,000 scans per second. Optical depth resolution is approximately 7 $\mu$m, with digital resolution reaching 3.5 $\mu$m.[8]

To adapt for the optical qualities of the mouse eye, we mounted a commercially available 78-D double aspheric fundus lens (Volk Optical, Inc., Mentor, OH) directly in front of the camera unit. Imaging was performed with a proprietary software package (Eye Explorer, version 3.2.1.0; Heidelberg Engineering). Length of the reference pathway was adjusted manually according to manufacturer's instructions using the "OCT debug window" (press Ctrl/Shift/Alt/O simultaneously to open window in the active, calibrated OCT mode) to adjust for the optical length of the scanning pathway. The combination of scanning laser retinal imaging and SD-OCT allows for real-time tracking of eye movements and real-time averaging of OCT scans, reducing speckle noise in the OCT images considerably.[8] Resultant data were exported as 8-bit grayscale image files and were processed with a graphics editing program (Photoshop CS2; Adobe Systems, San Jose, CA). For quantification of central retinal thickness based on high-resolution volume scans, we used the proprietary software (Eye Explorer; Heidelberg Engineering). Briefly, each volume scan consisted of at least 70 B-scans recorded at 30° field-of-view centered on the optic disc, which were used to calculate an interpolated retinal thickness map across the scanned retinal area. Central retinal thickness was quantified using the circular OCT grid subfield at 3-mm diameter, with the center located on the optic disc.

### Histology

Three animals from each mouse line (*Rho*$^{-/-}$, *RPE65*$^{-/-}$, BALB/c, and C57/BL6) were killed, and their eyes were enucleated for histologic analysis. After orientation was marked, the eyes were fixed overnight in 2.5% glutaraldehyde prepared in 0.1 M cacodylate buffer and were processed as described previously.[20] Semithin sections (0.5 mm) of Epon-embedded tissue were prepared form the central retina, counterstained with methylene blue, and analyzed using a light microscope (Axiovision; Zeiss, Jena, Germany).

For the timeline analysis of *rd1* mice ($n$ = 3 for each group: rd1 P11, rd1 P28, wild-type P11, and wild-type P28), eyes were embedded unfixed in Jung tissue freezing medium (Leica Microsystems, Wetzlar, Germany), frozen, and sectioned (14 $\mu$m) in a cryotome (HM560; Microm, Walldorf, Germany). Sections were then stained using hematoxylin/eosin staining. Morphologic observations and light microscopy were performed on a microscope (Imager.Z1 Apotome; Zeiss) equipped with a digital camera (Axiocam MrN; Zeiss). Images were captured using corresponding software (Axiovision 4.6; Zeiss).

### SD-OCT versus Histology

For correlation of retinal thickness measurements, *inner retina* was defined as ranging from the inner limiting membrane to the outer plexiform layer (OPL) and *outer retina* was defined as ranging from the outer nuclear layer (ONL) to the retinal pigment epithelium (RPE). In case of morphometric assessment of histologic sections, all measurements were taken at 1.4 mm eccentricity from the optic nerve head to mirror the SD-OCT-based thickness measurement along a circular ring scan ($r$ = 1.4 mm) centered on the optic nerve head. Respective thickness was quantified by computer-assisted manual segmentation analysis using the proprietary software (Eye Explorer; Heidelberg Engineering) for SD-OCT data and the calibrated "line-tool" in Adobe (Photoshop CS2) for histologic micrographs.

Student's $t$-test was used to analyze statistical significance between respective inner and outer retinal thickness measurements (C57/Bl6 vs. *Rho*$^{-/-}$, *RPE65*$^{-/-}$, or BALB/c; C3H wild-type vs. C3H rd1/rd1 at P11 and P28). Correlation between thickness measurements by OCT versus histology was assessed by Pearson's correlation coefficient.

## Results

### C57BL/6

A basic examination using cSLO en face imaging was performed in 4-week-old C57BL/6 mice to confirm the presence of regular retinal and vascular structures typical for normal wild-type animals. The examination included native red-free (RF; 513 nm), infrared (IR; 830 nm), and autofluorescence (AF) modes fluorescein angiography and indocyanine green angiography (Fig. 1). The cross-sectional SD-OCT imaging in these animals provided detailed in vivo data on retinal layer composition (Fig. 1) and retinal thickness. In a central circular area of approximately 3-mm diameter, total retinal thickness was 237 $\pm$ 2 $\mu$m (mean $\pm$ SD). The laminar organization of the murine retina, as determined in vivo by SD-OCT, correlated well with ex vivo light microscopy studies (Fig. 1). Notably, some wild-type mice feature Bergmeister's papilla, a structural remnant of the developmental hyaloid vascular system (HVS) at the optic disc.[21] Indeed, angiography showed characteristic perfusion of the HVS in mice until approximately P10 (data not shown), after which the hyaloid artery usually obliterates and leaves behind the channel of Cloquet.[22] In some animals, however, this development remains incomplete, leading to Bergmeister's papilla, as seen in Figure 1F.

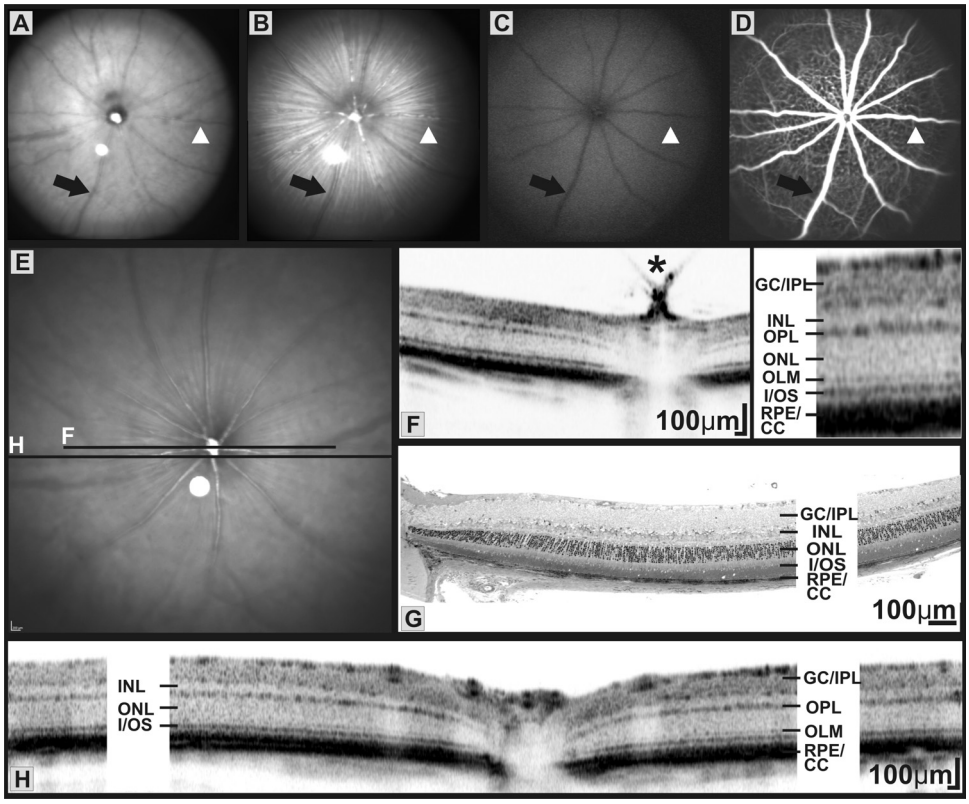


**FIGURE 1.** Retinal SLO imaging and OCT in C57BL/6 mice (PW4) with a regular retinal structure. (**A–D**) Representative example of en face imaging using cSLO. (**A**) Native IR (830 nm), (**B**) RF (513 nm), and (**C**) AF mode. (**D**) Fluorescein angiography (FLA) confirming an intact retinal vasculature (*arrowhead*, artery; *arrow*, vein). (**E–H**) Corresponding OCT data. (**E**) Fundus picture with indicated orientation of cross-sectional SD-OCT scans. (**F**) Corresponding B-scan at the optic nerve head displaying a Bergmeister's papilla characterized by a structural remnant of the developmental hyaloid vascular system (*asterisk*), including enlarged image. (**G**) Light microscopic data of an age-matched C57BL/6 animal. (**H**) Representative B-scan with retinal layers labeled. GC/IPL, ganglion cell/inner plexiform layer; OLM, outer limiting membrane; RPE/ChC, RPE/choriocapillary complex.

## BALB/c

En face imaging in BALB/c mice (postnatal week [PW]10) using cSLO showed nonpigmented retinal structures in the native RF (513 nm), IR (830 nm), and AF modes (Fig. 2). Given that BALB/c mice are highly susceptible to light-induced retinal degeneration,[23,24] the hyperfluorescent dots in the AF mode may reflect lipid degradation products. Accordingly, overall retinal thickness in the central 3 mm, as determined by SD-OCT, was 211 ± 10 $\mu$m, considerably less than in the C57BL/6 strain, which would be hypothetically consistent with a mild light-induced photoreceptor loss. Virtual cross-sections displayed identical laminar organization in the inner retina compared with C57BL/6. However, because lack of pigmentation in BALB/c mice resulted in altered optical characteristics in the outer retina, signal composition of SD-OCT scans distal of the external limiting membrane (ELM) differed considerably (Fig. 2). Specifically, instead of two highly reflective layers (HRLs) thought to represent the inner/outer segment border (I/OS) and RPE (Fig. 1), SD-OCT scans in BALB/c mice demonstrated two additional HRLs possibly demarcating the nonpigmented choriocapillary and choroidal structures (Fig. 2).

## *Rho*$^{-/-}$

The visual pigment of the rod photoreceptors, rhodopsin, is an essential element of the phototransduction cascade and serves as a structural protein of the discs in the rod outer segments (ROS). Hence, in rhodopsin-deficient mice (*Rho*$^{-/-}$), ROS are never formed, and rod-derived ERG signals cannot be generated.[15] En face imaging in *Rho*$^{-/-}$ mice (PW4) using cSLO showed characteristic signs of retinal degeneration with RPE irregularities visible in the native RF (513 nm, not shown), IR (830 nm), and AF modes (Fig. 3). SD-OCT imaging revealed a complete lack of ROS, whereas the ONL appeared only marginally thinner than the wild-type retina. Accordingly, central retinal thickness in *Rho*$^{-/-}$ mice was reduced to 193 ± 2 $\mu$m. The entire retina showed an absence of ROS, but the outer limiting membrane seemed not to be disturbed and could be distinguished from the RPE signal by a distance roughly equivalent to the extent of inner segment remnants (Fig. 3). Similarly, histologic sections showed an absence of ROS, whereas the outer nuclear layer appeared essentially intact with approximately six to eight rows of nuclei (Fig. 3).

## *Rpe65*$^{-/-}$

Mutations in the gene encoding *RPE65* causes LCA2, a major form of Leber's congenital amaurosis,[25–27] which is targeted in current clinical gene therapy trials.[28,29] The protein RPE65 is expressed in the RPE, where it plays a pivotal role in maintaining normal vision by regenerating the visual pigment rhodopsin.[16] In *Rpe65*$^{-/-}$ mice, the blocked visual cycle causes an accumulation of retinyl esters in RPE cells, where they form large lipid droplets (Fig. 4A). Cone photoreceptors degenerate

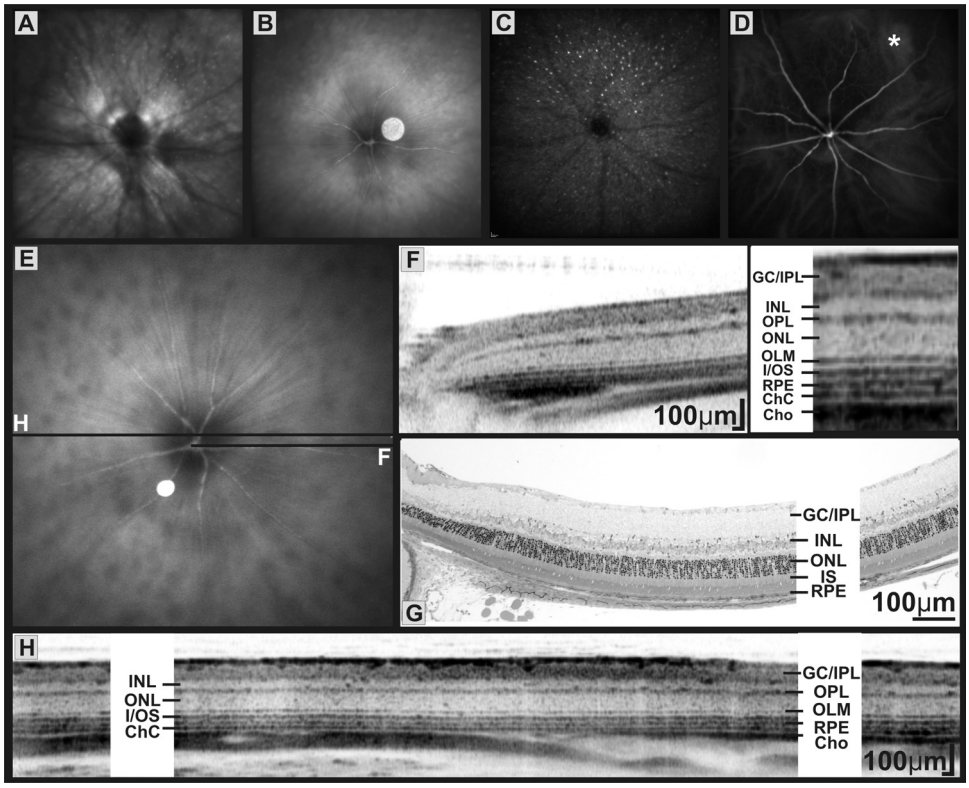


**FIGURE 2.** Retinal SLO imaging and OCT in BALB/c mice (PW10). Typical results of cSLO en face imaging in the presence of nonpigmented retinal structures in (**A**) native IR (830 nm), (**B**) RF (513 nm), and (**C**) AF modes. (**D**) Fluorescein angiography in BALB/c mice displayed both retinal and choroidal vasculature (*asterisk*) because lack of pigment allowed light at $\lambda = 488$ nm to better penetrate the RPE/choriocapillary complex. (**E**) Fundus image with indicated orientation (**F**, **H**) of corresponding B-scans. (**G**) Representative histologic data of an age-matched BALB/c mouse. (**H**) Virtual cross-section with designation of the different retinal layers. Note the altered signal composition in the outer retina because of the absence of pigmentation in BALB/c mice (**F**). There are four HRLs possibly demarcating the I/OS, RPE, nonpigmented choriocapillary, and choroidal structures. GC/IPL, ganglion cell/inner plexiform layer; OLM, outer limiting membrane; RPE/ChC, RPE/choriocapillary complex; Cho, choroid.

rapidly, whereas the remaining rods are the exclusive source of electrophysiological response and start to degenerate slowly only after approximately 6 months of age.[30,31] En face imaging at postnatal month (PM) 11 showed a characteristic pattern of hyperfluorescent flecks in the AF mode, which may again indicate metabolic remnants of photoreceptor outer segments (Fig. 4). Image resolution of SD-OCT in *Rpe65*$^{-/-}$ mice was insufficient to resolve intracellular lipid accumulations in vivo.

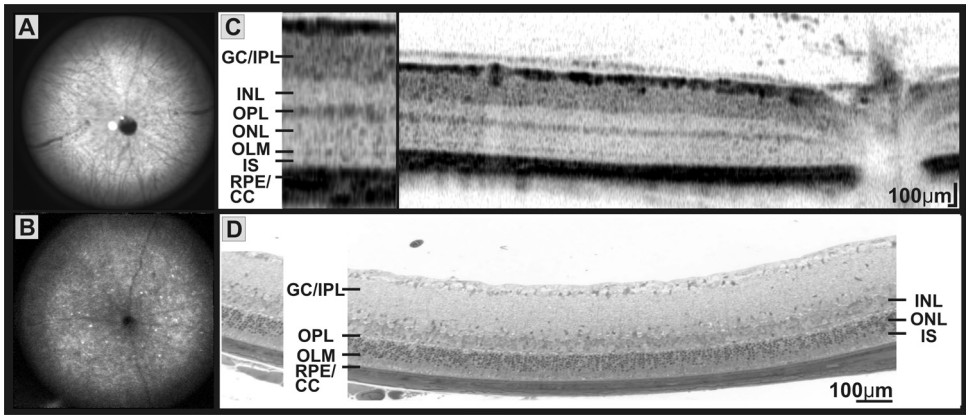


**FIGURE 3.** Retinal degeneration and RPE irregularities in the *Rho*$^{-/-}$ mouse model (PW4). (**A**) Native IR (830 nm) and (**B**) AF mode cSLO data. (**C**) SD-OCT section and enlarged image, revealing a complete absence of ROS together with an apparent thinning of the ONL. (**D**) Ex vivo histology for comparison, confirming the observed reduction in ONL thickness and the lack of ROS. GC/IPL, ganglion cell/inner plexiform layer; OLM, outer limiting membrane; IS, photoreceptor inner segments; RPE/ChC, RPE/choriocapillary complex.

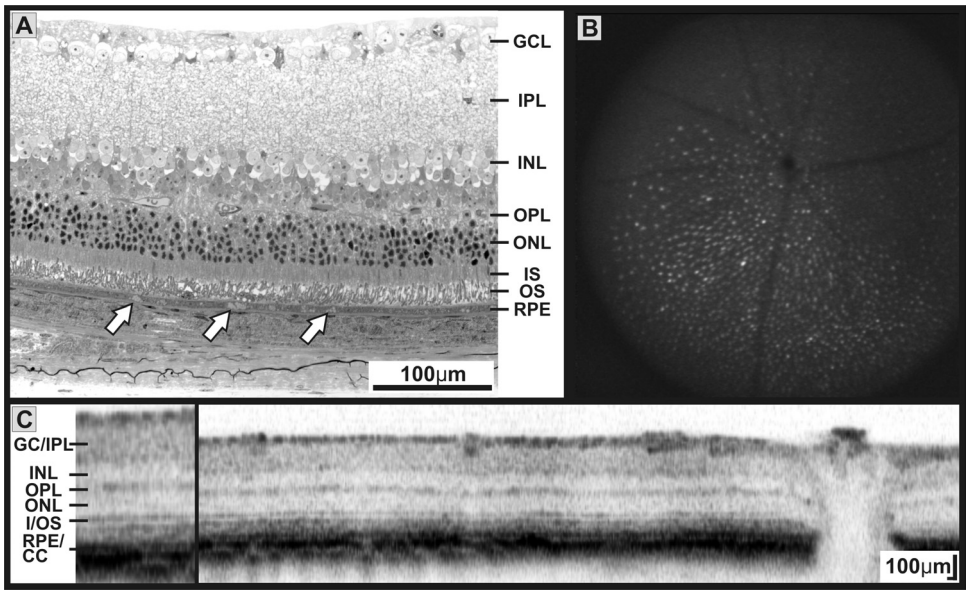


**Figure 4.** Retinal degeneration and RPE irregularities in the *Rpe65*$^{-/-}$ mouse model (PM11). (**A**) Histology showing lipid droplets from stored retinyl esters (*arrows*) in the RPE, together with a reduced retinal thickness. (**B**) Spots of hyperfluorescence in the AF mode, suggesting the presence of photoreceptor debris. (**C**) OCT cross-sectional image confirming a reduction of ONL thickness, though laminar organization (enlarged image) was not as clearly delineated as in wild-type mice. GC/IPL, ganglion cell/inner plexiform layer OLM, outer limiting membrane; RPE/ChC, RPE/choriocapillary complex.

However, cross-sectional images revealed a reduction of ONL size, resulting in decreased total central retinal thickness of 193 ± 2 μm, which is more than the expected roughly 10% reduction with age and would be consistent with the observed AF.[32] Laminar organization in *Rpe65*$^{-/-}$ mice was not as clearly delineated, perhaps because of a generalized reaction to the ongoing photoreceptor loss. Indeed, it has been shown that the genetic response in *Rpe65*$^{-/-}$ mice includes modified expression of cytoskeletal elements and components of the extracellular matrix.[33] Such a global response might reasonably affect the optical characteristics of the retinal sublayers.

### *rd1*

The autosomal recessive retinal degeneration in the *rd1* mouse is caused by a loss-of-function mutation in the gene encoding the β subunit of the rod cGMP phosphodiesterase 6 (PDE6β).[34] Numerous mutations in the catalytic domain of the human homolog, *PDE6β*, have been found in human patients with autosomal recessive retinitis pigmentosa (arRP).[35,36] Hence, the *rd1* mouse and other mouse strains harboring PDE6β mutant alleles are considered relevant animal models of retinitis pigmentosa.

First signs of rod photoreceptors cell loss in *rd1* mice become evident at approximately, P10 when looking at TUNEL stainings, whereas ONL reduction become evident at age P12 and P13 and most rod photoreceptor nuclei have disappeared by P21.[37,38] En face imaging in *rd1* mice at P11 failed to detect signs of retinal degeneration. In contrast, *rd1* mice at P28 revealed significant retinal degeneration both in the cSLO and SD-OCT imaging (Fig. 5). Cross-sectional images showed an intact inner retina, whereas the inner nuclear layer (INL) seemed to border the RPE almost directly with the OPL/ONL and photoreceptor segments virtually nonexistent. Although central retinal thickness in *rd1* at P28 showed a marked reduction to only 145 ± 5 μm, *rd1* mice at P11 featured a central retinal thickness at 246 ± 2 μm. The rapid progression of retinal degeneration in the *rd1* model has been analyzed before using a custom-made SD-OCT device.[5] This study adds to the published data by presenting the onset of retinal degeneration in this model and resolving the retinal architecture before photoreceptor cell death (P11).

### SD-OCT versus Histology

Direct comparison of inner and outer retinal thickness assessed either by SD-OCT or histomorphometric analysis revealed excellent correlation (Figs. 6A–D). Consistent with existing data based largely on histologic assessment,[15,31,37] SD-OCT data revealed a significant reduction of the outer retinal thickness in *Rho*$^{-/-}$, *RPE65*$^{-/-}$, and BALB/c mice compared with C57/Bl6 animals (Fig. 6A). Similarly, timeline analysis of C3H wild-type versus C3H rd1/rd1 mice at P11 and P28 showed significant changes only in the rd1 mice at P28 (Fig. 6B). Traditional histomorphometric assessment mirrored the findings gained by SD-OCT data analysis (Fig. 6C), and direct comparison between the two data sets revealed excellent correlation coefficients for the whole retinal thickness ($R^2$ = 0.897) and outer retinal thickness, respectively ($R^2$ = 0.978). When analyzing the two data sets stemming from different protocols for histology separately (data not shown), the protocol using overnight fixation (*Rho*$^{-/-}$, *RPE65*$^{-/-}$, BALB/c, and C57/Bl6) featured the lower correlation coefficient ($r^2$ = 0.802) compared with the protocol using direct embedding, freezing, and sectioning (C3H wild-type and C3H rd1/rd1 mice at P11 and P28 [$r^2$ = 0.954]). This could arguably be attributed to differential shrinkage during processing for histology, and it highlights the benefit of noninvasive assessment of retinal thickness by SD-OCT.

## Discussion

OCT has emerged as a valuable tool to analyze and monitor structural changes in the retina. Although noninvasive in character, the resolution of cross-sectional images obtained by third-generation OCT begins to approach the level of low-power micrographs gained from light microscopy. This allows for detailed in vivo structural analysis of retinal disorders and

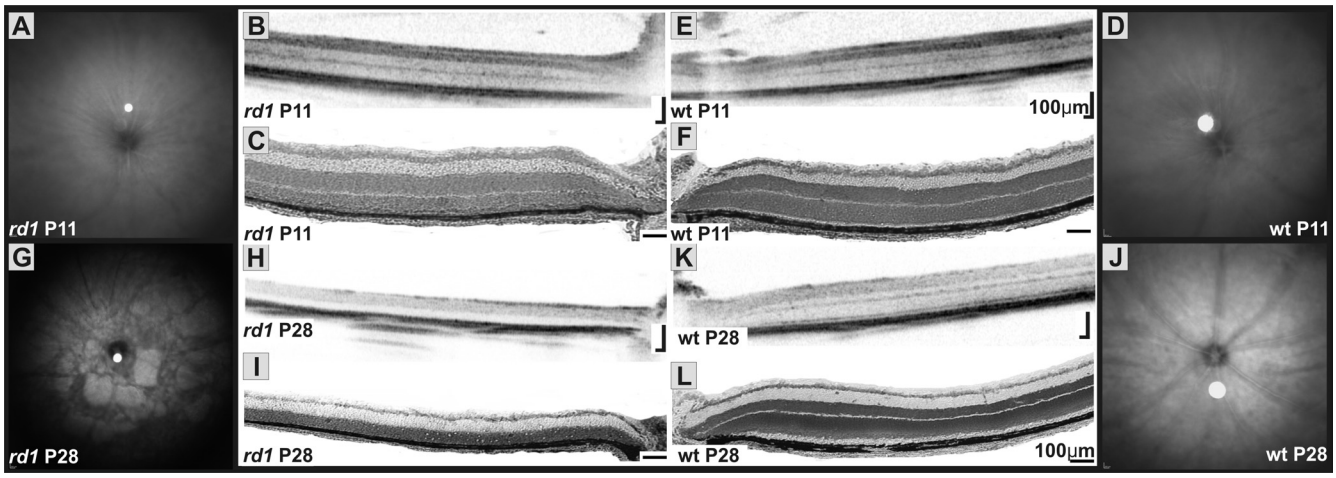


**FIGURE 5.** En face and SD-OCT imaging in *rd1* and corresponding wild-type control mice at P11 and P28. At P11, no signs of retinal degeneration were evident in (**A**, **D**) cSLO or (**B**, **E**) SD-OCT imaging. (**C**, **F**) Histology confirmed normal ONL thickness. In contrast, *rd1* mice at P28 revealed significant retinal degeneration (**G**). This pattern was also evident in the SD-OCT cross-sectional images (**H**) and corresponding histology (**I**), where inner retinal layers appeared intact, whereas the INL seemed to border the RPE almost directly. OPL/ONL and photoreceptor segments were virtually nonexistent. (**J**–**L**) Wild-type controls at P28 showed no signs of retinal degeneration. Scale bars, 100 μm.

bears importance for a refined genotype/phenotype correlation in a clinical setting and for noninvasive longitudinal studies on animal models that mimic respective disease characteristics. Indeed, various prototype OCT setups have been reported to allow noninvasive, high-resolution imaging of rodent retina.[6,7] Srinivasan et al.[7] used a custom build OCT setup to scan a normal C57/Bl6 mouse and to analyze the retinal thickness in a virtual cross-section obtained from a Long-Evans rat. Ruggeri et al.[6] demonstrated noninvasive retinal imaging (e.g., in a mouse model of retinal degeneration, $Rho^{-/-}$) using an experimental OCT system. Both studies compare single virtual cross-sections with conventional histology without quantification, whereas others have used custom OCT systems to monitor the dynamic changes of natural disease progression in respective animal models.[2,3,5] Yet the potential to evaluate therapeutic or adverse effects of experimental interventions in time-course experiments might prove to be even more important. Consequently, comparability between individual preclinical studies and preferably also between the preclinical and clinical setting will be of eminent importance. This is a challenge that is best addressed using commercially available equipment already approved for clinical use. In this study, we present data from frequently used wild-type mice and models of hereditary retinal degeneration using a commercially available third-generation OCT device approved for clinical diagnostic use.

The identity of signal composition in linear A- and two-dimensional B-scans acquired by OCT imaging has been subject to debate. However, it is generally thought[1,39,40] that—from vitreous to sclera—the first thin dark band resembles the nerve fiber layer followed by the lighter ganglion cell layer. The consecutive thick band of higher intensity illustrates the inner plexiform layer (IPL), approximated by a light band, the INL. The OPL appears as a thin stripe with signal intensity comparable to that of the IPL. The outer retina is composed of a thick light band, and ONL signal intensity is similar to that of INL. Apparently, both nuclear layers share the low signal intensity because they scatter or reflect light to a lesser extent than do both plexiform layers, which appear much darker. Located just distal to the ONL is the ELM, which is formed by adherence junctions between apical villi of Müller glia cells and distal photoreceptor cell bodies. Photoreceptor inner segments appear with the same signal intensity as the cell bodies, whereas the I/OS generates a strong signal possibly because of the high mitochondrial content in the ellipsoid region of the outer segment.[39] The photoreceptor outer segments are visible between the I/OS border and the equally strong signal of the RPE/choriocapillary complex. In pigmented retinas, choroidal structures cannot be reliably detected because light is almost completely scattered or reflected as it travels through the more proximal layers. In nonpigmented retinas, the signal composition is considerably different distal of the ELM (Fig. 2), which argues for scatter/reflection attributed to melanin granules as playing the main part in this phenomenon.

Earlier work exploring the correlation between OCT and histology in mice was performed primarily with second-generation, time-domain[2] or custom-made, high-resolution OCT devices[5] and reported a substantial overestimation of retinal thickness by OCT.[3] In this study we used a commercially available SD-OCT device and obtained high overall correlation of total retinal thickness ($R^2 = 0.897$) with only minor overestimation (2.5%) of retinal thickness by OCT. Interestingly, correlation of outer retinal thickness representing the photoreceptor cell layer separately showed an even higher Pearson's correlation coefficient ($R^2 = 0.978$, Fig. 6D). Overall, the results obtained in vivo are in good agreement with earlier studies on the three animal models for retinal degeneration.[15,31,37]

Although conventional histology features higher resolution, OCT delivers the advantage of producing morphologic data undistorted by handling, fixating, and staining procedures while being coregistered with en face topologic information. The latter aspect is particularly useful when assessing retinal degeneration types that do not show a uniform progression in the entire retina. OCT-based screening may also be useful for breeding purposes because it enables a noninvasive assessment of retinal health in mouse strains that are prone to develop sporadic retinal degeneration.

Analogous to electroretinography, by which the use of identical hardware in the clinical setting and laboratory has led to new insights,[31] the application of a clinically approved OCT device for animal studies bears the potential to translate insights from bench to bedside in an efficient and timely manner. Here, we present evidence on the efficacy of a commercially available SD-OCT in small animal retinal imaging and provide in vivo structural data on mouse models of retinal degeneration. This should facilitate further studies on dynamic changes of retinal structure through the natural course of disease and

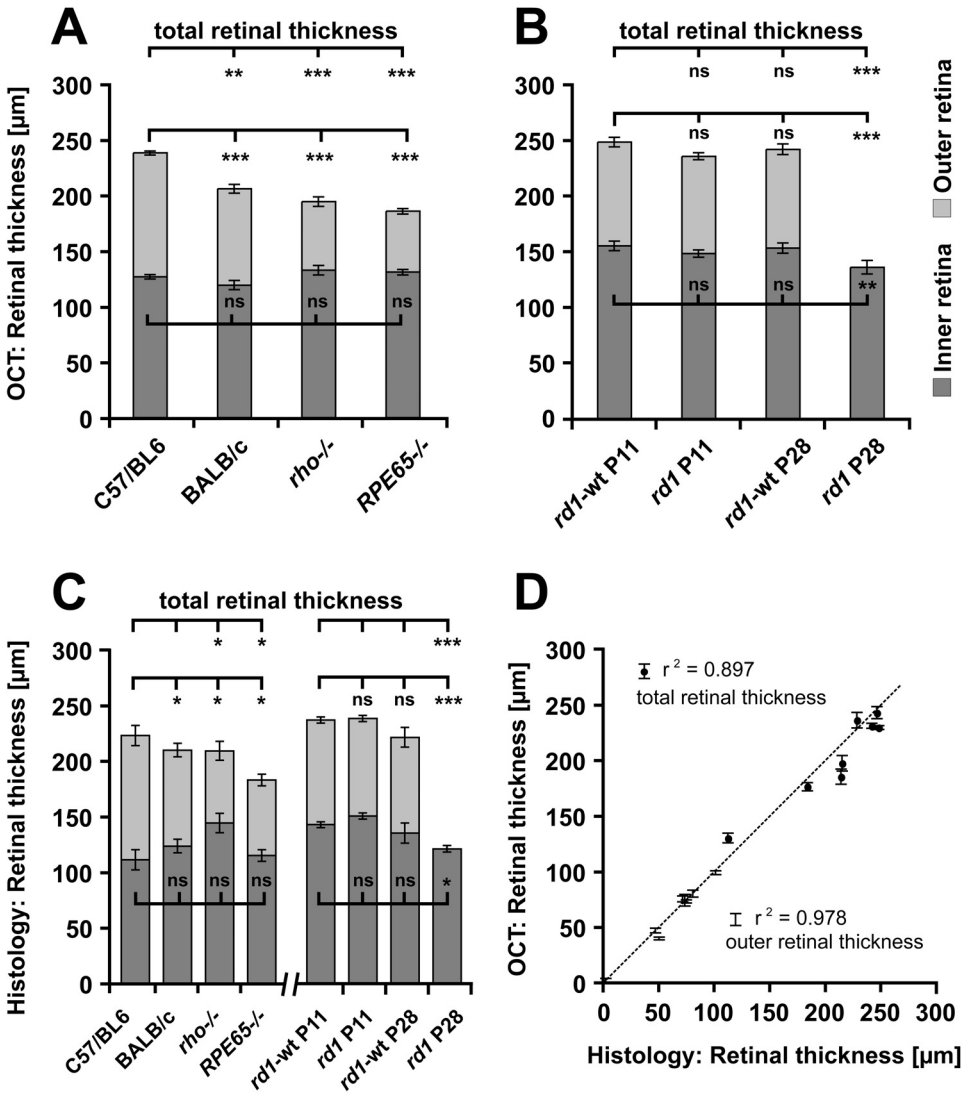


**Figure 6.** Evaluation of inner and outer retinal thickness in wild-type mice and animal models of hereditary retinal degeneration using either SD-OCT in vivo imaging or conventional morphometric assessment by histology. (**A–C**) Bar graphs indicate inner (*dark*) and outer (*light*) retinal thickness. (**A**) Note statistically significant reduction of outer but not inner retinal thickness in BALB/c, $Rho^{-/-}$ and $RPE65^{-/-}$ compared with C57/BL6 mice. (**B**) There is no statistical significant difference between *rd1* and wild-type mice at P11. Although outer retina remained unchanged in the wild-type mice at P28, there is complete loss of outer retina in the age-matched *rd1* mice. (**C**) Conventional morphometric assessment of retinal thickness in histologic sections with similar changes as reported by SD-OCT (**A**, **B**). Significance was calculated using Student's *t*-test. ns, not significant ($P > 0.01$); $^{*}P \leq 0.01$; $^{**}P \leq 0.001$; $^{***}P \leq 0.0001$. (**D**) Scatter plot shows the correlation of histologic versus OCT data on total (*dots*) and outer (*error bars* only) retinal thickness from C57/BL6, BALB/c, $Rho^{-/-}$, $RPE65^{-/-}$, *rd1-wt* P11, *rd1* P11, *rd1-wt* P28, and *rd1* P28 mice. Pearson's correlation coefficients ($r^2$) are displayed for total retinal thickness ($y = 0.975x$) and outer retinal thickness ($y = 1.018x$) separately. All data are reported as mean ± SD (*error bars*).

should help to monitor putative therapeutic effects of novel interventional strategies.

## *References*


1. Drexler W, Fujimoto JG. State-of-the-art retinal optical coherence tomography. *Prog Retin Eye Res.* 2008;27:45–88.
2. Horio N, Kachi S, Hori K, et al. Progressive change of optical coherence tomography scans in retinal degeneration slow mice. *Arch Ophthalmol.* 2001;119:1329–1332.
3. Li Q, Timmers AM, Hunter K, et al. Noninvasive imaging by optical coherence tomography to monitor retinal degeneration in the mouse. *Invest Ophthalmol Vis Sci.* 2001;42:2981–2989.
4. Anger EM, Unterhuber A, Hermann B, et al. Ultrahigh resolution optical coherence tomography of the monkey fovea: identification of retinal sublayers by correlation with semithin histology sections. *Exp Eye Res.* 2004;78:1117–1125.
5. Kim KH, Puoris'haag M, Maguluri GN, et al. Monitoring mouse retinal degeneration with high-resolution spectral-domain optical coherence tomography. *J Vis.* 2008;17:1–11.
6. Ruggeri M, Wehbe H, Jiao S, et al. In vivo three-dimensional high-resolution imaging of rodent retina with spectral-domain optical coherence tomography. *Invest Ophthalmol Vis Sci.* 2007;48:1808–1814.
7. Srinivasan VJ, Ko TH, Wojtkowski M, et al. Noninvasive volumetric imaging and morphometry of the rodent retina with high-speed,

ultrahigh-resolution optical coherence tomography. *Invest Ophthalmol Vis Sci.* 2006;47:5522–5528.
8. Wolf-Schnurrbusch UE, Enzmann V, Brinkmann CK, Wolf S. Morphological changes in patients with geographic atrophy assessed with a novel spectral OCT-SLO combination. *Invest Ophthalmol Vis Sci.* 2008;49:3095–3099.
9. Chang B, Hawes NL, Hurd RE, Davisson MT, Nusinowitz S, Heckenlively JR. Retinal degeneration mutants in the mouse. *Vision Res.* 2002;42:517–525.
10. Seeliger MW, Beck SC, Pereyra-Munoz N, et al. In vivo confocal imaging of the retina in animal models using scanning laser ophthalmoscopy. *Vision Res.* 2005;45:3512–3519.
11. Buttery RG, Hinrichsen CF, Weller WL, Haight JR. How thick should a retina be? A comparative study of mammalian species with and without intraretinal vasculature. *Vision Res.* 1991;31:169–187.
12. Hanstede JG, Gerrits PO. The effects of embedding in water-soluble plastics on the final dimensions of liver sections. *J Microsc.* 1983;131:79–86.
13. O'Steen WK, Sweatt AJ, Eldridge JC, Brodish A. Gender and chronic stress effects on the neural retina of young and mid-aged Fischer-344 rats. *Neurobiol Aging.* 1987;8:449–455.
14. Chaudhuri A, Hallett PE, Parker JA. Aspheric curvatures, refractive indices and chromatic aberration for the rat eye. *Vision Res.* 1983;23:1351–1363.
15. Humphries MM, Rancourt D, Farrar GJ, et al. Retinopathy induced in mice by targeted disruption of the rhodopsin gene. *Nat Genet.* 1997;15:216–219.
16. Redmond TM, Yu S, Lee E, et al. Rpe65 is necessary for production of 11-cis-vitamin A in the retinal visual cycle. *Nat Genet.* 1998;20:344–351.
17. Frasson M, Picaud S, Leveillard T, et al. Glial cell line-derived neurotrophic factor induces histologic and functional protection of rod photoreceptors in the rd/rd mouse. *Invest Ophthalmol Vis Sci.* 1999;40:2724–2734.
18. Azadi S, Paquet-Durand F, Medstrand P, van Veen T, Ekstrom PA. Up-regulation and increased phosphorylation of protein kinase C (PKC) delta, mu and theta in the degenerating rd1 mouse retina. *Mol Cell Neurosci.* 2006;31:759–773.
19. Hauck SM, Ekstrom PA, Ahuja-Jensen P, et al. Differential modification of phosducin protein in degenerating rd1 retina is associated with constitutively active Ca2+/calmodulin kinase II in rod outer segments. *Mol Cell Proteomics.* 2006;5:324–336.
20. Samardzija M, Wenzel A, Aufenberg S, Thiersch M, Reme C, Grimm C. Differential role of Jak-STAT signaling in retinal degenerations. *FASEB J.* 2006;20:2411–2413.
21. Jaffe NS. The vitreous. *Arch Ophthalmol.* 1971;85:501–509.
22. Eisner G. [Postmortem slitlamp study of the vitreous body, II: pattern of vitreous structures made visible by the slitbeam]. *Albrecht Von Graefes Arch Klin Exp Ophthalmol.* 1971;182:8–22.
23. LaVail MM, Gorrin GM, Repaci MA. Strain differences in sensitivity to light-induced photoreceptor degeneration in albino mice. *Curr Eye Res.* 1987;6:825–834.
24. LaVail MM, Gorrin GM, Repaci MA, Thomas LA, Ginsberg HM. Genetic regulation of light damage to photoreceptors. *Invest Ophthalmol Vis Sci.* 1987;28:1043–1048.
25. Gu SM, Thompson DA, Srikumari CR, et al. Mutations in RPE65 cause autosomal recessive childhood-onset severe retinal dystrophy. *Nat Genet.* 1997;17:194–197.
26. Lorenz B, Gyurus P, Preising M, et al. Early-onset severe rod-cone dystrophy in young children with RPE65 mutations. *Invest Ophthalmol Vis Sci.* 2000;41:2735–2742.
27. Marlhens F, Bareil C, Griffoin JM, et al. Mutations in RPE65 cause Leber's congenital amaurosis. *Nat Genet.* 1997;17:139–141.
28. Bainbridge JW, Smith AJ, Barker SS, et al. Effect of gene therapy on visual function in Leber's congenital amaurosis. *N Engl J Med.* 2008;358:2231–2239.
29. Maguire AM, Simonelli F, Pierce EA, et al. Safety and efficacy of gene transfer for Leber's congenital amaurosis. *N Engl J Med.* 2008;358:2240–2248.
30. Rohrer B, Lohr HR, Humphries P, Redmond TM, Seeliger MW, Crouch RK. Cone opsin mislocalization in Rpe65$^{-/-}$ mice: a defect that can be corrected by 11-cis retinal. *Invest Ophthalmol Vis Sci.* 2005;46:3876–3882.
31. Seeliger MW, Grimm C, Stahlberg F, et al. New views on RPE65 deficiency: the rod system is the source of vision in a mouse model of Leber congenital amaurosis. *Nat Genet.* 2001;29:70–74.
32. Gresh J, Goletz PW, Crouch RK, Rohrer B. Structure-function analysis of rods and cones in juvenile, adult, and aged C57BL/6 and Balb/c mice. *Vis Neurosci.* 2003;20:211–220.
33. Cottet S, Michaut L, Boisset G, Schlecht U, Gehring W, Schorderet DF. Biological characterization of gene response in Rpe65$^{-/-}$ mouse model of Leber's congenital amaurosis during progression of the disease. *FASEB J.* 2006;20:2036–2049.
34. Bowes C, Li T, Danciger M, Baxter LC, Applebury ML, Farber DB. Retinal degeneration in the rd mouse is caused by a defect in the beta subunit of rod cGMP-phosphodiesterase. *Nature.* 1990;347:677–680.
35. McLaughlin ME, Ehrhart TL, Berson EL, Dryja TP. Mutation spectrum of the gene encoding the beta subunit of rod phosphodiesterase among patients with autosomal recessive retinitis pigmentosa. *Proc Natl Acad Sci U S A.* 1995;92:3249–3253.
36. McLaughlin ME, Sandberg MA, Berson EL, Dryja TP. Recessive mutations in the gene encoding the beta-subunit of rod phosphodiesterase in patients with retinitis pigmentosa. *Nat Genet.* 1993;4:130–134.
37. Paquet-Durand F, Silva J, Talukdar T, et al. Excessive activation of poly(ADP-ribose) polymerase contributes to inherited photoreceptor degeneration in the retinal degeneration 1 mouse. *J Neurosci.* 2007;27:10311–10319.
38. Sancho-Pelluz J, Arango-Gonzalez B, Kustermann S, et al. Photoreceptor cell death mechanisms in inherited retinal degeneration. *Mol Neurobiol.* 2008;38:253–269.
39. Fischer MD, Fleischhauer JC, Gillies MC, Sutter FK, Helbig H, Barthelmes D. A new method to monitor visual field defects caused by photoreceptor degeneration by quantitative optical coherence tomography. *Invest Ophthalmol Vis Sci.* 2008;49:3617–3621.
40. Srinivasan VJ, Monson BK, Wojtkowski M, et al. Characterization of outer retinal morphology with high-speed, ultrahigh-resolution optical coherence tomography. *Invest Ophthalmol Vis Sci.* 2008;49:1571–1579.

# Excessive HDAC activation critical for neurodegeneration in the *rd1* mouse.

*Sancho-Pelluz J, Alavi M,* ***Sahaboglu A****, Kustermann S, Farinelli P, Azadi S, Van Veen T, Romero F.J, Paquet-Durand F, Ekström P.*

*Published in "Cell Death & Disease" doi:10.1038/cddis.2010.4. (2010)*

Citation: Cell Death and Disease (2010) 1, e24; doi:10.1038/cddis.2010.4

www.nature.com/cddis

# Excessive HDAC activation is critical for neurodegeneration in the *rd1* mouse

J Sancho-Pelluz[1,2], MV Alavi[3,4], A Sahaboglu[1], S Kustermann[1], P Farinelli[4], S Azadi[5], T van Veen[1,4], FJ Romero[2], F Paquet-Durand*[,1] and P Ekström[4]

**Inherited retinal degenerations, collectively termed retinitis pigmentosa (RP), constitute one of the leading causes of blindness in the developed world. RP is at present untreatable and the underlying neurodegenerative mechanisms are unknown, even though the genetic causes are often established. Acetylation and deacetylation of histones, carried out by histone acetyltransferases (HATs) and histone deacetylases (HDACs), respectively, affects cellular division, differentiation, death and survival. We found acetylation of histones and probably other proteins to be dramatically reduced in degenerating photoreceptors in the *rd1* human homologous mouse model for RP. Using a custom developed *in situ* HDAC activity assay, we show that overactivation of HDAC classes I/II temporally precedes photoreceptor degeneration. Moreover, pharmacological inhibition of HDACs I/II activity in *rd1* organotypic retinal explants decreased activity of poly-ADP-ribose-polymerase and strongly reduced photoreceptor cell death. These findings highlight the importance of protein acetylation for photoreceptor cell death and survival and propose certain HDAC classes as novel targets for the pharmacological intervention in RP.**

*Cell Death and Disease* (2010) **1,** e24; doi:10.1038/cddis.2010.4; published online 11 February 2010
**Subject Category:** Neuroscience



Retinitis pigmentosa (RP) is a group of inherited neurodegenerative diseases that result in selective cell death of retinal photoreceptors. Usually the mutations first lead to degeneration of the rod photoreceptor cells followed by a mutation-independent secondary degeneration of cone photoreceptors. With a prevalence of about 1 : 3500, RP is considered as the main cause of blindness among the working age population in the developed world. At least 40 RP causing mutations have been identified so far, but the metabolic pathways leading to photoreceptor cell death have not been resolved, and no adequate RP treatment is available.[1]

The *rd1* mouse is one of the most studied human homologous RP animal models and carries a loss-of-function mutation in the gene encoding for the $\beta$-subunit of rod photoreceptor cGMP phosphodiesterase-6.[2] This leads to an accumulation of cGMP, which eventually causes photoreceptor cell death.[3,4] In microarray experiments, we and others found *rd1* degeneration to be accompanied by extensive changes in gene expression.[5–7] Although some changes may result from direct and specific effects of cGMP on defined genes,[8] it is likely that also more generalized alterations of the transcriptional machinery are involved. Previously, we have shown that *rd1* photoreceptor degeneration is in part caused by a strong activation of poly-ADP-ribose-polymerase (PARP),[9] which may have a bearing on transcriptional activity.[10] However, as PARP activity was found to occur only relatively late during *rd1* degeneration, we hypothesized that there might be yet other mechanisms causing dysregulation of gene expression.

Gene regulation is to a large extent governed by epigenetic mechanisms, among which acetylation of histones[11] appears to be one of the most important.[12] Histone acetylation and deacetylation is mediated by histone acetyltransferases (HATs) and histone deacetylases (HDACs), respectively.[13] The HDAC family is subdivided into three main classes (HDAC I, II, and III), depending on their similarity with homologous yeast genes. Class I (HDAC 1–3 and 8) and class II (HDAC 4–7, 9, and 10) are inhibited by trichostatin A (TSA).[13] Class III HDACs, also referred to as sirtuins (isoforms: sirt1–7) form a structurally distinct class of

[1]Division of Experimental Ophthalmology, Institute for Ophthalmic Research, University of Tübingen, Tübingen, Germany; [2]Fundación Oftalmológica del Mediterráneo, Universidad Cardenal Herrera-CEU, Valencia, Spain; [3]Molecular Genetics Laboratory, Institute for Ophthalmic Research, University of Tübingen, Tübingen, Germany; [4]Department of Ophthalmology, Clinical Sciences, Lund, University of Lund, Sweden and [5]Department of Biochemistry and Molecular Biology, University of British Columbia, BC, Canada
*Corresponding author: F Paquet-Durand, Institute for Ophthalmic Research, University Eye Clinic Tübingen, Röntgenweg 11, Tübingen 72076, Germany.
Tel: + +49 (0) 7071 29 87430; Fax: + +49 (0) 7071 29 5777; E-mail: francois.paquet-durand@klinikum.uni-tuebingen.de
**Keywords:** epigenetic; neuroprotection; trichostatin A; retina; sirtuin; retinitis pigmentosa
**Abbreviations:** ab, antibody; abs, antibodies; CBP, CREB-binding-protein; CREB, cyclic AMP-response-element-binding; CRX, cone-rod-homeobox; GCL, ganglion cell layer; HDAC, histone deacetylase; INL, inner nuclear layer; $NAD^+$, nicotinamide dinucleotide; NAM, nicotinamide; ONL, outer nuclear layer; P, post-natal day; PFA, paraformaldehyde; PBS, phosphate buffered saline; PDE6, phosphodiesterase-6; PAR, poly-ADP-ribose; PARP, poly-ADP-ribose-polymerase; RP, retinitis pigmentosa; SEM, standard error of the mean; TUNEL, terminal deoxynucleotidyl transferase dUTP nick end labelling; TSA, trichostatin A; WB, western blot
Received 23.12.09; accepted 04.1.10; Edited by A Verkhratsky

$NAD^+$-dependent enzymes that can be inhibited by nicotinamide (NAM).[14]

Although a number of studies have related transcription of photoreceptor genes and photoreceptor viability with histone acetylation,[15–17] information regarding whether and how HDAC activity connects to degenerating photoreceptors is lacking. Here, we analyzed enzymatic activities of different HDAC classes *in situ* on retinal tissue sections and studied how various inhibitors affect retinal cell viability. Activity of HDACs I/II was strongly elevated in *rd1* photoreceptors and causally related to their death, suggesting HDAC inhibition as a novel approach for neuroprotection in retinal degeneration.

## Results

**Expression of HDACs in *wt* and *rd1* retina.** Microarray analysis of the expression of 13 different HDAC genes did not identify any significant differences between wild type (*wt*) and *rd1* (Figure 1a). Immunohistology revealed that HDACs representing all three major classes were present in *wt* and *rd1* retina at post-natal day (P) 11. Both class I HDAC2 (Figure 1a, d) and class II HDAC5 (Figure 1b, e) were prominently expressed in nuclei of the outer nuclear layer (ONL), inner nuclear layer (INL), and ganglion cell layer. In contrast, class III HDAC Sirt2 (Figure 1c, f) was expressed predominantly in non-nuclear structures including photoreceptor segments, neuritic processes in the ONL, and different INL cells. No obvious differences in expression or localization between *wt* and *rd1* at P11 were detected for any of the HDACs.

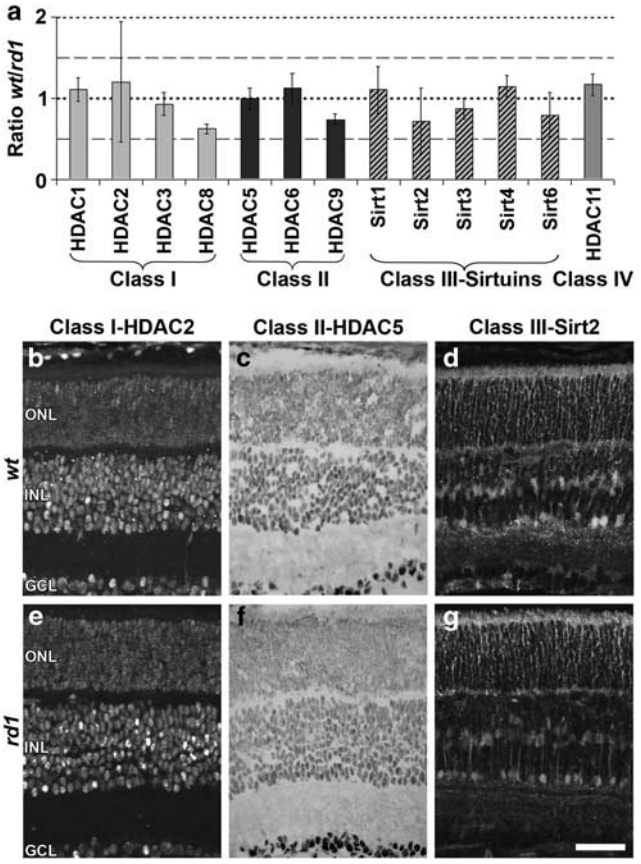


**Figure 1** Micro-array analysis and immunodetection of different HDAC isoforms in *wt* and *rd1* retinae at P11 *in vivo*. mRNA expression for 14 different HDAC isoforms pertaining to all four HDAC classes was assessed using micro-array analysis. (**a**) For all studied HDAC isoforms, the ratio of mRNA expression *wt/rd1* was not significantly different from 1, indicating that expression was not changed. Values are mean ± SEM from five independent hybridization experiments, each containing retinae from four male *wt* and four *rd1* animals. Immunostaining was performed for three different HDAC isoforms representing HDAC classes I–III. HDAC2 (**b**, **e**) and HDAC5 (**c**, **f**) were expressed in the nuclei of ONL, INL, and GCL, while Sirt2 (**d**, **g**) was expressed in photoreceptor segments and neuritic processes in the ONL and different INL cell types. No obvious differences between *wt* (**b**-**d**) and *rd1* (**e**-**g**) were found. Scale bar: 50 $\mu$m

***rd1* photoreceptor nuclei show hypoacetylation.** Acetylation of lysine residues was studied in *wt* and *rd1* retinae using acetylation-specific antibodies (Abs). In the ONL of *wt* mice at P11, an Ab detecting general acetylation of lysine residues showed homogeneous staining of the photoreceptor population (Figure 2a-c). In contrast, the P11 *rd1* ONL presented staining 'gaps' that contained unlabeled photoreceptor nuclei (Figure 2d-f). Such lack of staining encompassed decreased histone acetylation, as confirmed by several Abs directed against specific acetylated histones (Supplementary Figure 1). No obvious signs for hypoacetylation for any of the Abs used were found in the inner retina of neither *wt* nor *rd1*. Western blot (WB) of P11 *in vivo* retinae with the acetyl-lysine Ab (Figure 2g) mainly revealed bands between 12 and 17 kDa that corresponded to the reported molecular weights of different histones and showed numerically decreased acetylation levels in the *rd1* retina (*wt*: 100%; *rd1*: 89.8% ± 40, $n = 3$).

**HDAC activity is increased in *rd1* photoreceptors.** To investigate whether the decreased *rd1* photoreceptor acetylation was related to increased activity of HDACs, we adapted a technique originally intended to measure tissue homogenates[18] for the use on retinal tissue sections.

Whole fixed retinal cryosections revealed deacetylation activity. By specifically blocking either HDACs I/II with TSA or HDAC III with NAM, we were able to distinguish the relative contributions of different classes of HDACs to the total activity, and to follow their kinetics with different substrate concentrations. As proof of principle for the HDAC assay, we determined the $K_m$ values for total HDAC activity on retinae of *rd1* and *wt* mice (Supplementary Figure 2). The $K_m$ value for the fluorogenic substrate of 83 $\mu$M at 500 $\mu$M $NAD^+$ is in good agreement with previous reports.[19] When studied with cellular resolution, both *wt* and *rd1* tissue displayed HDAC activity in photoreceptor segments. All nuclear layers of *wt* retina were essentially devoid of visible activity (Figure 3a). In contrast, the *rd1* ONL carried a subset of cells, displaying typical nuclear morphology of photoreceptors, with highly elevated HDAC activity (Figure 3b). Inhibition of either class I/II HDACs (Figure 3c) or HDAC III (Figure 3d) suggested that most of the excessive HDAC activity in *rd1* photoreceptor originated from HDAC I/II. Together, these results implied that *rd1* photoreceptor hypoacetylation was due to an excessive activation of HDACs, and most likely HDAC I/II.

**HDAC activity and cell death.** To test whether the high HDAC activity observed in *rd1* photoreceptors was related to

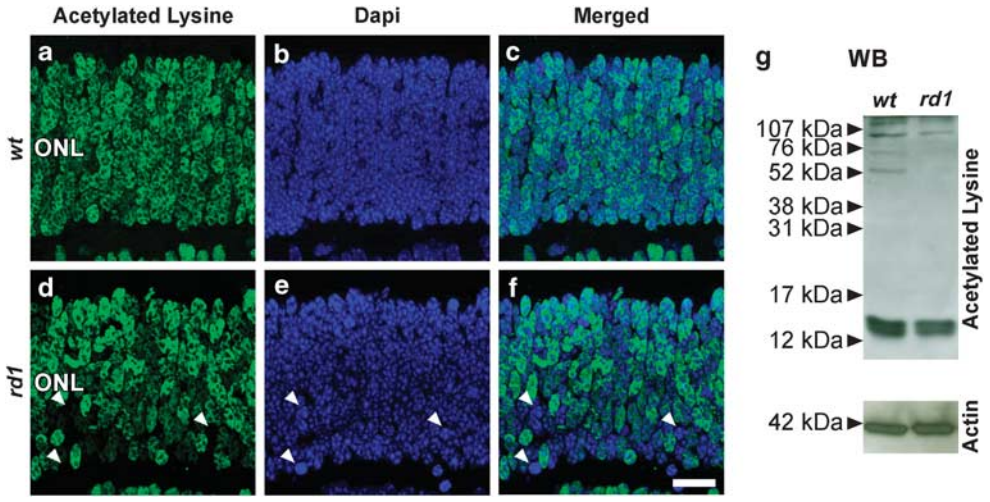


**Figure 2** Decreased acetylation in *rd1* photoreceptors *in vivo*. At P11 immunofluorescence for acetylated lysine residues (green) on *wt* (**a**) and *rd1* (**d**) retinae revealed a number of DAPI-stained *rd1* photoreceptor nuclei (**b**, **e**; blue) with very low levels of protein acetylation. (Merged pictures in **c**, **f**, arrowheads indicate nuclei showing low acetylation levels.) WB with the same Ab mainly labeled bands corresponding to the molecular weight of histones (**g**). Scale bar: 20 $\mu$m

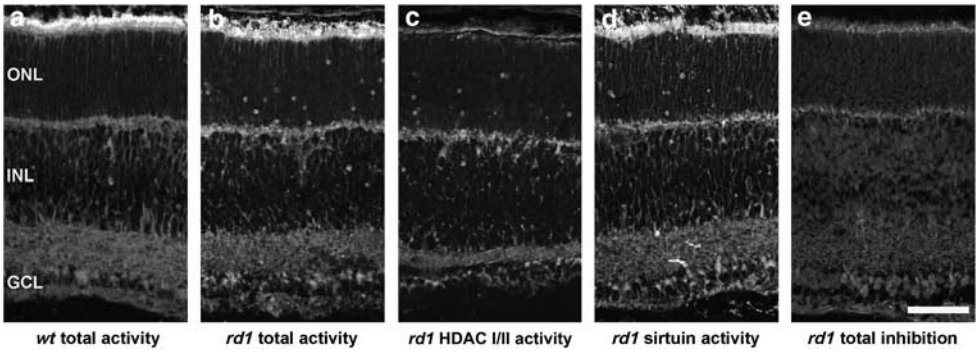


**Figure 3** HDAC activity in the retina *in vivo*. HDAC activity was detected *in situ* in particular in the segment layers of both *wt* (**a**) and *rd1* (**b**) retina. In contrast to *wt*, *rd1* retina displayed a subset of ONL cells with strongly increased HDAC activity. Activity of HDAC I/II (**c**) was studied by inhibition of HDAC III with NAM. Conversely, sirtuin activity (**d**) was assessed by inhibiting HDACs I/II with TSA. Combined inhibition with TSA and NAM was used as negative control (**e**). Scale bar: 50 $\mu$m

their degeneration, staining for acetylated lysine was combined with the TUNEL assay for dying cells. Most of the cells lacking acetylation (94.3% $\pm$ 7.3 S.E.M., $n=3$) were also TUNEL positive (Figure 4a–c). In another co-labeling experiment, *rd1* HDAC activity colocalized only partially (32.5% $\pm$ 6.7 S.E.M., $n=3$) with TUNEL-positive cells (Figure 4d–f) implying that the activity generally preceded the final stages of cell death. To confirm this hypothesis, we assessed the number of HDAC activity positive cells in the ONL of *wt* and *rd1* retinas at various time points during the second post-natal week (i.e., during onset and peak of *rd1* degeneration). The analysis of the temporal progression of HDAC activity showed a marked increase in the number of HDAC activity positive cells at P9, with a peak in activity already at P11 (Figure 4g). Comparison with previously published data on cell death (TUNEL assay) and PARP activity[9] indicated that the peak in HDAC activity preceded the peak of the degeneration by $\sim$2 days. Overall, this suggested that an acetylation/deacetylation imbalance might have an important role in *rd1* photoreceptor degeneration.

**HDAC I/II inhibitors protect *rd1* photoreceptors.** We then exposed retinal explants in a short-term culture paradigm (until P11) to inhibitors specific for the three main classes of HDACs and evaluated the outcome on photoreceptor viability using the TUNEL assay.

The HDAC I/II inhibitor TSA (1 $\mu$M) did not affect the number of TUNEL-positive cells in the ONL of P11 *wt* retinal cultures (TSA: 1.6 $\pm$ 0.2%, $n=6$ retinal cultures from six different animals *versus* vehicle controls: 1.7 $\pm$ 0.2%, $n=9$; Figure 5a, b). In the *rd1* retina, however, 1 $\mu$M TSA significantly decreased the rate of cell death (TSA: 2.2 $\pm$ 0.4%, $n=12$ *versus* vehicle: 3.5 $\pm$ 0.2%, $n=27$, $P<0.001$; Figure 5c, d; quantification in panel e). A second HDAC I/II inhibitor, Scriptaid (6 $\mu$M), also conferred a significant neuroprotective effect to *rd1* photoreceptors (Scriptaid: 2.6 $\pm$ 0.1%, $n=6$, *versus* vehicle: 3.5 $\pm$ 0.2%, $n=27$, $P<0.05$). The HDAC III inhibitor NAM (200 $\mu$M and 1 mM) had no measurable effect on photoreceptor viability (NAM 200 $\mu$M: 3.9 $\pm$ 0.2%, $n=5$ *versus* vehicle: 3.5 $\pm$ 0.2%, $n=27$; Figure 5e). Neither of the above treatments affected the number of photoreceptor rows (quantification in Figure 5e). Successful *in vitro* HDAC

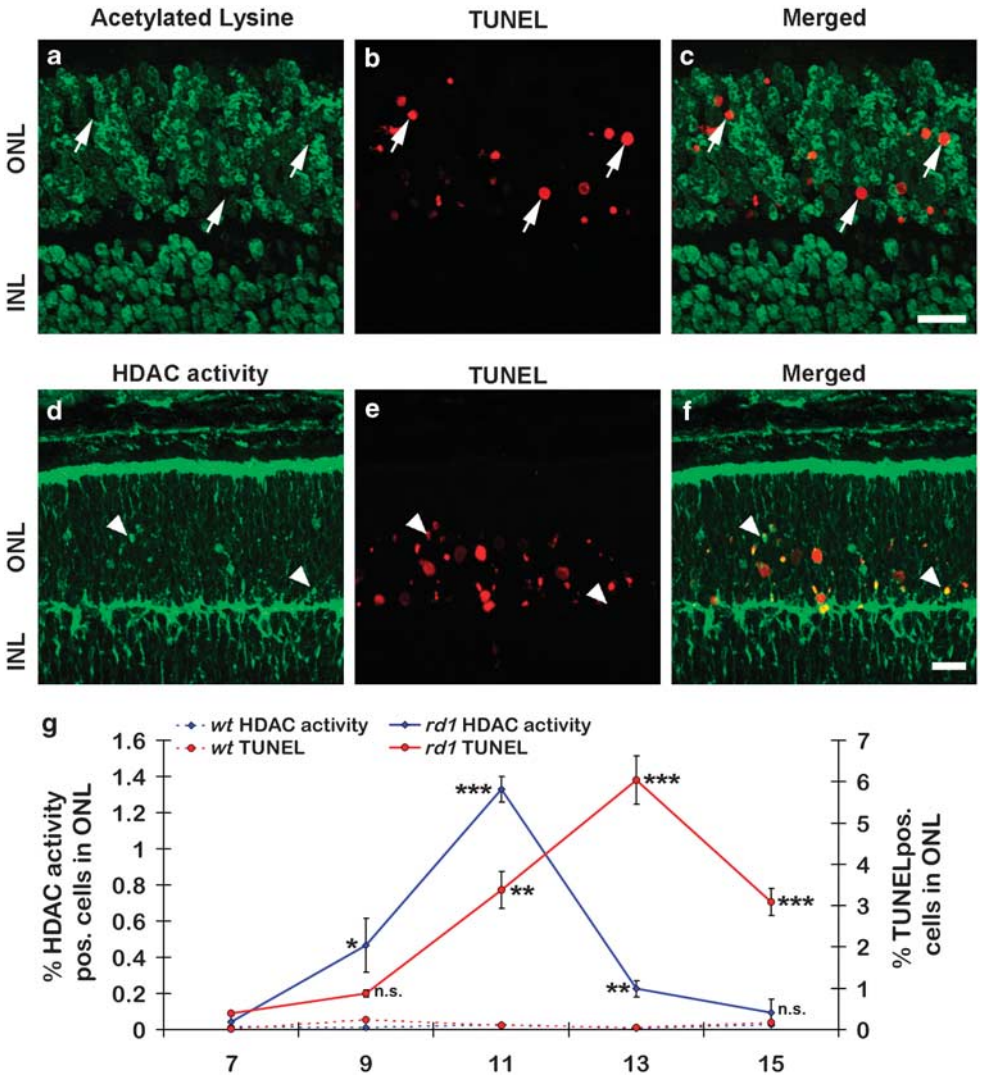


**Figure 4** Protein acetylation and temporal progression of HDAC activity and cell death *in vivo*. At P11, immunostaining for acetylated lysine residues (**a**, green) in *rd1* ONL showed characteristic "gaps", which were partly filled by TUNEL staining (red) for dying cells (**b**) (merged in **c**), suggesting hypoacetylation to contribute to photoreceptor cell death. Conversely, the HDAC activity assay (**d**, **f**) colocalized in part with TUNEL staining at P11 (**e**) in the *rd1* ONL (merged in **f**). Scale bar: 20$\mu$M. The graph in **g** shows the temporal progression of HDAC activity (blue line) in *wt* and *rd1* ONL during the second postnatal week, and relates it to the time-course for TUNEL-positive cells (red). Note that the peak of HDAC activity markedly precedes the peak of TUNEL. n $\geqslant$ 3 for each time point and genotype, data for TUNEL assay were previously published in Paquet-Durand *et al*., 2007 and are shown here for reference purposes only

inhibition by TSA was confirmed using both a tissue-based analysis (WB for acetylated lysine; Figure 5f) and an *in situ* approach (HDAC activity; Supplementary Figure 3).

Although we did not observe any negative properties of TSA in our cultures, a previous study on acute *wt* retinal explants showed proapoptotic effects of TSA at early developmental stages.[16] To address the possibility of a transient TSA effect on retinal cell viability, we treated P5 *rd1* retinal explants with 1 $\mu$M TSA for 24 h, but this did not affect the percentage of TUNEL-positive cells in the P6 *in vitro* retina (TSA: 1.7 $\pm$ 0.2%, vehicle: 1.5 $\pm$ 0.3%; $n = 3$; Supplementary Figure 4). Furthermore, when extending the culture period for another 5 days without TSA (P5 + 1 + 5 = P11), to match with the end point used in our previous experiments, the treated *rd1* retina again showed a markedly reduced number of TUNEL-positive cells (TSA: 1.0 $\pm$ 0.2%; vehicle: 3.8 $\pm$ 0.5%, $n = 3$, $P < 0.05$). At the same time, the number of photoreceptor rows was not significantly affected by the treatment (TSA: 7.1 $\pm$ 0.2, vehicle: 7.5 $\pm$ 0.1; $n = 3$).

To test whether the strong neuroprotective effect of TSA in the different short-term paradigms would translate into improved long-term survival of photoreceptors, *in vitro* treatment was prolonged until P28. TSA treatment almost doubled the number of surviving *rd1* photoreceptor rows (TSA: 4.1 $\pm$ 0.3; vehicle: 2.1 $\pm$ 0.2, $n = 6$, $P < 0.001$; Figure 5i).

Expression of rhodopsin was then analyzed as an indication of rod photoreceptor identity. In *wt* retina, *in vivo* rhodopsin expression is restricted to the outer segments of rod photoreceptors, whereas in *rd1* retina, where outer segments do not develop properly, it is partly mislocalized and also observed throughout the cytoplasm of photoreceptors.[20] This phenomenon intensifies under *in vitro* conditions where

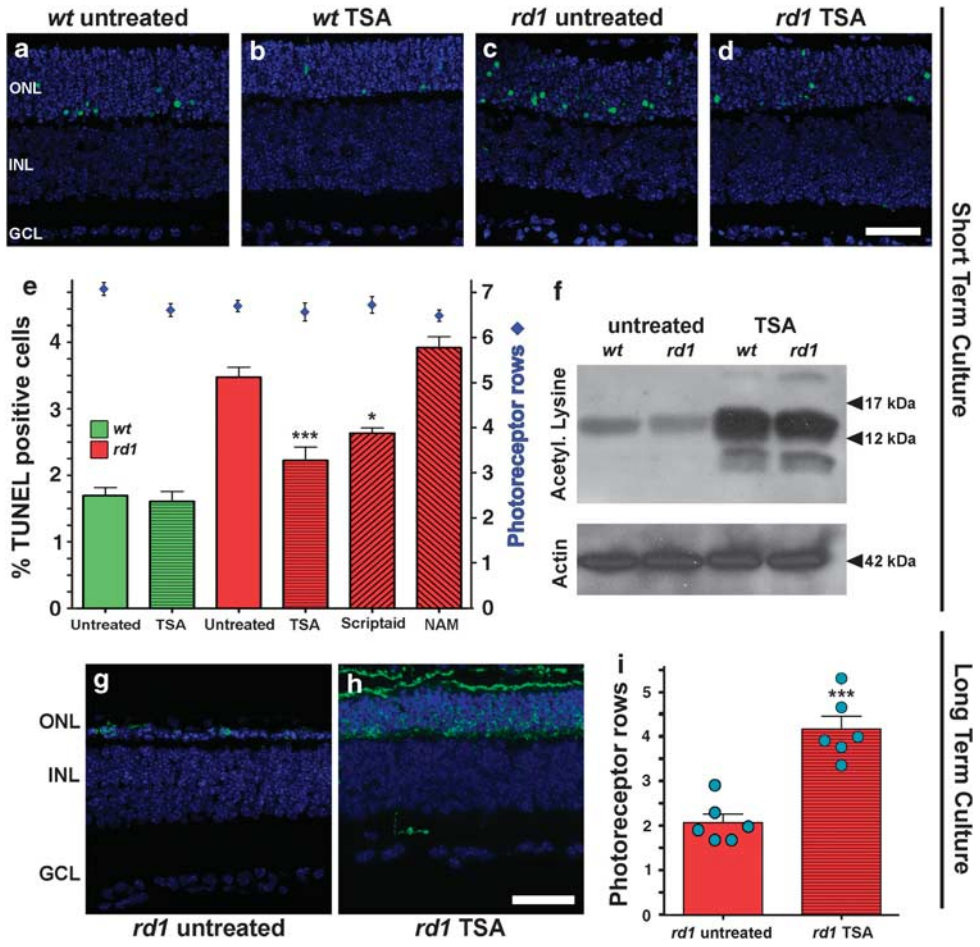


**Figure 5** HDAC inhibition reduces photoreceptor cell death *in vitro*. Short-term retinal explant cultures from *rd1* and *wt* animals were exposed to control conditions or 1 $\mu$M TSA from P7 to P11 (**a**-**d**). In untreated specimens (**a**, **c**), TUNEL assay (green) showed the characteristic increase of dying cells in *rd1* ONL compared with *wt*. TSA treatment (**b**, **d**) reduced the number of degenerating photoreceptors in *rd1*, but did not alter viability of *wt*. The bar graph (**e**) summarizes effects of TSA, 6 $\mu$M Scriptaid, and 200 $\mu$M NAM on photoreceptor viability. HDAC I/II inhibitors, TSA and Scriptaid, significantly reduced the amount of dying cells, whereas HDAC III inhibitor NAM had no effect on cell survival. Immunoblotting for acetylated lysine residues (**f**) showed an increase in protein acetylation after TSA treatment in both *wt* and *rd1* retinae. Long-term cultures of *rd1* retinae (until P28; **g**, **h**) treated with TSA showed a marked increase in the number of rhodopsin-positive cell bodies and overall size of their ONL when compared with untreated situation (quantification in **i**). DAPI (blue) was used as nuclear counterstain; actin immunoblotting was used as loading control in **f**; $n \geqslant 6$, Scale bars in **d** and **h** are 50 and 20 $\mu$M respectively

rhodopsin mislocalization is observed in both *wt* and *rd1* photoreceptors (Supplementary Figure 5). In long-term TSA-treated explants, rhodopsin expression was found in most of the surviving *rd1* photoreceptors, whereas in the untreated situation most remaining ONL cells were rhodopsin negative and most likely predominantly cones (Figure 5g, h). Significantly, rhodopsin-positive photoreceptor outer segments were observed in TSA-treated specimens, when at the same time in the untreated situation, outer segments were completely absent. This supported the idea that TSA indeed upheld survival of rod photoreceptors and promoted growth of *rd1* outer segments.

All in all, TSA treatment in both short- and long-term retinal culture demonstrated a strong prosurvival effect, whereas NAM had no such protective effects. The experiments therefore suggested a major contribution of HDAC I/II, but not III, to mutation-induced *rd1* photoreceptor death.

**HDAC I/II regulate PARP activity.** As we had previously found PARP activity to be involved in *rd1* photoreceptor cell death,[9] we wanted to investigate a possible interaction between HDACs and PARP. When immunostainings for acetylated lysines and for poly-ADP-ribose (PAR) – the product of PARP activity – were combined, the merged images revealed PAR-positive photoreceptor nuclei exclusively in cases where acetylation was absent (Figure 6a–d). Together with the data on the progression of HDAC activity (Figure 4g), this suggested that hypoacetylation and hence HDAC activity was preceding PARP activity.

We then tested whether HDAC I/II inhibition by TSA indirectly also affected PARP activity. With respect to PAR immunostaining, there was a moderate amount of positive photoreceptor nuclei in *wt* retinal explant cultures at P11 (*wt* vehicle: 0.25% $\pm$ 0.1, $n = 3$), and a comparatively much higher number in *rd1* explants (*rd1* vehicle: 0.9% $\pm$ 0.1; Figure 6e, g). The presence of PAR-positive photoreceptors in *wt* explants is likely due to the stress that these undergo during culture. In both *wt* and *rd1* explants, the number of PAR-positive cells was reduced by TSA treatment, and this reduction was

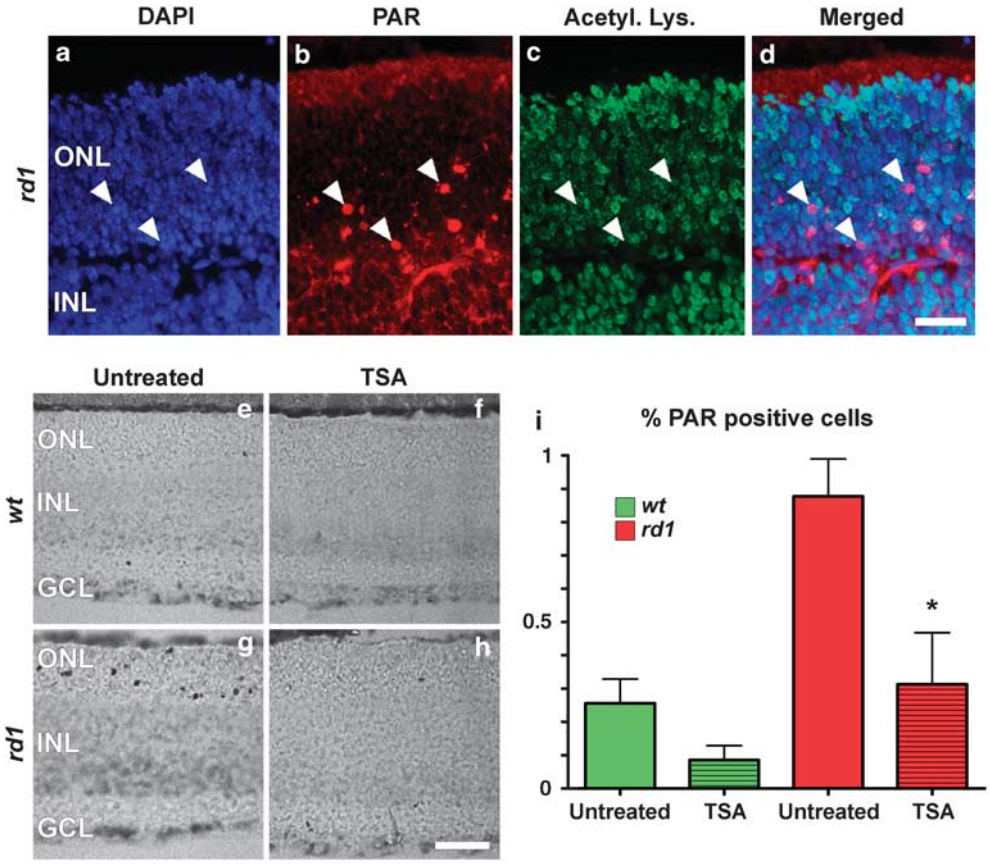


**Figure 6** HDAC and PARP activities are connected. In *rd1* P11 *in vivo* specimens, a subset of ONL nuclei showed unusual chromatin condensation as evidenced by DAPI nuclear counterstain (**a**, blue). In most of these cells a strong accumulation of poly-ADP-ribose (PAR) (**b**, red) colocalized with hypoacetylation (**c**, green; merged in **d**; white arrowheads), suggesting a functional connection between acetylation and PARP activity. In short-term retinal explant cultures at P11, photoreceptors showing PAR accumulation were observed in untreated *wt* (**e**) and *rd1* retina (**g**), their number being much higher in the latter case. This number was strongly reduced by TSA treatment in both *wt* (**f**) and *rd1* retina (**h**; quantification in **i**), implying that activation of PARP occurred downstream of HDAC I/II activity. $n = 3$; Scale bar in **d**, **h** = 20 $\mu$M. Some of the PAR immunostaining between ONL and INL relates to IGG staining in blood vessels

statistically significant in the *rd1* situation (*rd1* TSA: $0.3\% \pm 0.2$, $n = 3$, $P < 0.05$; Figure 6f, h). These results supported the notion that activation of PARP in *rd1* photoreceptors occurred downstream of HDAC I/II activity.

## Discussion

The activity of HDACs has previously been connected to a variety of different cellular processes, notably regulation of gene expression, cytoskeletal rearrangements, division, and differentiation.[13] Here, we show that HDAC activity was causally related to inherited photoreceptor cell death in the *rd1* mouse and that this detrimental effect was tied to HDACs I/II. HDACs III did not seem to be involved in the degeneration, which corresponds to observations on weakened HDAC III action in degenerating retina.[21] The strong neuroprotection afforded by HDAC I/II inhibitors in both short- and long-term retinal explant cultures proposes them as novel lead compounds to prevent or delay retinal neurodegeneration.

**HDAC and gene regulation.** Given the extensive effects of acetylation/deacetylation on gene regulation, the observed HDAC hyperactivation would likely result in significantly altered *rd1* gene transcription, which matches with previous microarray data.[5–7] On the other hand, we can at present not exclude the possibility that the observed histone deacetylation was due in part also to a decreased activity of HATs. Our observations that *rd1* gene alterations include downregulation of the transcription factor CREB[6,8,22] is of particular interest here, as CREB not only appears to confer neuroprotection[6,8,22] but also has several links to cellular acetylation events. For example, different HDAC I/II isoforms can recruit protein phosphatase-1 to dephosphorylate and inactivate CREB,[23] which might be related to its downregulation in the *rd1* retina. Moreover, CREB target gene transcription is facilitated by its co-factor CREB-binding protein (CBP), which has HAT activity,[24] and therefore connects CREB activation with histone acetylation. Accordingly, some of the effects on neuronal gene regulation seen when acetylation is increased by HDAC inhibition may be routed through enhanced activity of CREB and CBP.[25] The expression of opsin and other photoreceptor genes is controlled by the photoreceptor-specific transcription factor cone-rod-homeobox (CRX).[26] In conjunction with histone acetylation and CBP, CRX drives expression of these critical photoreceptor genes in Y79 retinoblastoma cells and in the mouse retina.[15,27]

**Cross-talk between HDAC and PARP activity.** PARP activity is involved in DNA damage repair and hence often seen as a benign factor, although excessive PARP activity may compromise cellular viability.[10] Increased PARP activity, as seen in *rd1* photoreceptors,[9] consumes $NAD^+$ and generates NAM, which in turn negatively regulates HDAC III activity and thereby favors acetylation of its target proteins.[14] As HDAC III-dependent deacetylation of the automodification domain of PARP blocks its activity,[28] low $NAD^+$ levels could trigger a positive feedback loop accounting for both the high PARP activity and the low HDAC III activity observed in *rd1* photoreceptors. Yet other reports demonstrate that acetylation by p300/CBP promotes the ability of PARP-1 to act as a co-activator in transcription[30], whereas acetylation by histone acetyltransferases PCAF and GCN5L reduces PARP-2 catalytic activity.[29,30] The findings highlight a possibility for hyperactive HDAC I/II to intervene with various PARP types, perhaps causing abnormal stimulation of these enzymes. In such a scheme, HDAC I/II activity would be upstream of PARP activation in *rd1* photoreceptor degeneration, which is in accord with our results, where TSA treatment reduced accumulation of PAR. In addition, PARP activity accompanies the event of dying, TUNEL-positive photoreceptors and colocalizes to a large extent with them,[9] whereas in this study, TUNEL colocalization with HDAC activity was only minor. This again implies that HDAC activity was upstream of PARP activation.

**HDAC activity in cell death and survival.** Experimental evidence suggests that both overactivation of HDACs I/II or their inhibition promotes cell death.[13] Similarly, HDAC III activity can have both pro- and antiapoptotic effects depending on cell type and proliferation state,[31] and the right balance between the activities of different HDAC classes therefore seems to be crucial for maintaining cellular viability.[13] In addition, individual members of each HDAC class could have distinct cell type-specific roles,[32] perhaps related to their expression levels, which may in part explain the opposing effects of HDAC inhibitors observed in different neurodegeneration paradigms.[12] The protective effects of TSA and Scriptaid comply with a number of studies on post-mitotic neurons, where HDAC inhibitors also conferred neuroprotection,[12,33,34] possibly in part due to the prevention of oxidative stress[35] and reactivation of CREB signaling.[36,37] Furthermore, it is conceivable that in the *rd1* situation HDAC inhibition may induce expression or increase the stability of neuroprotective genes and proteins that are not directly related to the pathological mechanism. In this context, the chaperone HSP90, which is a target for HDAC-dependent deacetylation, appears to have a prominent role in neurodegeneration. Acetylation at its K294 residue inhibits HSP90[38] and hence HDAC inhibitors indirectly also block HSP90 activity.[39] Interestingly, HSP90 inhibition induces an upregulation of the neuroprotective chaperone HSP70 and strongly increases neuronal survival.[40,41] Our finding that decreased histone acetylation combines with increased HDAC activity corresponds to very similar observations made in motorneurons in a mouse model for amyotrophic lateral sclerosis, where HDAC inhibition also resulted in neuroprotection.[36] In the *in vivo* retina, HDAC inhibition has been shown to promote survival of ganglion cells after optic nerve crush.[37]

## Conclusion

The mechanisms governing inherited photoreceptor cell death have remained elusive to date.[1] Our discovery that HDAC activity was involved in photoreceptor degeneration may thus help to close a major gap of knowledge between the immediate effects of a single gene mutation[2] and the observed massive changes at the transcriptional level.[6] Moreover, increased HDAC activity appeared to be responsible for an activation of PARP in degenerating *rd1* photoreceptors. The exact interplay between PARP and HDAC activity warrants further studies, as it may potentially explain crucial events in the pathological process. This study not only brings up HDAC activity as a 'missing link,' uniting several other findings on the mechanisms of photoreceptor cell death, but also highlights HDACs as novel targets for the development of neuroprotective therapies aimed to halt or delay inherited retinal degeneration in humans.

## Material and Methods

**Animals.** Animals were housed under standard white cyclic lighting, had free access to food and water, and were used irrespective of gender. C3H *rd1*/*rd1* (*rd1*) and control C3H *wt* mice were used.[42] All procedures were performed in accordance with the local ethics committee in Lund (permits M225-04 and M242-07), the Tübingen University (§4 registration from 23–01–08), and the ARVO statement for the use of animals in ophthalmic and visual research. All efforts were made to minimize the number of animals used and their suffering. Because of the critical changes at P11,[22,43] most comparisons between *rd1* and *wt* were carried out at this age. Day of birth was considered as P0.

**Microarray analyis.** Details of the transcription assay performed on a custom-made mouse gene chip were described in Azadi *et al*.[6] Two times up- or downregulation in at least three out of five hybridizations was considered as significant variation. Results not pertaining to this study are published elsewhere.

***In vitro* retinal explant cultures.** Retinae from P5 *rd1* and *wt* animals were used to generate retinal explants as described before.[4,44] In brief, animals were killed and the eyes enucleated in an aseptic environment. Afterwards, the entire eyes were incubated in R16 serum-free culture medium (Invitrogen Life Technologies, Paisley, UK; 07490743A) containing 0.12% proteinase K (MP Biomedicals, Solon, OH, USA; 193504) at 37 °C for 15 min, to allow preparation of retinal cultures with RPE attached. Proteinase K was inactivated with 10% fetal calf serum (Invitrogen Life Technologies; PET10108165) in R16 medium, and the eyes dissected aseptically in a Petri dish containing R16 medium. The anterior segment, lens, vitreous, sclera, and choroids were carefully removed, and the retina was cut perpendicular to its edges, resulting in a cloverleaf-like shape. Subsequently, the retina was transferred to a Millicell culture dish filter insert (Millipore AB, Solna, Sweden; PIHA03050) with the retinal pigment epithelium layer facing the membrane. The insert was put into a six-well culture plate and incubated in R16 nutrient medium at 37 °C. Every second day, the full volume of nutrient medium, 1.5 ml per dish, was replaced with fresh medium.

The first 2 days, the retina was left in R16 culture medium without treatment to adapt to culture conditions. At P7, cultures were either exposed to different treatments (TSA 1 $\mu$M, Scriptaid 6 $\mu$M, NAM 200 $\mu$M, and 1000 $\mu$M; all from Sigma, Munich, Germany), or kept as untreated control. NAM is a constituent of the culturing medium and present at about 22 $\mu$M, which should be less than half the reported $IC_{50}$ value in cell-free studies.[45] Explants were cultured until P11 for short-term cultures (P5 + 2 + 4), or until P28, for long-term cultures (P5 + 2 + 21). Culturing was stopped by 2 h fixation in 4% paraformaldehyde (PFA), washed 4 × 15 min in phosphate-buffered saline (PBS), then cryoprotected first with PBS + 10% sucrose, and subsequently with PBS + 25% sucrose. Explants were frozen and embedded in Jung tissue freezing medium (Leica Microsystems, Nussloch, Germany) for cryosectioning (12 $\mu$m).

**HDAC assay.** HDAC activity assays were performed on cryosections of 4% PFA P11 fixed eyes. The assay is based on an adaptation of the Fluor de Lys Fluorescent Assay System (Biomol, Hamburg, Germany). Retinal sections were exposed to

different concentrations of Fluor de Lys-SIRT2 deacetylase substrate (Biomol) with 2 or 100 $\mu$M TSA (Sigma, Steinheim, Germany), 2 mM NAM (Sigma), and 500 $\mu$M $NAD^+$ (Biomol) in assay buffer (50 mM Tris/HCl, pH 8.0; 137 mM NaCl; 2.7 mM KCl; 1 mM $MgCl_2$; 1 mg/ml BSA) and 0.1% NP40 and 0.5 $\times$ Developer II (Biomol). Images were captured at indicated time points with a fixed exposure time of 2 s using a Zeiss (Jena, Germany) Axiophot microscope ( $\times$ 20 magnification) and Zeiss Axiovision 4.2 software; densitometry was performed with the aid of ImageJ (National Institutes of Health, Bethesda, MD, USA). The reaction rate was determined in at least four independent experiments, as the slope of the linear regression fitted to the data points in the linear range of a time course, using SigmaPlot (Systat software, Erkrath, Germany) software. For the calculation of $K_m$ values, the slope of time courses with different substrate concentrations was plotted against the corresponding substrate concentrations; a hyperbolic regression fitted to the data points revealed $K_m$ values and $V_{max}$.

*In situ* deacetylation activity was determined on retinal sections incubated for 3 h with 200 $\mu$M Fluor de Lys-SIRT2 deacetylase substrate in assay buffer with/without inhibitors. Sections were then washed in PBS and fixed in methanol at $-80\,^{\circ}C$ for 20 min. $\times$ 0.5 developer (Biomol) in assay buffer was applied and pictures taken immediately in an Apotome microscope (Zeiss), at $\times$ 20 using the DAPI filter.

**TUNEL assay.** The terminal deoxynucleotidyl transferase dUTP nick end labeling (TUNEL) assay was performed on cryosections from treated and untreated *rd1* retinas, using an *in situ* cell death detection kit conjugated with tetramethyl-rhodamine or fluorescein isothiocyanate (Roche Diagnostics, Mannheim, Germany). For controls, terminal deoxynucleotidyl transferase enzyme was either omitted from the labeling solution (negative control), or sections were pretreated for 30 min with DNAse I (Roche Diagnostics, 3 U/ml) in 50 mM Tris-HCl, pH 7.5, 1 mg/ml BSA to induce DNA-strand breaks (positive control). Negative control showed no staining at all, whereas positive control stained all nuclei in all layers of the retina.[9]

**Immunostaining.** Frozen retinal sections from P11 animals or cultured retinae were dried for 30–60 min at 37 °C. Subsequently, the tissue was rehydrated in PBS, and preincubated for 1 h at room temperature (RT) in blocking solution, containing 10% normal serum, and 0.1 or 0.3% Triton in PBS (PBST). Immunohistochemistry was performed overnight at 4 °C, using primary Abs (acetylated lysine; acetylated H2A, H2B, H3, H4; Sirt2; HDAC2; HDAC5; PAR) diluted 1 : 100 in blocking solution. Primary Abs were purchased from Cell Signaling (Danvers, MA, USA) except PAR Ab (Alexis Biochemicals, Lörrach, Germany) and Rhodopsin Ab (Millipore, Schwalbach, Germany). The tissue was rinsed with PBST, and incubated for 1 h with a corresponding secondary Ab, Alexa 488 (1 : 200–1 : 750, Invitrogen), diluted in PBST. Sections were rinsed in PBS, and mounted in Vectashield with DAPI (Vector Laboratories, Burlingame, CA, USA).

**Western Blot.** Retinae from P11 animals were enucleated and stored at $-80\,^{\circ}C$. Later on, the tissue was homogenized in buffer (10 mM Tris, 1 mM EDTA, 150 mM NaCl, 1 mM $Na_3VO_4$, 50 nM okadaic acid, 2% SDS, 10% glycerol, 0.0625 M Tris-HCl, and protease inhibitor cocktail 10 $\mu$l/ml (Calbiochem, Darmstadt, Germany); pH 6.8) with a Heidolph DIAX 600 homogenizer (Heidolph, Schwabach, Germany) or a manual homogenizer (glass to glass). Retinal explant cultures, both treated and untreated with TSA, from *wt* and *rd1* mice were homogenized using the same process. Bradford assay was used to measure protein concentration. Proteins were then separated by SDS-PAGE 4–12% gradient gel (at 55 V), and transferred to a PVDF membrane (Amersham Biosciences, Buckinghamshire, UK). Membranes were incubated in Roti block (Roth, Karlsruhe, Germany) blocking buffer for 3 h at RT. After washing, primary Abs (acetylated lysine; acetylated H2A, H2B, H3, H4; actin) were added at a dilution of 1 : 1000 in buffer containing TBS-T and 5% dried milk (Roth), and incubated overnight at 4 °C. Primary Abs were purchased from Cell Signaling, except for actin Ab which was from Chemicon (Schwalbach, Germany). After washing, the membranes were treated with buffer containing HRP-conjugated secondary Ab (Amersham Biosciences) overnight at 4 °C. The membranes were developed using Hyperfilm (Amersham Biosciences) detection system. Quantification was performed after film scanning using ImageJ (NIH).

**Microscopy, cell counting, and statistics.** Morphological observations and routine light microscopy were performed on a Zeiss Imager Z1 Apotome Microscope, equipped with a Zeiss Axiocam digital camera. Images were captured using Zeiss Axiovision 4.7 software; image overlays and contrast enhancement were performed using Adobe Photoshop CS3. Images shown in figures are representative for least three different animals for each genotype/treatment. Percentages of TUNEL-positive cells were assessed and calculated in a blinded manner as reported previously.[4,9] The mean value for photoreceptor rows in the ONL after *in vitro* culture was determined using DAPI nuclear counterstaining. Values are given as mean $\pm$ S.E.M. Statistical significance was tested using one-way ANOVA with Bonferroni correction and Prism (GraphPad Software, San Diego, CA, USA), significance levels were $P<0.05$ (*), $P<0.01$ (**), and $P<0.001$ (***).

## Conflict of interest

The authors declare no conflict of interest.

**Acknowledgements**. We thank H Abdalle, B Klefbohm, K Dengler, and S Kurz-Bernhard for excellent technical assistance and Y Arsenijevic, M-T Perez, and B Wissinger for helpful comments and discussions. This study was supported by grants from the EU (RETNET: MRTN-CT-2003–504003, EVI-GENORET: LSHG-CT-2005–512036, NEUROTRAIN: MEST-CT-2005–020235), Fundación Oftalmológica del Mediterráneo (FOM), KMA, Synfrämjandets Forskningsfond, Stiftelsen för synskadade i f.d. Malmöhus län, Foundation Fighting Blindness (FFB), Swedish Medical Research Council (VRM), Crafoord foundation, Kerstan Foundation, Torsten och Ragnar Söderbergs Foundation, and Deutsche Forschungsgemeinschaft (DFG; PA1751/1–1).

1. Sancho-Pelluz J, Arango-Gonzalez B, Kustermann S, Romero FJ, van Veen T, Zrenner E *et al*. Photoreceptor cell death mechanisms in inherited retinal degeneration. *Mol Neurobiol* 2008; **38**: 253–269.
2. Bowes C, Li T, Danciger M, Baxter LC, Applebury ML, Farber DB. Retinal degeneration in the rd mouse is caused by a defect in the beta subunit of rod cGMP-phosphodiesterase. *Nature* 1990; **347**: 677–680.
3. Farber DB, Lolley RN. Cyclic guanosine monophosphate: elevation in degenerating photoreceptor cells of the C3H mouse retina. *Science* 1974; **186**: 449–451.
4. Paquet-Durand F, Hauck SM, van Veen T, Ueffing M, Ekstrom P. PKG activity causes photoreceptor cell death in two retinitis pigmentosa models. *J Neurochem* 2009; **108**: 796–810.
5. Rohrer B, Pinto FR, Hulse KE, Lohr HR, Zhang L, Almeida JS. Multidestructive pathways triggered in photoreceptor cell death of the rd mouse as determined through gene expression profiling. *J Biol Chem* 2004; **279**: 41903–41910.
6. Azadi S, Paquet-Durand F, Medstrand P, van Veen T, Ekstrom PA. Up-regulation and increased phosphorylation of protein kinase C (PKC) delta, mu and theta in the degenerating rd1 mouse retina. *Mol Cell Neurosci* 2006; **31**: 759–773.
7. Hackam AS, Strom R, Liu D, Qian J, Wang C, Otteson D *et al*. Identification of gene expression changes associated with the progression of retinal degeneration in the rd1 mouse. *Invest Ophthalmol Vis Sci* 2004; **45**: 2929–2942.
8. Pilz RB, Broderick KE. Role of cyclic GMP in gene regulation. *Front Biosci* 2005; **10**: 1239–1268.
9. Paquet-Durand F, Silva J, Talukdar T, Johnson LE, Azadi S, van Veen T *et al*. Excessive activation of poly(ADP-ribose) polymerase contributes to inherited photoreceptor degeneration in the retinal degeneration mouse 1. *J Neurosci* 2007; **27**: 10311–10319.
10. Schreiber V, Dantzer F, Ame JC, de Murcia G. Poly(ADP-ribose): novel functions for an old molecule. *Nat Rev Mol Cell Biol* 2006; **7**: 517–528.
11. Egger G, Liang G, Aparicio A, Jones PA. Epigenetics in human disease and prospects for epigenetic therapy. *Nature* 2004; **429**: 457–463.
12. Morrison BE, Majdzadeh N, D'Mello SR. Histone deacetylases: focus on the nervous system. *Cell Mol Life Sci* 2007; **64**: 2258–2269.
13. Haberland M, Montgomery RL, Olson EN. The many roles of histone deacetylases in development and physiology: implications for disease and therapy. *Nat Rev Genet* 2009; **10**: 32–42.
14. Kruszewski M, Szumiel I. Sirtuins (histone deacetylases III) in the cellular response to DNA damage—facts and hypotheses. *DNA Repair (Amst)* 2005; **4**: 1306–1313.
15. Peng GH, Chen S. Crx activates opsin transcription by recruiting HAT-containing co-activators and promoting histone acetylation. *Hum Mol Genet* 2007; **16**: 2433–2452.
16. Wallace DM, Donovan M, Cotter TG. Histone deacetylase activity regulates apaf-1 and caspase 3 expression in the developing mouse retina. *Invest Ophthalmol Vis Sci* 2006; **47**: 2765–2772.
17. Chen B, Cepko CL. Requirement of histone deacetylase activity for the expression of critical photoreceptor genes. *BMC Dev Biol* 2007; **7**: 78.
18. Wood JG, Rogina B, Lavu S, Howitz K, Helfand SL, Tatar M *et al*. Sirtuin activators mimic caloric restriction and delay ageing in metazoans. *Nature* 2004; **430**: 686–689.
19. Fan Y, Ludewig R, Scriba GK. 9-Fluorenylmethoxycarbonyl-labeled peptides as substrates in a capillary electrophoresis-based assay for sirtuin enzymes. *Anal Biochem* 2009; **387**: 243–248.
20. Bowes C, van Veen T, Farber DB. Opsin, G-protein and 48-kDa protein in normal and rd mouse retinas: developmental expression of mRNAs and proteins and light/dark cycling of mRNAs. *Exp Eye Res* 1988; **47**: 369–390.
21. Jaliffa C, Ameqrane I, Dansault A, Leemput J, Vieira V, Lacassagne E *et al*. Sirt1 involvement in rd10 mouse retinal degeneration. *Invest Ophthalmol Vis Sci* 2009; **50**: 3562–3572.

22. Paquet-Durand F, Azadi S, Hauck SM, Ueffing M, van Veen T, Ekstrom P. Calpain is activated in degenerating photoreceptors in the rd1 mouse. *J Neurochem* 2006; **96**: 802–814.
23. Gao J, Siddoway B, Huang Q, Xia H. Inactivation of CREB mediated gene transcription by HDAC8 bound protein phosphatase. *Biochem Biophys Res Commun* 2009; **379**: 1–5.
24. Kalkhoven E. CBP and p300: HATs for different occasions. *Biochem Pharmacol* 2004; **68**: 1145–1155.
25. Vecsey CG, Hawk JD, Lattal KM, Stein JM, Fabian SA, Attner MA *et al.* Histone deacetylase inhibitors enhance memory and synaptic plasticity via CREB: CBP-dependent transcriptional activation. *J Neurosci* 2007; **27**: 6128–6140.
26. Hennig AK, Peng GH, Chen S. Regulation of photoreceptor gene expression by Crx-associated transcription factor network. *Brain Res* 2008; **1192**: 114–133.
27. Palhan VB, Chen S, Peng GH, Tjernberg A, Gamper AM, Fan Y *et al.* Polyglutamine-expanded ataxin-7 inhibits STAGA histone acetyltransferase activity to produce retinal degeneration. *Proc Natl Acad Sci USA* 2005; **102**: 8472–8477.
28. Rajamohan SB, Pillai VB, Gupta M, Sundaresan NR, Birukov KG, Samant S *et al.* SIRT1 promotes cell survival under stress by deacetylation-dependent deactivation of poly (ADP-ribose) polymerase 1. *Mol Cell Biol* 2009; **29**: 4116–4129.
29. Haenni SS, Hassa PO, Altmeyer M, Fey M, Imhof R, Hottiger MO. Identification of lysines 36 and 37 of PARP-2 as targets for acetylation and auto-ADP-ribosylation. *Int J Biochem Cell Biol* 2008; **40**: 2274–2283.
30. Hassa PO, Haenni SS, Buerki C, Meier NI, Lane WS, Owen H *et al.* Acetylation of poly(ADP-ribose) polymerase-1 by p300/CREB-binding protein regulates coactivation of NF-kappaB-dependent transcription. *J Biol Chem* 2005; **280**: 40450–40464.
31. Gan L, Mucke L. Paths of convergence: sirtuins in aging and neurodegeneration. *Neuron* 2008; **58**: 10–14.
32. Chen B, Cepko CL. HDAC4 regulates neuronal survival in normal and diseased retinas. *Science* 2009; **323**: 256–259.
33. Leng Y, Liang MH, Ren M, Marinova Z, Leeds P, Chuang DM. Synergistic neuroprotective effects of lithium and valproic acid or other histone deacetylase inhibitors in neurons: roles of glycogen synthase kinase-3 inhibition. *J Neurosci* 2008; **28**: 2576–2588.
34. Bolger TA, Yao TP. Intracellular trafficking of histone deacetylase 4 regulates neuronal cell death. *J Neurosci* 2005; **25**: 9544–9553.
35. Ryu H, Lee J, Olofsson BA, Mwidau A, Dedeoglu A, Escudero M *et al.* Histone deacetylase inhibitors prevent oxidative neuronal death independent of expanded polyglutamine repeats via an Sp1-dependent pathway. *Proc Natl Acad Sci USA* 2003; **100**: 4281–4286.
36. Rouaux C, Panteleeva I, Rene F, Gonzalez de Aguilar JL, Echaniz-Laguna A, Dupuis L *et al.* Sodium valproate exerts neuroprotective effects *in vivo* through CREB-binding protein-dependent mechanisms but does not improve survival in an amyotrophic lateral sclerosis mouse model. *J Neurosci* 2007; **27**: 5535–5545.
37. Biermann J, Grieshaber P, Goebel U, Martin G, Thanos S, Di Giovanni S, Lagréze WA. Valproic acid-mediated neuroprotection and regeneration in injured retinal ganglion cells. *Invest Ophthalmol Vis Sci.* 2010; **51**: 526–534. Epub 2009 Jul 23.
38. Scroggins BT, Robzyk K, Wang D, Marcu MG, Tsutsumi S, Beebe K *et al.* An acetylation site in the middle domain of Hsp90 regulates chaperone function. *Mol Cell* 2007; **25**: 151–159.
39. Kekatpure VD, Dannenberg AJ, Subbaramaiah K. HDAC6 modulates Hsp90 chaperone activity and regulates activation of aryl hydrocarbon receptor signaling. *J Biol Chem* 2009; **284**: 7436–7445.
40. Shen HY, He JC, Wang Y, Huang QY, Chen JF. Geldanamycin induces heat shock protein 70 and protects against MPTP-induced dopaminergic neurotoxicity in mice. *J Biol Chem* 2005; **280**: 39962–39969.
41. Wen XR, Li C, Zong YY, Yu CZ, Xu J, Han D *et al.* Dual inhibitory roles of geldanamycin on the c-Jun NH2-terminal kinase 3 signal pathway through suppressing the expression of mixed-lineage kinase 3 and attenuating the activation of apoptosis signal-regulating kinase 1 via facilitating the activation of Akt in ischemic brain injury. *Neuroscience* 2008; **156**: 483–497.
42. Sanyal S, Bal AK. Comparative light and electron microscopic study of retinal histogenesis in normal and rd mutant mice. *Z Anat Entwicklungsgesch* 1973; **142**: 219–238.
43. Hauck SM, Ekstrom PA, Ahuja-Jensen P, Suppmann S, Paquet-Durand F, van Veen T *et al.* Differential modification of phosducin protein in degenerating rd1 retina is associated with constitutively active Ca2+/calmodulin kinase II in rod outer segments. *Mol Cell Proteomics* 2006; **5**: 324–336.
44. Sanz MM, Johnson LE, Ahuja S, Ekstrom PA, Romero J, van Veen T. Significant photoreceptor rescue by treatment with a combination of antioxidants in an animal model for retinal degeneration. *Neuroscience* 2007; **145**: 1120–1129.
45. Bitterman KJ, Anderson RM, Cohen HY, Latorre-Esteves M, Sinclair DA. Inhibition of silencing and accelerated aging by nicotinamide, a putative negative regulator of yeast sir2 and human SIRT1. *J Biol Chem* 2002; **277**: 45099–45107.



Supplementary Information accompanies the paper on Cell Death and Disease website (http://www.nature.com/cddis)

# PARP1 gene knock-out increases resistance to retinal degeneration without affecting retinal function.

***Sahaboglu A****, Tanimoto N, Kaur J, Sancho-Pelluz J, Huber G, Fahl E, Arango-Gonzalez B, Zrenner E, Ekström P, Löwenheim H, Seeliger M, Paquet-Durand F.*

*Published in "PLoS ONE"* PLoS ONE 5(11): e15495. *(2010)*

OPEN ACCESS Freely available online

PLoS one

# PARP1 Gene Knock-Out Increases Resistance to Retinal Degeneration without Affecting Retinal Function

**Ayse Sahaboglu[1], Naoyuki Tanimoto[2], Jasvir Kaur[1], Javier Sancho-Pelluz[1¤], Gesine Huber[2], Edda Fahl[2], Blanca Arango-Gonzalez[1], Eberhart Zrenner[1], Per Ekström[3], Hubert Löwenheim[4], Mathias Seeliger[2], François Paquet-Durand[1]***

**1** Division of Experimental Ophthalmology, Institute for Ophthalmic Research, University of Tübingen, Tübingen, Germany, **2** Ocular Neurodegeneration Research Group, Centre for Ophthalmology, Institute for Ophthalmic Research, University of Tübingen, Tübingen, Germany, **3** Department of Ophthalmology, Clinical Sciences Lund, University of Lund, Lund, Sweden, **4** Otolaryngology Department, University of Tübingen, Tübingen, Germany

## Abstract

Retinitis pigmentosa (RP) is a group of inherited neurodegenerative diseases affecting photoreceptors and causing blindness in humans. Previously, excessive activation of enzymes belonging to the poly-ADP-ribose polymerase (PARP) group was shown to be involved in photoreceptor degeneration in the human homologous *rd1* mouse model for RP. Since there are at least 16 different PARP isoforms, we investigated the exact relevance of the predominant isoform - PARP1 - for photoreceptor cell death using PARP1 knock-out (KO) mice. *In vivo* and *ex vivo* morphological analysis using optic coherence tomography (OCT) and conventional histology revealed no major alterations of retinal phenotype when compared to wild-type (*wt*). Likewise, retinal function as assessed by electroretinography (ERG) was normal in PARP1 KO animals. We then used retinal explant cultures derived from *wt*, *rd1*, and PARP1 KO animals to test their susceptibility to chemically induced photoreceptor degeneration. Since photoreceptor degeneration in the *rd1* retina is triggered by a loss-of-function in phosphodiesterase-6 (PDE6), we used selective PDE6 inhibition to emulate the *rd1* situation on non-*rd1* genotypes. While *wt* retina subjected to PDE6 inhibition showed massive photoreceptor degeneration comparable to *rd1* retina, in the PARP1 KO situation, cell death was robustly reduced. Together, these findings demonstrate that PARP1 activity is in principle dispensable for normal retinal function, but is of major importance for photoreceptor degeneration under pathological conditions. Moreover, our results suggest that PARP dependent cell death or PARthanatos may play a major role in retinal degeneration and highlight the possibility to use specific PARP inhibitors for the treatment of RP.

**Citation:** Sahaboglu A, Tanimoto N, Kaur J, Sancho-Pelluz J, Huber G, et al. (2010) PARP1 Gene Knock-Out Increases Resistance to Retinal Degeneration without Affecting Retinal Function. PLoS ONE 5(11): e15495. doi:10.1371/journal.pone.0015495

**Editor:** Ted M. Dawson, Johns Hopkins, United States of America

**Received** August 2, 2010; **Accepted** October 3, 2010; **Published** November 23, 2010



**Funding:** This work has been supported by grants from the Charlotte and Tistou Kerstan Foundation, the European Union (EVI-GENORET: LSHG-CT-2005-512036, NEUROTRAIN: MEST-CT-2005-020235, HEALTH-F2-2008-200234), Fundación Oftalmológica del Mediterráneo (FOM), Deutsche Forschungsgemeinschaft (DFG; PA1751/1-1, Se837/5-2, Se837/6-1, Se837/7-1), and the Werner Reichhardt Centre for Integrative Neuroscience (CIN, No. PP2009-20). The funders had no role in study design, data collection and analysis, decision to publish, or preparation of the manuscript.

**Competing Interests:** The authors have declared that no competing interests exist.

* E-mail: francois.paquet-durand@klinikum.uni-tuebingen.de

¤ Current address: Department of Ophthalmology, Columbia University, Edward S. Harkness Eye Institute Research Annex, New York, New York, United States of America

## Introduction

Blindness is a devastating condition that severely affects the quality of human life. Retinitis pigmentosa (RP) is a group of inherited neurodegenerative diseases that result in selective cell death of photoreceptors and is regarded as the main cause of blindness among the working age population in the developed world [1]. Many of the genetic mutations causing RP have been identified in recent years (for a recent list see RETNET webpage: www.sph.uth.tmc.edu/retnet) but, nevertheless, the precise mechanisms eventually causing cell death remain unknown and to date no adequate treatment for RP is available [2].

The retinal degeneration 1 (*rd1* or rd) human homologous mouse model for RP is characterized by a loss-of-function mutation in the gene encoding for the β-subunit of rod photoreceptor cGMP phosphodiesterase 6 (PDE6) [3]. The *rd1* mouse is considered a relevant model for human RP, since about 4–5% of patients are suffering from mutations in the PDE6 beta gene [4]. Non-functional PDE6 leads to accumulation of cGMP which occupies a key role in the vertebrate phototransduction cascade; however, excessively high cGMP levels trigger photoreceptor degeneration [5,6]. The *rd1* mouse is one of the most studied animal models for RP and previously we demonstrated an involvement of excessive poly (ADP-ribose) polymerase (PARP) activity in *rd1* photoreceptor cell death [7].

PARP enzymes use $NAD^+$ as a substrate to transfer ADP-ribose onto acceptor proteins [8,9]. There are at least 16 different PARP isoforms among which PARP1 - one of the most abundant nuclear enzymes - appears to be responsible for most of the cellular poly (ADP-ribosy)lation activity [10]. PARP1 is activated by DNA strand breaks and facilitates the DNA repair process [11,12]. On the other hand, over-activation of PARP may lead to cell death and PARP has been proposed to be a major constituent of a novel cell death mechanism termed PARthanatos [13,14]. Accordingly, pharmacological inhibition of PARP was shown to increase cellular viability in a number of experimental systems and

particularly so in the context of neurodegenerative diseases [11,15]. Similarly, PARP inhibition protected *rd1* mouse photoreceptors [7]. Notably, though, the question which PARP isoform precisely was most important for the degeneration of photoreceptors remained open, which prevents the full understanding of the pathology.

Here, we examined the phenotype of PARP1 KO retina *in vivo*, *ex vivo* and *in vitro*. While, the retina of PARP1 KO animals appeared essentially normal in terms of morphology and function, photoreceptor cell death was greatly decreased under a specific stress paradigm that mimics inherited retinal degeneration. These results, for the first time, attribute an important role in photoreceptor cell death to PARP1 specifically and emphasize its importance for future treatments of RP.

## Results

### Comparative analysis of PARP1 KO retinal morphology and function

An initial comparison of *wt*, *rd1 and* PARP1 KO *ex vivo* retinal morphology revealed no major differences between the *wt* and PARP1 KO and genotypes at P11 (data not shown) or at P30 (Fig. 1A–C), although at this age the ONL in PARP1 KO did not completely reach the thickness of *wt* (*wt*: 62 µm ±0.3 SEM, n = 4, *rd1*: 8 µm ±0.3 SEM, n = 3, PARP1 KO: 54 µm ±0.6 SEM, n = 4; $p<0.05$) (Fig. 1D). The latter was also reflected in the number of ONL photoreceptor rows (*wt*: 12.7±0.3 SEM, n = 3, *rd1*: 0.9±0.1 SEM, n = 3, PARP1 KO: 11.5±0.3 SEM, n = 4; $p<0.05$). Consistent with these histological data, *in vivo* optic coherence tomography (OCT) examination showed an apparently normal retinal morphology and layering together with a somewhat thinner ONL in PARP1 KO (Fig. 1E–G).

Absence of the characteristic 116 kDa band in PARP1 western blot confirmed the deficiency in protein expression in PARP1 KO (Fig. 1H). To test for possible alterations in retinal function of PARP1 KO mice, single flash ERGs were recorded from PARP1 KO and *wt* control (SV129) mice under scotopic and photopic conditions at an age of 5 weeks (Fig. 1I, J). Both rod and cone photoreceptor signalling appeared to be normal in PARP1 KO, since neither type of measurement revealed any signs of impaired retinal function.

### Cell death markers in *wt, rd1* and PARP1 KO retina

In the *rd1* mouse model, retinal degeneration starts at around P11 [2] and consequently we chose this time-point for a comparative analysis of different cell death markers in *wt*, *rd1*, and PARP1 KO retina. cGMP levels were studied using immunofluorescent detection with a selective and well validated antibody [16] on *ex vivo* sections from *wt*, *rd1* and PARP KO mice at P11. While *wt* retina was essentially devoid of cGMP positive cells, many positive cells were observed in *rd1* ONL due to PDE6 dysfunction in this genotype (*wt*: 0.01% ±0.004 SEM, n = 4; *rd1*: 6.3% ±0.9 SEM, n = 4, $p<0.01$) (Fig. 2A, B). cGMP-positive cells were rarely seen PARP1 KO (0.004% ±0.003 SEM, n = 5) (Fig. 2C). Accumulation of cGMP corresponded to PDE6 beta expression, which was readily detectable in photoreceptor outer segments of both *wt* and PARP1 KO, but absent in the *rd1* situation (Fig. S1).

The analysis of *in situ* PARP activity at P11 (Fig. 2D–F), showed few PARP activity positive cells in the *wt* retina (0.02% ±0.008 SEM, n = 3), large numbers of PARP activity positive cells in *rd1* ONL (2.6% ±0.1 SEM, n = 3), and no detectable activity in the PARP1 KO (0.0% ±0.0 SEM, n = 3). Differences between PARP1 KO and *rd1* ($p<0.01$), and PARP1 KO and *wt* ($p<0.05$) were statistically significant.

Accumulation of poly(ADP-ribosyl)ated proteins is considered an indirect measure to confirm PARP activity. Previous studies showed that PARP activity and correspondingly accumulation of PAR were increased in *rd1* photoreceptors at P11 [7]. In the present study immunohistochemistry demonstrated very low levels of PAR accumulation in the *wt* situation (0.02% ±0.005 SEM, n = 6), high levels in *rd1* ONL (1.5% ±0.2 SEM, n = 4), and no detection in PARP1 KO (0.0% ±0.0 SEM, n = 5) (Fig. 2G–I). There were significant differences between *in vivo* PARP1 KO and *rd1* ($p<0.01$) as well as PARP1 KO and *wt* ($p<0.05$). Western blot analysis for PAR confirmed the immunohistochemical results showing a strong accumulation of high molecular weight poly(ADP-ribosyl)ated proteins only in *rd1* retinal tissue samples (Fig. 2O).

We then used the TUNEL assay to identify degenerating cells in the different genotypes. In the ONL, *wt* retinae showed only very few TUNEL positive, dying cells, while much higher numbers were detected in the *rd1* situation (*wt*: 0.1% ±0.006 SEM, n = 3; *rd1*: 4.5% ±0.4 SEM, n = 3) (Fig. 2J, K). Similar to *wt*, PARP1 KO retinae showed very low numbers of TUNEL positive cells (PARP1 KO: 0.04% ±0.01 SEM, n = 3) (Fig. 2L). Quantification and statistical analysis revealed no significant difference ($p = 0.31$) between *wt* and PARP1 KO but a significant difference ($p<0.01$) between PARP1 KO and *rd1* (Fig. 2M). In line with the histological data, these results indicated that there was no major degeneration phenotype in the ONL of PARP1 KO, which therefore, in all aspects studied here, appeared to behave like *wt*.

### PARP1 KO reduces photoreceptor cell death induced by PDE6 inhibition

Zaprinast is a selective PDE5/6 inhibitor [17,18] which in a concentration dependent manner raises intracellular cGMP levels and causes cGMP-dependent photoreceptor degeneration closely resembling the *rd1* degeneration (Fig. S2) [6,19]. Here, 100 µM zaprinast was used to mimic the *rd1* situation on *wt* and PARP1 KO retinal explants cultured between postnatal days 5–11. Successful PDE6 inhibition was confirmed by an increased cGMP immunofluorescence. While untreated *wt* retina is essentially devoid of cGMP immunoreactivity (0.7% ±0.4 SEM, n = 5), the zaprinast treated *wt* ONL showed large numbers of cGMP positive cells (7.8% ±0.1 SEM, n = 4), comparable to the *rd1* situation (10.6% ±0.7 SEM, n = 7) (Fig. 3A–C). Untreated PARP1 KO displayed very low cGMP immunoreactivity (0.2% ±0.1 SEM, n = 3), which was strongly increased by zaprinast treatment (4.2% ±0.3 SEM, n = 4) (Fig. 3D, E). The zaprinast induced increase in cGMP positivity was significantly lower in PARP1 KO when compared to *wt* ($p<0.01$). However, in relative terms the zaprinast induced elevation in cGMP was more pronounced in PARP1 KO (21-fold increase) than in *wt* (11-fold increase).

Immunohistochemistry for PAR illustrated few positive cells in the ONL of untreated *wt* situation (0.1% ±0.02 SEM, n = 3), larger numbers of positive cells in zaprinast treated *wt* (0.7% ±0.07 SEM, n = 5) and *rd1* ONL (1.3% ±0.3 SEM, n = 3), and very few positive cells in untreated (0.05% ±0.01 SEM, n = 3, $p<0.05$) and zaprinast treated PARP1 KO retinae (0.1% ±0.02 SEM, n = 3, $p<0.05$) (Fig. 3F–J).

The TUNEL assay for dying cells identified only very few positive cell in P11 *wt* ONL i*n vitro* (*wt*: 1.3% ±0.1 SEM, n = 3), while zaprinast treatment raised their number to levels comparable to untreated *rd1* retina (*wt* + zaprinast: 3.9% ±0.1 SEM, n = 6; *rd1*: 5.3% ±0.3 SEM, n = 5) (Fig. 3K–M). Untreated PARP1 KO retina displayed very low numbers of TUNEL positive cells (0.6%

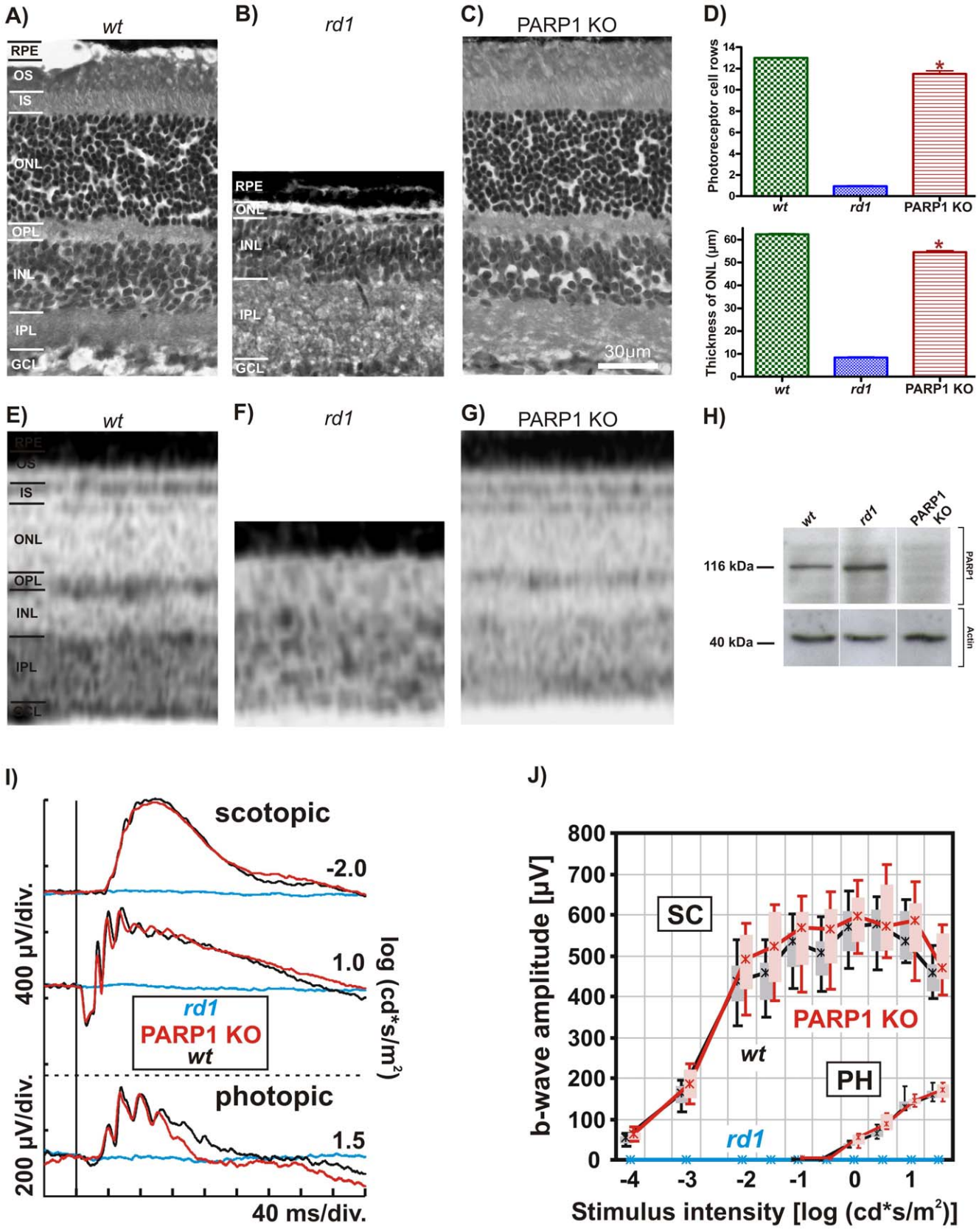


**Figure 1. Histological and functional analysis of PARP1 KO retina.** Haematoxylin/eosin staining at PN30 revealed normal morphology and layering of *wt* (**A**) retina, while in the *rd1* situation (**B**) the ONL had almost completely disappeared. In contrast, PARP1 KO retinae (**C**) appeared essentially normal, although direct comparisons with *wt* showed lower PARP1 KO values for ONL thickness and number of photoreceptor rows

(quantification in **D**). SD-OCT *in vivo* imaging of *wt* (**E**), *rd1* (**F**), and PARP1 KO (**G**) retinae showed a similar picture, with PARP1 KO retina appearing slightly thinner than its *wt* counterpart. Absence of the 116 kDa PARP1 protein was confirmed using western blot (**H**). In spite of the subtle morphological changes seen in PARP1 KO, functional *in vivo* analysis using ERG under both scotopic and photopic conditions in 5 weeks old animals did not detect any differences between PARP1 KO (red traces) and *wt* control (black traces). In *rd1* animals (blue traces), however, retinal function was essentially abolished. Representative single flash ERG recordings from dark-adapted (top) and light-adapted (bottom) states are shown in (**I**), while a statistical evaluation (box-and-whisker plot) of dark-adapted (scotopic; SC) and light-adapted (photopic; PH) single flash ERG b-wave amplitudes in *wt*, *rd1*, and PARP1 KO mice is shown in (**J**). Boxes indicate the 25% and 75% quantile range, whiskers indicate the 5% and 95% quantiles, and solid lines connect the medians of the data. For each of the different experimental investigations, n = 3–4 animals from each genotype were used and analyzed independently. Error bars in (**D**) represent SEM. GCL, ganglion cell layer; IPL, inner plexiform layer; INL, inner nuclear layer; OPL, outer plexiform layer; IS, inner segment; OS, outer segment; RPE, retinal pigment epithelium.
doi:10.1371/journal.pone.0015495.g001

$\pm$0.1 SEM, n = 3) similar to untreated *wt*. Importantly, zaprinast treatment resulted only in a minor elevation of cell death in PARP1 KO retina when compared to zaprinast treated *wt* (PARP1 KO + zaprinast: 0.7% $\pm$0.04 SEM, n = 5, $p<0.01$) (Fig. 3N, O). In relative terms, zaprinast treatment resulted in a 200% elevation of cell death in *wt* retina, compared to only 17% increase in PARP1 KO (Fig. 3P).

Together, these results suggest that the photoreceptor cell death that follows upon PDE6 inhibition and subsequent accumulation of cGMP, to a major extent is dependent on PARP1 activity, since PARP1 KO displayed strong resistance to this paradigm of induced photoreceptor degeneration.

## Discussion

Cell death, in particular in the context of neurodegenerative diseases, has frequently been found to be associated with excessive PARP activity [10,11] and we have previously found strong PARP activation to be causally connected to photoreceptor cell death [7]. Nevertheless, at the beginning of this study it was not clear which one of the 16 different PARP isoforms might be responsible for this detrimental effect. Here, we show that PARP activity during photoreceptor neurodegeneration is caused to a major extent by the PARP1 isoform specifically. While *wt* photoreceptors were highly susceptible to a stress paradigm mimicking the *rd1* type of inherited retinal degeneration, PARP1 KO photoreceptors were resistant to such stress.

### PARP activity in cellular physiology

PARP enzymes play ambiguous roles in cellular physiology. They are important mediators of DNA repair and strongly protect cells against genotoxic stressors [20,21], notably because poly(ADP-ribosyl)ation of DNA associated histones causes relaxation of the chromatin structure, allowing DNA repair enzymes to access the site of the strand break, thereby facilitating the DNA repair process [10,12]. On the other hand, an excessive PARP activation may overstrain the cellular metabolism, leading to an energetic collapse and eventually cell death [22,23]. In this respect excessive consumption of the PARP substrate $NAD^+$ seems to be of particular importance, since this will indirectly result in depletion of cellular ATP [10,22].

In conjunction with its antagonist poly-ADP-ribose-glycohydrolase (PARG), PARP activity may result in the generation of free PAR polymers. These may cause release of a mitochondrial protein termed apoptosis inducing factor (AIF) resulting in its translocation to the nucleus, widespread DNA fragmentation and cell death [24], as seen in PARP dependent cell death of primary cortical neurons [25]. Alternatively, free PAR may act on transient-receptor-potential (TRP) ion channels causing excessive calcium influx [26,27] with potential repercussions on calcium-dependent calpain-type protease activation and therefore photoreceptor cell death [28]. Interestingly, auditory receptor cell death following acoustic trauma and cochlear ischemia has also been connected with excessive PARP activation, suggesting that sensory cells might be particularly susceptible to undergo PARP dependent cell death [29,30].

PARP1 KO mice develop normally and show no particular phenotype. However, these animals are susceptible to developing epidermal hyperplasia and obesity at older ages [31] and cells lacking PARP1 are susceptible to genotoxic stress [21]. Future investigations will have to determine whether reduced DNA repair capabilities, or other PARP related actions, are responsible for the slight decrease in retinal thickness observed in PARP1 KO animals. Interestingly, PARP1 KO animals display increased resistance to streptozotocin induced cell death of pancreatic beta cells [32], ischaemic brain injury [33], and ocular deprivation induced cell death in the lateral geniculate nucleus [34]. Indeed, PARP is supposed to play a central role in a novel form of caspase-independent cell death which involves excessive activation of PARP, formation of poly-ADP-ribose polymers, translocation of AIF protein from mitochondria to the nucleus, chromatin condensation, and large DNA fragmentation. Because of its dependence on PARP activity and the generation of PAR polymers this cell death mechanism was tentatively termed PARthanatos [13,35]. Taken together, PARP1, apart from its functions during normal cell physiology appears to be of major importance for cell death, particularly in neuronal cells.

### PARP and photoreceptor cell death mechanisms

It has previously been shown that photoreceptor cell death in the *rd1* mouse is associated with nuclear translocation of AIF [36] and oxidative DNA damage, factors which both colocalizes with PARP activity in photoreceptor nuclei [7]. Our finding that PARP1 KO photoreceptors are highly resistant to PDE6 inhibition induced degeneration confirms these previous results and points to the PARP1 isoform as a major contributor to PARP dependent photoreceptor cell death. However, while PARP1 KO dramatically reduced the accumulation of PAR in all situations tested, PAR accumulation was not abolished altogether. This suggests that other PARP isoforms such as PARP2 [21,37,38,39] may, to a limited extent, compensate for the lack of PARP1 expression.

Apart from PARP activity, photoreceptor cell death in the *rd1* mouse model for RP has been found to be characterized by an elevation of cGMP levels, activation of PKG, calpains and histone deacetylases (HDACs) [5,6,40]. The PARP activity in *rd1* photoreceptors might have a bearing on calpain activation [15] and could itself be governed by the activity of HDACs, since HDAC inhibition in *rd1* retina also abolished PARP activity [38]. Moreover, deacetylation and poly(ADP-ribose)ylation were exactly coincidental in degenerating *rd1* photoreceptors [40] also suggesting a sequential activation of first HDAC then PARP during cell death.

Even though photoreceptor degeneration has in the past often been addressed as an apoptotic process, it takes place independent of critical features of apoptosis such as *de novo* protein biosynthesis, caspase activation, or cytochrome *c* release (*reviewed in:* 2). The finding that photoreceptor degeneration induced by PDE6 inhibition was strongly reduced in PARP1 deficient animals

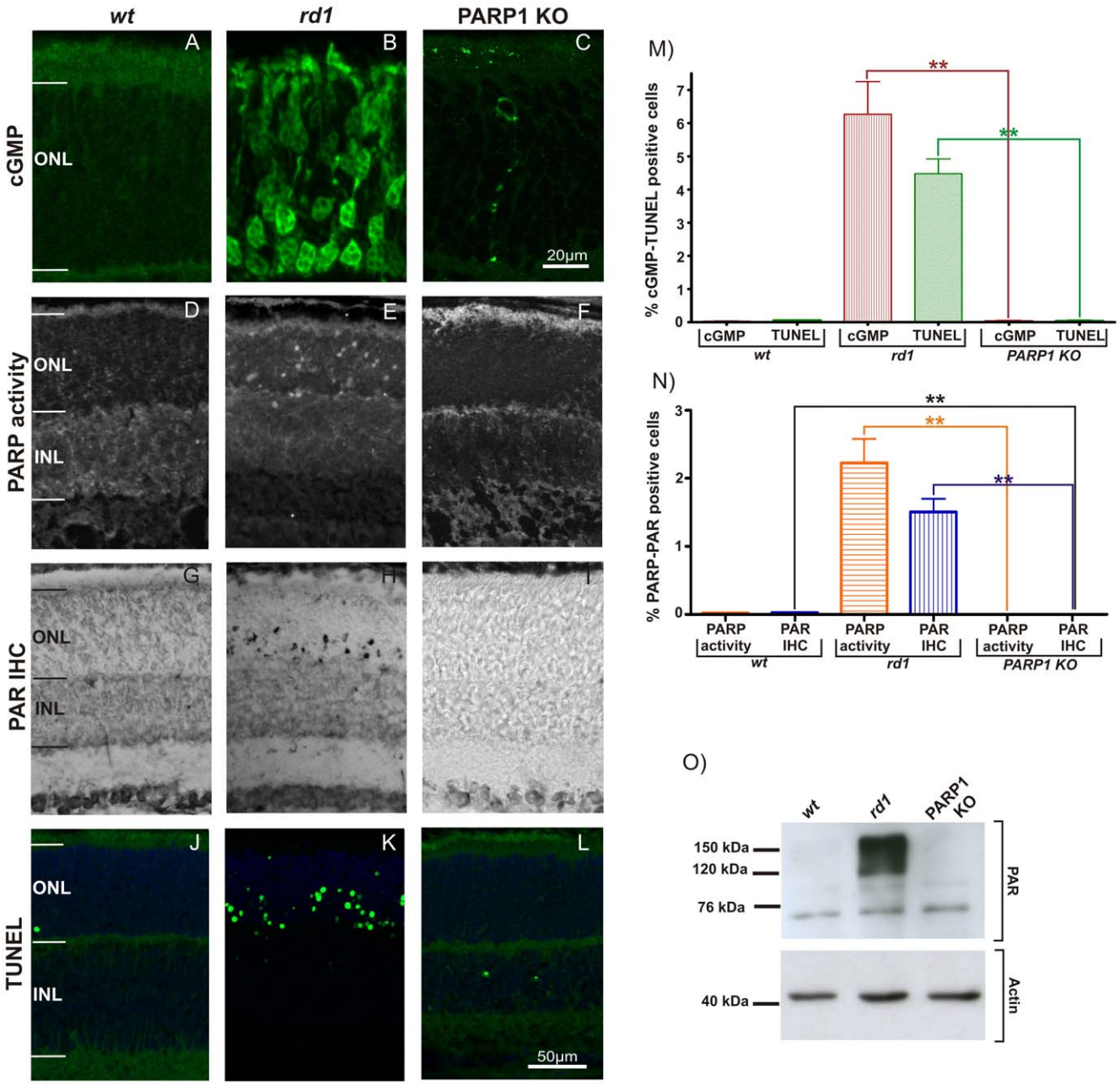


**Figure 2. cGMP, PARP activity and TUNEL in *wt*, *rd1*, and PARP1 KO retina.** At P11, immunoreactivity for cGMP was essentially absent in both *wt* and PARP1 KO retina, while in the *rd1* ONL a large number of photoreceptor cell bodies, neurites and segments were stained (**A**–**C**). The *in situ* PARP activity assay (**D**–**F**) and accumulation of PAR (**G**–**I**) as an indirect marker for PARP activity labeled photoreceptor nuclei only in the *rd1* situation but not in *wt* nor PARP1 KO retina. The bar graphs display the quantification of the percentages of ONL cells positive for cGMP and TUNEL (**M**), and PARP activity and PAR accumulation (**N**), respectively. Strong accumulation of PAR in *rd1* retina was confirmed using western blot (**O**). The TUNEL assay for dying cells identified large numbers of cells only in the *rd1* ONL (**J**–**L**), Retinae from n = 3–6 animals were used for each analysis and genotype. Error bars represent SEM.
doi:10.1371/journal.pone.0015495.g002

suggests that PARthanatos or a closely related mechanism is responsible for cell death in this situation. If this was the case then in turn the wealth of knowledge available for the *rd1* degeneration might also be used to improve the understanding of this novel cell death mechanism.

## Conclusion

We have shown a causal involvement of PARP1 in a retinal photoreceptor degeneration paradigm, that mimics inherited neurodegeneration as it occurs in the human homologous *rd1* mouse model. PARP1 KO prevented photoreceptor cell death *in vitro*, a result that highlights the importance of PARP1 as a novel therapeutic target in retinal degeneration both for pharmacological and genetic treatment approaches. A reduced PARP1 activity would most likely not compromise retinal function, since absence of PARP1 does not alter retinal function. These findings also propose that photoreceptor cell death may be governed by an alternative cell death mechanism, possibly related to the recently described PARthanatos.

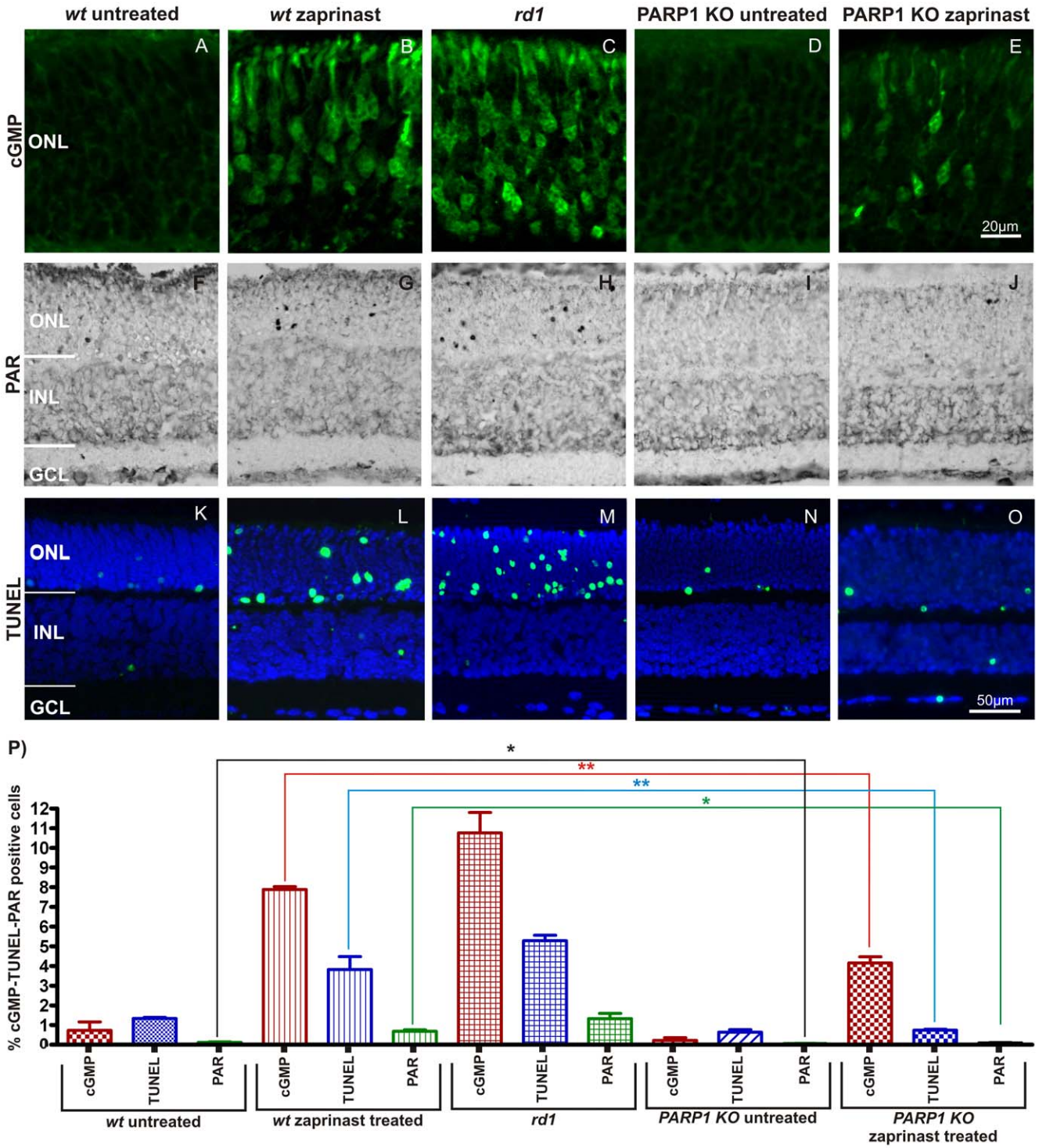


**Figure 3. PARP1 KO animals are resistant to PDE6 inhibition induced photoreceptor cell death.** Organotypic retinal explant cultures obtained from *wt* and PARP1 KO animals were treated with the PDE6 inhibitor zaprinast and compared to untreated *wt*, *rd1* and PARP1 KO cultured retinae. Control *wt* retinae at P11 *in vitro* showed minimal immunoreactivity to cGMP-antibody in the ONL (**A**). Zaprinast treated *wt* retinae exhibited strongly increased intracellular cGMP levels (**B**), similar to what was observed in PDE6 mutant *rd1* retina (**C**). While PARP1 KO did not display cGMP immunoreactivity (**D**), it responded to zaprinast treatment with a moderate, but significant, elevation of cGMP positive ONL cells (**E**). Accumulation of PAR as an indirect marker for PARP activity (**F**–**J**) was found in large amounts only in zaprinast treated *wt* or *rd1* ONL but notably absent in PARP1 KO preparations and *wt* retinae. The TUNEL assay for dying cells generally followed a similar pattern (**K**–**O**): The *rd1* mutant or PDE6 inhibition resulted in marked increases of positive cells in the ONL only. The bar graph (**P**) illustrates the quantification of the three parameters assayed. Explant cultures from n = 3–6 animals were used for each treatment situation and genotype. Error bars represent SEM.
doi:10.1371/journal.pone.0015495.g003

## Materials and Methods

### Experimental animals

Animals were housed under standard white cyclic lighting, had free access to food and water, and were used irrespective of gender. C3H *rd1* mice [41], PARP1 KO mice [31] and wild-type (*wt*) SV129 mice were used. All procedures were approved by the Tübingen University committee on animal protection (Einrichtung für Tierschutz, Tierärztlichen Dienst und Labortierkunde directed by Dr. Franz Iglauer) and performed in accordance with the ARVO statement for the use of animals in ophthalmic and visual research. Protocols compliant with §4 of the German law on animal protection were reviewed and approved by Dr. Ulf Scheurlen and Dr. Susanne Gerold (Einrichtung für Tierschutz, Tierärztlichen Dienst und Labortierkunde; Registration No.: 16/12/08-1, 10/02/10-1). Since experiments were carried out on *ex vivo* retinal explants (see below), no further permits were required. Because in the *rd1* retina critical changes are apparent at postnatal day 11 (P11) [30,42], most comparisons were carried out at this age.

### Morphological characterization

Haematoxylin/Eosin staining was used for *ex vivo* characterization of PARP1 KO retinae. Fixed cryosectioned retinae were stained in Harris haematoxylin solution (Vector Laboratories, CA, USA, H-3401) for 3 minutes and then washed in bidestilled water for 1 minute. Following a brief, 2s exposure to 25% hydrochloric acid in ethanol, the sections were washed again and counterstained in Accustain eosin Y solution (Sigma-Aldrich, Munich, Germany, HT-110-1-16) for 30 seconds to 1 minute. The sections were dehydrated in a 70% –96% –100% alcohol series, washed in xylene for 2 minutes, and then mounted with DPX mounting medium for histology (Sigma-Aldrich).

### Electroretinographic Analysis

Electroretinograms (ERGs) were recorded binocularly according to previously described procedures [43,44]. The ERG equipment consisted of a Ganzfeld bowl, a direct current amplifier, and a PC-based control and recording unit (Multiliner Vision; VIASYS Healthcare GmbH, Hoechberg, Germany). Mice of 5 weeks age were dark-adapted overnight and anaesthetised with ketamine (66.7 mg/kg body weight) and xylazine (11.7 mg/kg body weight). The pupils were dilated and single flash ERG responses were obtained under dark-adapted (scotopic) and light-adapted (photopic) conditions. Light adaptation was accomplished with a background illumination of 30 candela (cd) per square meter starting 10 minutes before recording. Single white-flash stimulus intensity ranged from $-4$ to 1.5 log cd*s/m$^2$ under scotopic and from $-2$ to 1.5 log cd*s/m$^2$ under photopic conditions, divided into 10 and 8 steps, respectively. Ten responses were averaged with an inter-stimulus interval of either five seconds or 17 seconds (for 0, 0.5, 1, and 1.5 log cd*s/m$^2$).

### Spectral domain optical coherence tomography (SD-OCT)

SD-OCT imaging was performed immediately following ERG, i.e. animals remained anaesthetized. Mouse eyes were subjected to SD-OCT using the commercially available Spectralis$^{TM}$ HRA+OCT device from Heidelberg Engineering (Heidelberg, Germany) featuring a broadband superluminescent diode at $\lambda = 870$ nm as low coherent light source. Each two-dimensional B-Scan recorded at 30° field of view consisted of 1536 A-Scans, which were acquired at a speed of 40,000 scans per second. Optical depth resolution was approximately 7 µm with digital resolution reaching 3.5 µm [45]. The adaptation for the optical qualities of the mouse eye was described previously [46].

### Retinal explant cultures

Organotypic retinal cultures that included the retinal pigment epithelium (RPE) were prepared in principle as previously published [47]. Briefly, P5 animals were sacrificed, the eyes enucleated and pretreated with 12% proteinase K (ICN Biomedicals Inc., OH, USA; 193504) for 15 minutes at 37°C in R16 serum free culture medium (Invitrogen Life Technologies, Paisley, UK; 07490743A). Proteinase K was blocked by addition of 10% fetal bovine serum, followed by rinsing in serum-free medium. In the following, cornea, lens, sclera and choroid were removed carefully, with only the RPE remaining attached to the retina. The explant was then cut into four wedges to give a cloverleaf like structure which was transferred to a culture membrane insert (Millipore AB, Solna, Sweden; PIHA03050) with the RPE facing the membrane. The membrane inserts were placed into six well culture plates and 1.4 ml of R16 medium with supplements [47] was added. The cultures were incubated at 37°C in a humidified 5% $CO_2$ incubator. The culture medium was changed every 2 days during 6 culturing days. Retinal explants were left without treatment for 2 days (until P7), followed by zaprinast (100 or 200 µM; Sigma Z0878) treatment. Zaprinast was prepared in dimethyl sulfoxide (DMSO; Sigma D2650) and diluted in R16 serum free culture medium with supplements. For controls, the same amount of DMSO was diluted in culture medium.

### TUNEL Assay

The terminal deoxynucleotidyl transferase dUTP nick end labeling (TUNEL) assay was performed on cryosections from treated/untreated *wt*, PARP1 KO, and *rd1* retinae, using an *in situ* cell death detection kit conjugated with fluorescein isothiocyanate (Roche Diagnostics, Mannheim, Germany). For controls, terminal deoxynucleotidyl transferase enzyme was either omitted from the labelling solution (negative control), or sections were pre-treated for 30 min with DNAse I (Roche, 3 U/ml) in 50 mM Tris-HCl, pH 7.5, 1 mg/ml BSA to induce DNA strand breaks (positive control). Negative control gave no staining at all, while positive control stained all nuclei in all layers of the retina (not shown, *see:* 7).

### Immunostaining

4% PFA fixed, frozen retinal sections from P11 animals or cultured retinae, were dried for 30–60 minutes at 37°C. Subsequently, the tissue was rehydrated in PBS, and pre-incubated for 1 hour at RT in blocking solution, containing 10% normal serum, and 0.1% or 0.3% Triton in PBS (PBST). Immunohistochemistry was performed overnight at 4°C, using primary antibodies directed against cGMP (obtained from Jan de Vente, Maastricht University; *see:* 16; dilution 1:500), PAR (Alexis Biochemicals, Lörrach, Germany; dilution 1:200; Order No.: 804-220), and PDE6 beta (Affinity Bioreagents; dilution 1:400; Order No.: PA1-722) diluted in blocking solution. The tissue was rinsed in PBST, and incubated for 1 hour with Alexa 488 conjugated secondary antibody, (1:200-1:750, Invitrogen), diluted in PBST. Sections were rinsed in PBS, and mounted in Vectashield with DAPI (Vector, Burlingame, CA, USA).

### Western blot (WB)

Retinal tissue from PARP1 KO, *wt* and *rd1* mice were homogenized in buffer as described previously [7] with a Heidolph DIAX 600 homogenizer (Heidolph, Schwabach, Germany) or a

manual homogenizer (glass to glass). Bradford assay was used for determination of protein concentration. For separation of proteins, SDS-PAGE 10–12% gradient gel (at 55 V) was used and 27 µg protein was loaded per well. Subsequently, the proteins were transferred to PVDF membranes (GE Healthcare, UK). Membranes were blocked in Roti block (Roth, Karlsruhe, Germany) blocking buffer for 1 hour at room temperature (RT). Membranes were incubated in primary antibodies against PARP1 (BD Pharmingen, Heidelberg, Germany; 556362), PAR (see above), actin (Sigma-Aldrich; A 2668) at a dilution of 1:1000 in buffer containing PBST and 5% dried milk (Roth) overnight at 4°C. Membranes were washed with PBST and incubated with horseradish peroxidase conjugated secondary antibody (GE Healthcare, UK) for 1 hour at RT. Hyperfilm (GE Healthcare, UK) detection system was used as a membrane developer. Films were scanned and quantified using ImageJ (National Institutes of Health, Washington, USA).

### PARP activity assay

Eyes from PARP1 KO, *wt* and *rd1* mice were enucleated, frozen immediately on dry ice (−72°C), followed by cryosectioning. A biotin-avidin blocking kit (Vector) was used to block endogenous biotin and to reduce background. After incubation with PARP reaction mixture (10 mM $MgCl_2$, 1 mM dithiothreitol, 5 µM biotinylated NAD (Trevigen, Gaithersburg, MD, USA) in 100 mM Tris buffer with 0.2% Triton X100, pH 8.0) for 2.5 h at 37°C, the sections were washed with PBS, 3 times for 5 minutes. The biotin incorporated by PARP activity was then detected by fluorescently labeled avidin (1:800 in PBS, 1 h at RT). After 3 times 5 min washing in PBS, the sections were mounted in Vectashield (Vector). For controls, biotinylated-$NAD^+$ was omitted from the reaction mixture resulting in absence of detectable reaction product.

### Microscopy, Cell counting, and Statistics

Microscopy was performed using a Zeiss Imager Z1 Apotome Microscope. Images were taken with a Zeiss Axiocam digital camera, using Zeiss Axiovision 4.7 software. Image enhancements (Contrast, Colors) were done in paired fashion using Corel Draw X3 software.

The percentages of ONL cells positive in the different assays (PARP activity, PAR IHC, TUNEL) were assessed and calculated in a blinded fashion as reported previously [6,28]. For each animal the central areas (in proximity to the optic nerve) of at least 3 sections were quantified to yield an average value, and at least 3 different animals were analyzed for each time-point and genotype. Values are given as mean ± standard error of the mean (SEM).

Statistical analysis was performed using GraphPad Prism 4.01 software (GraphPad Software, La Jolla, CA, USA) and two-tailed Student's *t* test. Levels of significance were: * = $p<0.05$, ** = $p<0.01$, *** = $p<0.001$.

## Supporting Information

**Figure S1 PDE6 beta expression in *wt*, *rd1*, and PARP1 KO retinae.** At PN11, immunostaining revealed PDE6 beta expression (green) in photoreceptor outer segments of *wt* retina, while PDE6 beta protein was undetectable in *rd1* retina. In PARP1 KO retina PDE6 beta expression followed the pattern of *wt*. DAPI (blue) was used as nuclear counterstain. The images shown are representative for immunostainings performed on retinal cross-sections from at least 3 different animals for each genotype.
(TIF)

**Figure S2 Zaprinast treatment induces cGMP accumulation and cell death in a concentration dependent manner.** Untreated organotypic retinal cultures derived from *wt* animals showed very few cGMP (**A**) and TUNEL (**D**) positive cells at P11 *in vitro*. PDE6 inhibition with zaprinast caused cGMP accumulation (**B**, **C**) and cell death (**E**, **F**) that increased together with zaprinast concentration (Quantification in **G**). Explant cultures from n = 3-8 *wt* animals were used for each treatment situation. Error bars represent SEM.
(TIF)

## Acknowledgments

We thank S. Bernhard-Kurz, K. Bekure-Nemariam, and K. Gültig for excellent technical assistance and D. Trifunovic and C. Harteneck for helpful comments and discussions. The PARP1 KO-mice were kindly provided by Zhao-Qi Wang, Leibniz Institute for Age Research, Fritz Lipmann Institute, Jena. The cGMP antibody was kindly provided by Jan de Vente, University of Maastricht.

## Author Contributions

Conceived and designed the experiments: FP-D MWS PE. Performed the experiments: AS NT JK JS-P GH EF. Analyzed the data: AS NT GH BA-G MWS FP-D. Contributed reagents/materials/analysis tools: HL EZ PE. Wrote the paper: AS NT GH BA-G FP-D PE.

## References

1. Herse P (2005) Retinitis pigmentosa: visual function and multidisciplinary management. Clin Exp Optom 88: 335–350.
2. Sancho-Pelluz J, Arango-Gonzalez B, Kustermann S, Romero FJ, van Veen T, et al. (2008) Photoreceptor cell death mechanism in inherited retinal degeneration. Mol Neurobiol 38: 253–269.
3. Bowes C, Li T, Danciger M, Baxter LC, Applebury ML, et al. (1990) Retinal degeneration in the rd mouse is caused by a defect in the beta subunit of rod cGMP-phosphodiesterase. Nature 347: 677–80.
4. McLaughlin ME, Ehrhart TL, Berson EL, Dryja TP (1995) Mutation spectrum of the gene encoding the β subunit of rod phosphodiesterase among patients with autosomal recessive retinitis pigmentosa. Proc Natl Acad Sci USA 92: 3249–3253.
5. Farber DB, Lolley RN (1974) Cyclic guanosine monophosphate: elevation in degenerating photoreceptor cells of the C3H mouse retina. Science 186.4162: 449–51.
6. Paquet-Durand F, Hauck SM, van Veen T, Ueffing M, Ekström P (2009) PKG activity causes photoreceptor cell death in two retinitis pigmentosa models. J Neurochem 108: 796–810.
7. Paquet-Durand F, Silva J, Talukdar T, Jonhnson LE, Azadi S, et al. (2007) Excessive activation of poly(ADP-ribose) ploymerase contributes to inherited photoreceptor degeneration in the retinal degeneration 1 mouse The Journal of Neuroscience 27(38): 10311–10319.
8. Beneke S, Diefenbach J, Burkle A (2004) Poly(ADP-ribosyl)ation inhibitors: promising drug candidates for a wide variety of pathophysiologic conditions. Int J Cancer 111: 813–818.
9. Smith S (2001) The World according to PARP. Trends in Biochemical Sciences 26: 174–179.
10. Rouleau M, Patel A, Hendzel MJ, Kaufmann SH, Poirier GG (2010) PARP inhibition: PARP1 and beyond. Nat Rev Cancer 10(4): 293–301.
11. Jagtap P, Szabo C (2005) Poly(ADP-ribose) polymerase and the therapeutic effects of its inhibitors. Nat Rev Drug Discov 4: 421–440.
12. Herceg C, Wang ZQ (2001) Functions of poly(ADP-ribose) polymerase (PARP) in DNA repair, genomic integrity and cell death. Mutation Research 477: 97–110.
13. Wang Y, Dawson VL, Dawson TM (2009) Poly(ADP-ribose) signals to mitochondrial AIF: a key event in parthanatos. Exp Neurol 218(2): 193–202.
14. Ghezzi D, Sevrioukova I, Invernizzi F, Lamperti C, Mora M, et al. (2010) Severe X-linked mitochondrial encephalomyopathy associated with a mutation in apoptosis-inducing factor. Am J Hum Genet 86(4): 639–49.
15. Vosler PS, Sun D, Wang S, Gao Y, Kintner DB, et al. (2009) Calcium dysregulation induces apoptosis-inducing factor release: cross-talk between PARP-1- and calpain-signaling pathways. Exp Neurol 218(2): 213–20.

16. de Vente J, Steinbusch HWM, Schipper J (1987) A new approach to immunocytochemistry of 3′,5′-cyclic guanosine monophosphate: preparation, specificity, and initial application of a new antiserum against formaldehyde-fixed 3′,5′-cyclic guanosine monophosphate. Neuroscience 22: 361–73.
17. Contin MA, Verra DM, Guido ME (2006) An invertebrate-like phototransduction cascade mediates light detection in the chicken retinal ganglion cells FASEB J 20: 2648–2650.
18. Morin F, Lugnier C, Kameni J, Voisin P (2001) Expression and role of phosphodiesterase 6 in the chicken pineal gland. Journal of Neurochemistry 78: 88–99.
19. Vallazza-Deschamps G, Cia D, Gong J, Jellali A, Duboc A, et al. (2005) Excessive activation of cyclic nucleotide-gated channels contributes to neuronal degeneration of photoreceptors. Eur J Neurosci 22: 1013–22.
20. Hong SJ, Dowson TM, Dowson VL (2004) Nuclear and mitochondrial conversations in cell death: PARP-1 and AIF signaling. TRENDs in Pharmacological Sciences 25: 259–264.
21. Schreiber V, Ame JC, Dolle P, Schultz I, Rinaldi B, et al. (2002) Poly(ADP-ribose) polymerase-2 (PARP-2) is required for efficient base excision DNA repair in association with PARP-1 and XRCC1. J Biol Chem 277: 23028–23036.
22. Sims JL, Berger SJ, Berger NA (1983) Poly(ADP-ribose) Polymerase inhibitors preserve nicotinamide adenine dinucleotide and adenosine 5′-triphosphate pools in DNA-damaged cells: mechanism of stimulation of unscheduled DNA synthesis. Biochemistry 22: 5188–5194.
23. Du L, Zhang X, Han YY, Burke NA, Kochanek PM, et al. (2003) Intra-mitochondrial poly(ADP-ribosylation) contributes to NAD+ depletion and cell death induced by oxidative stress. J Biol Chem 278: 18426–18433.
24. Susin SA, Lorenzo HK, Zamzami N, Marzo I, Snow BE, et al. (1999) Molecular characterization of mitochondrial apoptosis-inducing factor. Nature 397(6718): 441–6.
25. Andrabi SA, Kim NS, Yu SW, Wang H, Koh DW, et al. (2006) Poly(ADP-ribose) (PAR) polymer is a death signal. Proc Natl Acad Sci USA 103(48): 18308–18313.
26. Kraft R, Grimm C, Grosse K, Hoffmann A, Sauerbruch S, et al. (2004) Hydrogen peroxide and ADP-ribose induce TRPM2-mediated calcium influx and cation currents in microglia. Am J Physiol Cell Physiol 286(1): C129–C137.
27. Buelow B, Song Y, Scharenberg AM (2008) The Poly(ADP-ribose) polymerase PARP-1 is required for oxidative stress-induced TRPM2 activation in lymphocytes. J Biol Chem 283: 24571–24583.
28. Paquet-Durand F, Azadi S, Hauck SM, Ueffing M, van Veen T, et al. (2006) Calpain is activated in degenerating photoreceptors in the rd1 mouse. J Neurochem 96: 802–14.
29. Murashita H, Tabuchi K, Hoshino T, Tsuji S, Hara A (2006) The effects of tempol, 3-aminobenzamide and nitric oxide synthase inhibitors on acoustic injury of the mouse cochlea. Hear Res 214(1-2): 1–6.
30. Tabuchi K, Ito Z, Tsuji S, Nakagawa A, Serizawa F, et al. (2001) Poly(adenosine diphosphate-ribose) synthetase inhibitor 3-aminobenzamide alleviates cochlear dysfunction induced by transient ischemia. Ann Otol Rhinol Laryngol 110(2): 118–21.
31. Wang ZQ, Auer B, Stingl L, Berghammer H, Haidacher D, et al. (1995) Mice lacking ADPRT and poly(ADP-ribosyl)ation develop normally but are susceptible to skin disease. Genes Dev 9(5): 509–20.
32. Burkart V, Wang ZQ, Radons J, Heller B, Herceg Z, et al. (1999) Mice lacking the poly(ADP-ribose) polymerase gene are resistant to pancreatic beta-cell destruction and diabetes development induced by streptozocin. Nat Med 5(3): 314–9.
33. Eliasson MJ, Sampei K, Mandir AS, Hurn PD, Traystman RJ, et al. (1997) Poly(ADP-ribose) polymerase gene disruption renders mice resistant to cerebral ischemia. Nat Med 3(10): 1089–95.
34. Nucci C, Piccirilli S, Rodinò P, Nisticò R, Grandinetti M, et al. (2000) Apoptosis in the dorsal lateral geniculate nucleus after monocular deprivation involves glutamate signaling, NO production, and PARP activation. Biochem Biophys Res Commun 19;278(2): 360–7.
35. Andrabi SA, Dawson TM, Dawson VL (2008) Mitochondrial and nuclear cross talk in cell death: parthanatos. Ann N Y Acad Sci 1147: 233–41.
36. Sanges D, Marigo V (2006) Cross-talk between two apoptotic pathways activated by endoplasmic reticulum stress: differential contribution of caspase-12 and AIF. Apoptosis 11: 1629–1641.
37. Shieh WM, Amé JC, Wilson MV, Wang ZQ, Koh DW, et al. (1998) Poly(ADP-ribose) polymerase null mouse cells synthesize ADP-ribose polymers. J Biol Chem 273(46): 30069–72.
38. Ame JC, Rolli V, Schreiber V, Niedergang C, Apiou F, et al. (1999) PARP-2, A novel mammalian DNA damage-dependent poly(ADP-ribose) polymerase. J Biol Chem 274: 17860–17868.
39. Menissier de Murcia J, Ricoul M, Tartier L, Niedergang C, Huber A, et al. (2003) Functional interaction between PARP-1 and PARP-2 in chromosome stability and embryonic development in mouse. Embo J 22: 2255–2263.
40. Sancho-Pelluz J, Alavi M, Sahaboglu A, Kustermann S, Farinelli P, et al. (2010) Excessive HDAC activation critical for neurodegeneration in the rd1 mouse. Cell Death & Disease. doi:10.1038/cddis.2010.4.
41. Sanyal S, Bal AK (1973) Comparative light and electron microscopic study of retinal histogenesis in normal and *rd* mutant mice. Z Anat EntwGesch 142: 219–238.
42. Hauck SM, Ekström PA, Ahuja-Jansen P, Supmann S, Paquet-Durand F, et al. (2006) Differential modification of phosducin protein in degenerating rd1 retina is associated with constitutively active $Ca^{+2}$/calmodulin kinase II in rod outer segments. Mol Cell Proteomics 5: 324–336.
43. Seeliger MW, Grimm C, Ståhlberg F, Friedburg C, Jaissle G, et al. (2001) New views on RPE65 deficiency: the rod system is the source of vision in a mouse model of Leber congenital amaurosis. Nat Genet 29: 70–74.
44. Tanimoto N, Muehlfriedel RL, Fischer MD, Fahl E, Humphries P, et al. (2009) Vision tests in the mouse: Functional phenotyping with electroretinography. Front Biosci 14: 2730–37.
45. Huber G, Beck SC, Grimm C, Sahaboglu-Tekgoz A, Paquet-Durand F, et al. (2009) Spectral domain optical coherence tomography in mouse models of retinal degeneration. Investigative Ophthalmology & Visual Science. doi:10.1167/iovs.09-3724.
46. Fischer MD, Huber G, Beck SC, Tanimoto N, Muehlfriedel R, et al. (2009) Noninvasive, in vivo assessment of mouse retinal structure using optical coherence tomography. PLoS One 2009 Oct 19;4(10): e7507.
47. Caffé AR, Ahuja P, Holmqvist B, Azadi S, Forsell J, et al. (2001) Mouse retina explants after long-term culture in serum free medium. J Chem Neuroanat 22: 263–273.